



UNIVERSITEIT VAN PRETORIA  
UNIVERSITY OF PRETORIA  
YUNIBESITHI YA PRETORIA

# **Effects of cadmium, chromium and mercury alone and in combination on lung tissue of Sprague-Dawley rats**

Sirasha Venketsamy Koopsamy Naidoo

11131978

## **MSc: Human Cell Biology**

Supervisor: Prof HM Oberholzer

Co-Supervisor: Prof MJ Bester

DEPARTMENT OF ANATOMY  
FACULTY OF HEALTH SCIENCES  
UNIVERSITY OF PRETORIA

2019



UNIVERSITEIT VAN PRETORIA  
UNIVERSITY OF PRETORIA  
YUNIBESITHI YA PRETORIA

# **Effects of cadmium, chromium and mercury alone and in combination on lung tissue of Sprague-Dawley rats**

**by**

SIRASHA VENKETSAMY KOOPSAMY NAIDOO

SUPERVISOR: Prof HM Oberholzer

CO-SUPERVISOR: Prof MJ Bester

DEGREE: MSc Human Cell Biology

## **Summary**

Heavy metals are widely used in numerous applications and environmental exposure has increased. The prevalence of respiratory disease worldwide has also increased dramatically and research has linked heavy metal exposure via inhalation to diseases of the respiratory system, particularly pulmonary fibrosis. The lungs are often overlooked when the toxicity of heavy metals after oral exposure is being investigated. Environmental exposure is not limited to a single metal but as part of mixtures of metals. In the South African milieu cadmium, chromium and mercury are common metal contaminants in water. Therefore, the aim of this study was to investigate the effects of exposure to 1000 times the World Health Organization's limits of cadmium, chromium and mercury alone and in combination on the lung tissue of Sprague-Dawley rats.

Sprague-Dawley rats (6 rats per group including controls) were daily orally gavaged with dosages equivalent to a 1000 times, the World Health Organisation's limits for cadmium, chromium and mercury alone and in combinations (Cd, Cr, Hg, Cd + Cr, Cd + Hg, Cr + Hg and Cd + Cr + Hg) for 28 days. After exposure the controls and exposed rats were terminated and the tissue and cellular structure of the bronchioles and lungs were evaluated. Tissue structure was evaluated using specific stains. Transmission electron microscopy was used to evaluate the ultrastructural changes in type I and II alveolar cells as well as the distribution of collagen and elastic fibers.

In the exposed groups, thickening of the intra-alveolar space, desquamation of epithelial cells of the bronchioles with increase in cellular debris was observed. Additionally, the presence of bronchus-associated lymphoid tissue was observed, with increased displacement and distribution of collagen type III to type I. Elastin fibres appeared more fragmented along the basement membrane of the exposed groups compared to the control. Ultrastructural analyses revealed the detachment of the nuclear membrane of alveolar type II cells, with a prominent increase in collagen and elastin bundles and the presence of mast cells near injured alveolar type II cells. Mercury alone and the combinations containing mercury, (Cr + Hg, Cd + Hg and Cd + Cr + Hg) were the most toxic.

In conclusion, this study identified, that following oral exposure to metals such as cadmium, chromium and mercury, the lungs are a specific target of toxicity. Therefore, in addition to aerosol heavy metal exposure, oral exposure can also contribute to lung damage and the development of lung fibrosis.

**Keywords:**

Heavy metals, cadmium, chromium, mercury, toxicity, collagen, lung disease



UNIVERSITEIT VAN PRETORIA  
UNIVERSITY OF PRETORIA  
YUNIBESITHI YA PRETORIA

**Declaration**

I, SVK Naidoo, hereby declare that this research is my own work and has not been presented by me for any degree at this or of any other University.

**Signed:**

A handwritten signature in black ink, appearing to read 'SVK Naidoo', written over a light grey rectangular background. Below the signature is a horizontal dashed line.

**Date:** 2019/05/02

Department of Anatomy, School of Medicine, Faculty of Health Sciences,

University of Pretoria

South Africa



UNIVERSITEIT VAN PRETORIA  
UNIVERSITY OF PRETORIA  
YUNIBESITHI YA PRETORIA

## Acknowledgements

Om Namo Narayan, I offer my obeisance to Acharya Shyam Ramanuj and Lord Sriman  
Narayana

*“If I have the belief that I can do it, I shall surely acquire the capacity to do it even if I may not have it  
at the beginning”*

By Mahatma Gandhi

- I humbly dedicate this MSc to my grandfather. I thank you for your confidence and belief in me. Thank you for the values and principles you had instilled within me, I hoped each day to carry each value as graceful as you. Your continuous encouragement and support is what drove me to new heights
- To my mother, I hope you are proud of me. Regardless of the distance, your support has been an unyielding factor which propelled me towards my goals. Your encouragement and determination helped me during sleepless nights.
- To my supervisor, Prof Oberholzer, I appreciate the support and guidance you have provided me, your endless patience and unlimited knowledge throughout this MSc. Your expertise and wisdom were invaluable towards the entire MSc.
- To my co-supervisor, Prof Bester, thank you for the valuable input and assistance during this MSc.
- To the staff of the Unit for Microscopy and Microanalysis, thank you for your constant assistance and advice during my data collection.
- To all my friends and colleagues, thank you for the strength, support and encouragement during this period.
- To my best friend and closets companion, Yatin Bholu Soni. Thank you for being my new-found strength and foundation to move forward. Thank you for believing in my abilities and the encouragement you have displayed since I met you. Life is float with you around and loads of fun.

- Lastly to, Acharya Shyam Ramanuj, thank you for introducing God back into my life. Thank you for teaching me the absolute truth and providing me with spiritual enlightenment towards self-realisation. This path is testing but well worth it.

## **Article published**

**Annexure 3:** Naidoo SVK, Bester MJ, Arbi S, Venter C, Dhanraj P and Oberholzer HM. 2019. Oral exposure to cadmium and mercury alone and in combination causes damage to the lung tissue of Sprague-Daley rats. *Environmental Toxicology and Pharmacology*. 69(2019): 86-94.

## Table of contents

<b>Summary</b>	<b>i</b>
<b>List of Abbreviations</b>	<b>ix</b>
<b>List of figures and tables</b>	<b>xi</b>
<b>Chapter 1: Introduction</b>	<b>1</b>
<b>Chapter 2: Literature review</b>	<b>3</b>
2.1 Heavy metals	3
2.1.1 Cadmium: Sources and associated lung disease	4
2.1.2 Chromium: Sources and associated disease	5
2.1.3 Mercury: Sources and associated disease	6
2.2 Heavy metal toxicokinetics	8
2.2.1 GSH and the anti-oxidant pathway as targets of metal toxicity	9
2.2.2 Role of metals in free radical formation	10
2.2.2.1 Superoxide generation in the mitochondria	10
2.2.2.2 Hydroxyl radical formation and the Fenton reaction	12
2.3 Cadmium and oxidative stress	13
2.4 Chromium and oxidative stress	13
2.5 Mercury and oxidative stress	14
2.6 Lungs as a target of heavy metal toxicity	15
2.6.1 Extracellular matrix proteins	18
2.7 Diseases of the airways and associated exposure to heavy metals	20
2.7.1 Asthma	20
2.8 Diseases affecting the alveoli	22
2.8.1 Emphysema	22
2.8.2 Pulmonary fibrosis	22
2.8.3 Lung cancer	22
2.9 Aim	23
<b>Chapter 3: Materials and methods</b>	<b>25</b>
3.1 Materials	25
3.2 Study design	26
3.3 Light microscopy sample preparation	27
3.4 Haematoxylin and eosin staining	28
3.5 Picro-Sirius Red staining	28
3.6 Verhoeff van Gieson stain	29
3.7 Transmission electron microscopy	30
3.8 Statistical considerations	31
3.9 Ethical considerations	32
<b>Chapter 4: Results</b>	<b>34</b>
4.1 General morphology of the alveoli and bronchiole tissue	33
4.2 PR Stain: Collagen distribution and deposition in alveoli and bronchiole tissue	37
4.3 Verhoeff van Gieson Stain: Elastin deposition and distribution in the alveoli and bronchioles	40
4.4 Transmission electron microscopy	45
<b>Chapter 5</b>	<b>53</b>

<b>Chapter 6: Conclusion</b>	<b>61</b>
6.1 Limitations to the study	63
6.2 Future perspectives	63
<b>CHAPTER 7: REFERENCES</b>	<b>64</b>
<b>Annexure 1</b>	<b>84</b>
<b>Annexure 2</b>	<b>85</b>
<b>Annexure 3</b>	<b>86</b>

## List of abbreviations, symbols and chemical formulae

### **A**

ABB	Air Blood Barrier
ADC	Adenocarcinomas
ADP	Adenosine diphosphate
Al	Aluminium
AP-1	Activator protein 1
As	Arsenic
ATP	Adenosine triphosphate
Au NP	Gold nanoparticles

### **B**

BAL	2,3-Dimercapto-1-propanol
BALT	Bronchus associated lymphoid tissue
BDH	British Drug House

### **C**

C <sub>6</sub> H <sub>3</sub> N <sub>3</sub> O <sub>7</sub>	Picric acid
CAT	Catalase
Cd	Cadmium as Cd(II)
Cd <sup>2+</sup>	Cadmium ions
Cl1-0	Carcinoma cell line
Co	Cobalt
CO <sub>2</sub>	Carbon dioxide
COPO	Chronic Obstructive Pulmonary Disease
Cr	Chromium as Cr(III)
Cu	Copper

### **D**

ddH <sub>2</sub> O	Double distilled water
DNA	Deoxyribonucleic acid

### **E**

ECM	Extracellular matrix
EMT	Epithelial to mesenchymal transition
EPA	Environmental Protective Agency
ER	Endoplasmic reticulum
EtOH	Ethanol

### **F**

FA	Formaldehyde
Fe	Iron

### **G**

GA	Glutaraldehyde
GIT	Gastrointestinal tract
GP <sub>x</sub>	Glutathione peroxidase
GR	Glutathione reductase
grsp	Glucose regulated proteins
GSH	Glutathione
GSSH	Glutathione disulphide

### **H**

H&E	Haematoxylin and eosin
Hg	Mercury as Hg(II)
hsp	Heat shock proteins
HIF-1 $\alpha$	Hypoxia-inducible factor 1-alpha
<b>I</b>	
IARC	International Agency for Research on Cancer
ICR	International cancer research
IHC	Immunohistochemistry
IPF	Idiopathic pulmonary fibrosis
<b>K</b>	
KAl(SO <sub>4</sub> ) <sub>2</sub> .12H <sub>2</sub> O	Potassium aluminium sulphate
KI	Potassium iodine
<b>L</b>	
LGC	Large cell cancer
LD50	Lethal dosage 50
LOP	Lipid peroxidation
LOX	Lysyl oxidase
<b>M</b>	
MAP	Mitogen-activated protein (MAP) kinase/AP-1
MDA	Malondialdehyde
MT	Metallothionein
MTF-1	Metal transcriptional factor-1
<b>N</b>	
Na <sub>2</sub> S <sub>2</sub> O <sub>3</sub> .5H <sub>2</sub> O	Sodium thiosulfate
NaCl	Sodium chloride
NADH	Nicotinamide adenine dinucleotide hydrogen
NADPH	Nicotinamide adenine dinucleotide phosphate
NaH <sub>2</sub> PO <sub>4</sub>	Sodium phosphate
NaIO <sub>3</sub>	Sodium iodate
NaOH	Sodium hydroxide
Ni	Nickel
NF- $\kappa$ B	Nuclear factor kappa B/Nuclear factor (erythroid
Nrf2	Nuclear factor (erythroid 2-related factor) - 2
<b>O</b>	
O-	Singlet oxygen
O <sub>2</sub>	Oxygen gas
O <sub>2</sub> <sup>-</sup>	Oxide ion
<b>P</b>	
p53	Phosphoprotein 53
Pb	Lead
ppm	Parts per million
PR	Picro-Sirius red
<b>R</b>	
RBC	Red blood cells
RER	Rough endoplasmic reticulum
RNA	Ribonucleic acid
ROS	Reactive oxygen species
<b>S</b>	
SCLC	Small cell cancer

SE	Stratification of the bronchiole epithelium
SM	Smooth muscle
SOD	Superoxide dismutase
SQC	Squamous cell carcinoma
<b>T</b>	
TBARS	Thiobarbituric acid reactive substances
TEM	Transmission electron microscopy
TGF- $\beta$	Transforming growth factor beta
<b>V</b>	
Vit C	Vitamin C
VvG	Verhoeff van Gieson
VEGF	vascular endothelial growth factor
<b>W</b>	
WHO	World Health Organisation
<b>Y</b>	
YAP1	Yes-associated protein 1
<b>Z</b>	
Zn	Zinc

### List of Figures

Number		Page
<b>Figure 2.1</b>	Flow diagram of the toxicokinetics of heavy metals	8
<b>Figure 2.2:</b>	Diagrammatic representation of the generation of ROS within the cell	11
<b>Figure 2.3:</b>	Fenton reactions showing the generation of radicals due to heavy metal toxicity	12
<b>Figure 2.4:</b>	Representation of the bronchial tree and the lungs.	15
<b>Figure 2.5:</b>	Representation of the bronchial tree and the lungs. The diagrammatic sketch annotates the various epithelium and cells found in the alveoli cell.	16
<b>Figure 3.1:</b>	Schematic representation of the objectives of this study	27
<b>Figure 4.1:</b>	The general structure of the alveoli.	34
<b>Figure 4.2:</b>	General structure of the bronchioles	36
<b>Figure 4.3:</b>	Polarised light micrographs of the alveoli from the exposed groups	38
<b>Figure 4.4:</b>	Polarised light micrographs of the bronchioles	39
<b>Figure 4.5:</b>	The structure of the alveoli and the air-blood barrier	41
<b>Figure 4.6:</b>	The structure of the bronchioles.	43
<b>Figure 4.7:</b>	Magnified images of parts of the bronchioles	44
<b>Figure 4.8:</b>	TEM micrographs of lung tissue from the control and single exposure groups, showing Type II pneumocytes	46
<b>Figure 4.9:</b>	TEM micrograph of lung tissue in the combination groups showing Type II pneumocytes	47
<b>Figure 4.10:</b>	TEM micrographs of the lung tissue of the control and exposed groups indicating fibrotic changes	49
<b>Figure 4.11:</b>	TEM micrographs showing mast cells within the lung tissue	51
<b>Figure 5.1:</b>	Flow diagram of the hypothesised method of action of Cd and Hg on lung tissue, contributing to lung pathologies associated with asthma, chronic bronchitis, COPD and pulmonary fibrosis.	59

## List of Tables

<b>Number</b>		<b>Page</b>
<b>Table 2.1:</b>	Collagen classification according to appearance, location in the body and main function.	19
<b>Table 2.2:</b>	Respiratory diseases of the lungs and associated histopathology	24
<b>Table 3.1:</b>	Animal groups, metal dosages and the number of rats per group	27
<b>Table 3.2:</b>	Animal groups, number of rats per group and sections/slides for each staining method	32
<b>Table 4.1:</b>	Summary of histological changes observed in light microscopy after the exposure of heavy metals alone and in combination	46
<b>Table 4.2:</b>	Summary of ultrastructural changes in lung tissue after heavy metals exposure	53

## **Chapter 1: Introduction**

Heavy metals are found throughout the earth's crust and are widely used in various industrial applications. Subsequently, the concentration of heavy metals in the environment has increased. As a result, human exposure has also increased with the main source of exposure being via anthropogenic sources such as transport, agriculture, mining and other related operations (Venter, 2014). The routes of absorption are through the skin, orally or via inhalation (Awofolu *et al.*, 2005). The degree of toxicity depends on the route of exposure, concentration of the heavy metal, the duration of the exposure as well as other factors such as age, sex and genetic factors. Exposure also does not only involve single metals but are often mixtures of metals and at different concentrations (Singh *et al.*, 2017; Omrane *et al.*, 2018). Chronic exposure to several of these metals may lead to histopathological changes to cellular, tissue and organ structure, leading to disease (Yuan *et al.*, 2014).

The mining industry is one of the biggest sectors in South Africa, particularly the mining of gold, diamonds, platinum and iron. During the process of extraction, different chemicals and metals are used. Any absorption of these metals throughout the extraction process or contact with by-waste containing heavy metals may compromise the health of an individual (Blaurock-Busch, 2010; Maskei *et al.*, 2017). Incorrect disposal of these metals may also pollute water sites through leaching into various reservoirs. The United States Environmental Protective Agency (EPA) in 2013 analysed municipal water supplies for the following heavy metals: aluminium (Al), copper (Cu), arsenic (As), mercury (Hg) and lead (Pb). Aluminium concentrations were found to exceed the limit of 1000 parts per billion (ppb), and the suggested source was due to industrial contamination of the municipal water supply. In addition, water levels of Pb in Phoenix, Arizona and Pleasanton, California exceeded the EPA limit for Pb 120.6 ppb (Adam, 2013). In South Africa elevated levels of heavy metals in the drinking water near the Witwatersrand region have been reported (Naicker *et al.*, 2003). The water in rivers, dams and soils have also become contaminated and these include mine villages of the East and West Rand (Durand, 2012). Another study assessed the health risk of heavy metals (As, Pb, Hg, Cd, Cr, Cobalt (Co), Nickel (Ni), Cu and Zinc (Zn)) leaching into soils from the Witswatersrand Gold Mining Basin. After further examination it was concluded that the carcinogenic risk values were significantly higher than the acceptable value being one individual in every 5882 adults and one child out of 2725 that may be affected. Carincross *et al.*, (2013) reported on the effect of extractive industries processes on the health of individuals. Symptoms and diseases included the development of asthma, cancer, stomach aches and chest pains. The overall concern is that there are multiple paths of

exposure that includes water, soil and occupational exposure which may result in several adverse health effects (Carincross *et al.*, 2013).

Metal absorption via the skin, inhalation and oral exposure leads to the disruption of normal cellular, tissue and organ structure and consequently physiological function is altered (Jaishankar *et al.*, 2014). Specific organs are targets of toxicity and these are typically associated with the routine of absorption [skin, lungs and gastrointestinal tract (GIT)], distribution (blood and vascular system), metabolism (liver and to a lesser degree other organs) and excretion (kidneys and parts of the GIT). In addition, to the disruption of normal cellular pathways, exposure can also lead to carcinogenesis and cancer (Ouyang *et al.*, 2012).

Inhalation of heavy metals often leads to respiratory disease (Jarup, 2003; Leem *et al.*, 2015; Mamuya *et al.*, 2007) which can affect the airways and other structures within the lungs (Athanasio, 2012; Perez-Campana *et al.*, 2013). The most common respiratory diseases are asthma, bronchitis, chronic cough, colds, chronic obstructive pulmonary disease (COPD), cystic fibrosis, idiopathic pulmonary fibrosis (IPF), influenza, lung cancer, pneumonia and tuberculosis. The World Health Organisation (WHO) in 2010 reported an increase in the prevalence of respiratory disease of 100 to 400 million from 2006 to 2010 (Mamuya *et al.*, 2007; Perez-Campana *et al.*, 2013). Respiratory symptoms that manifest early may be identified during routine health examinations. Additionally, routine examination can aid in facilitating the identification of risk or early onset disease (Ros and Slooff, 1987; Seidal *et al.*, 1993; Mamuya *et al.*, 2007). Several studies have identified a relationship between heavy metal exposure and the development of respiratory disease (Occupational Safety and Health Administration Cadmium, 2013; Terzano *et al.*, 2010; Lodovici and Bigagli, 2011). Usually exposure is not limited to a single metal, but a mixture of metals at different concentrations. Also, the duration of exposure is variable and can be acute, sub-acute or chronic. In South Africa, concentration levels of Hg, Cr and Cd are increased due to water source contamination (Venter *et al.*, 2017). Therefore, these metals have been chosen to be investigated for their possible adverse effects on the respiratory system of Sprague-Dawley rats.

The aim of this study was to determine the effects of oral exposure to sub-acute levels of Hg, Cr and Cd alone and in combinations on the respiratory system using a Sprague-Dawley rat animal model.

## **Chapter 2: Literature review**

### **2.1 Heavy metals**

Heavy metals are used in industrial, domestic, agriculture, medical and technological applications causing an increase in their distribution within the environment (Singh, 2007; Arruit *et al.*, 2010; Tchounwou *et al.*, 2012) and consequently human exposure has increased dramatically. Exposure is the result of anthropogenic activities, mining and smelting, industrial production and use, domestic and agricultural use (Blaurock-Busch, 2010). Additional exposure is via metal corrosion, atmospheric deposition and the leaking of heavy metals into soil and groundwater. Industrial sources include metal processing, burning of coal, petroleum combustion, nuclear power stations, wood preservations and paper processing plants (Begum and Huq, 2016). Toxicity depends on the dosage, route of exposure, chemical species, age, gender, genetics, and nutritional status of individuals (Tchounwou *et al.*, 2012).

As trace elements, heavy metals occur in low concentration ranges in environmental matrices. The bio-availability is dependent on physical properties such as temperature, phase association, absorption and chemical properties such as thermodynamics, equilibrium, complexation kinetics (movement of atoms that play a vital role in the determination of processing and properties of materials (Dillon *et al.*, 2007)), lipid solubility and water partition coefficient of these metals (Jaishankar *et al.*, 2013; Khelifi and Hamza-Chaffai, 2010). Some heavy metals are essential, and these include Cu and Cr, that play an important role in biochemical and physiological functions (Venter *et al.*, 2017). Insufficient levels in the human body can result in different diseases or syndromes, for example lack of Cr can lead to glucose intolerance. Cr is essential for fat, glucose and protein metabolism (Tchounwou *et al.*, 2012; Martin and Griswold, 2009). However, in excess, Cr may cause cellular and tissue damage leading to disease. There is a narrow range for Cr between beneficial and toxic concentrations (Flora *et al.*, 2008; Martin and Griswold, 2009; Tchounwou *et al.*, 2012).

Studies have shown that heavy metals in biological systems affect cell and organelle structure (Bartosz, 2008). These metal ions interact with cellular molecules such as deoxyribonucleic acid (DNA) and nuclear proteins causing DNA damage and conformational changes leading to cell cycle modulations, apoptosis or carcinogenesis (Flora *et al.*, 2008; Tchounwou *et al.*, 2012). Several studies found that the production of reactive oxygen species (ROS) and oxidative stress play a key role in the toxicity and carcinogenicity of metals such as Cd, Cr, Pb and Hg (Patra *et al.*, 2011; Tchounwou *et al.*, 2012; Sarkar *et al.*,

2013). These heavy metals have the highest degree of toxicity and consequently, exposure levels have been restricted to parts per million (ppm) (Occupational Safety and Health Administration, 1998). The systemic toxic effects of these metals include the induction of multi-organ damage at low levels of exposure. These metals have also been identified as probable human carcinogens based on epidemiological data and findings from experimental studies (Pesch *et al.*, 2000, IARC, 2002; Martin and Griswold, 2009; Tchounwou *et al.*, 2012). The following sections in this chapter will focus on the source, distribution and effects of Cd, Cr and Hg.

### **2.1.1 Cadmium: Sources and associated lung diseases**

Cadmium is distributed in the earth's crust at an average concentration of 0.1 mg/kg and accumulation increases environmental levels. Sedimentary rocks and marine phosphates contain about 15 mg/kg Cd (Szyzewski *et al.*, 2009). Cadmium has caused considerable environmental and occupational concerns as it is used in various industrial activities (Martin and Griswold, 2009). The main industrial application of Cd is as an alloy product and as a component of pigments and batteries. In recent years the use of Cd has increased, however, in developed countries there has been a decline in commercial use due to environmental concerns (Tchounwou *et al.*, 2012). Skin absorption is uncommon but Cd exposure via inhalation is common, particularly in cigarette smoke or ingested with foods such as liver, mushrooms, shellfish, mussels, cocoa powder and dried seaweed (Kazemipour *et al.*, 2008). Workers in primary metal industries are also at a risk of exposure, as Cd is a pulmonary irritant and fatal when chronically inhaled at levels exceeding WHO. An increased concentration of Cd in the human body is associated with a decrease in pulmonary function (Bertin and Averbeck, 2006; Nawrot *et al.*, 2010; Huff *et al.*, 2013). Rodent studies have shown that chronic inhalation of Cd causes pulmonary adenocarcinomas (Nawrot *et al.*, 2010; Tchounwou *et al.*, 2012).

The inhalation of Cd via different routes of exposure has been implicated in the development of emphysema, pulmonary fibrosis and lung carcinoma. It morphologically and metabolically resembles the type II pneumocytes that is the presumptive target site for Cd-induced lung carcinogenesis (Huff *et al.*, 2007). Acute respiratory toxicity from the exposure of Cd may result in shortness of breath, lung oedema and destruction of the mucous membranes leading to Cd-induced pneumonitis (Seidal *et al.*, 1993). The International Agency for Research on Cancer (IARC) has classified Cd as a potential carcinogenic agent within the respiratory system (Jin *et al.*, 2005; IARC, 2012; Odewumi *et al.*, 2016). Sorahan and Esmen, (2003) investigated the effect of cadmium hydroxide on factory workers in the progression of lung cancer. In these workers, the ROS levels were increased. However, the link to the mechanism of action of Cd in inducing carcinogenesis is not fully understood.

Several factors that may contribute to carcinogenesis include apoptotic resistance, inhibition of DNA repair mechanisms and upregulation of mitogenic signalling (Ilyasova, 2004; Godt *et al.*, 2006).

E-cadherin is vital for cell to cell adhesion and Cadmium ions ( $\text{Cd}^{2+}$ ) mediated change in adhesion may contribute to the development of various lung diseases. A study in rats showed that Cd exposure caused changes in the morphology of the epithelium and the characteristic features of apoptosis. The observed changes included cell shrinkage, detachment of the cell membrane, cytoplasmic and chromatin condensation and fragmentation of the nucleus (Bertin and Averbeck, 2006). Shrivastava and Sathyanesan (1988) showed that Cd inhalation resulted in pulmonary oedema and respiratory tract irritation. Additionally, chronic inhalation of Cd caused fibrosis and emphysematous changes in the lung tissue (Shrivastava and Sathyanesan, 1988).

### **2.1.2 Chromium: Sources and associated disease**

Chromium is a naturally occurring element present in the earth's crust and is more stable in the trivalent (Cr III) form which occurs in ores (Szyzewski *et al.*, 2009). Chromium VI is the second most stable form whereas Cr oxide (Cr O) does not occur naturally. Chromium III is an essential nutrient that plays a role in glucose, fat and protein metabolism by potentiating the action of insulin (Anderson, 2000). Chromium enters most elemental matrices such as air, water and soil, from a variety of natural and anthropogenic sources. The largest source of Cr is industrial production. Previous studies have shown it to have a devastating toxic and carcinogenic effect in humans (Mayans *et al.*, 1985; Langard, 1990) and it has been identified as a potent inducer of tumours in experimental animals (Costa and Klein, 2008). Chromium VI is reported to be more toxic than Cr III because it enters cells via the sulphate transport system and exists as an oxy-anion at physiological pH (Szyzewski *et al.*, 2009). Chromium VI levels exceeding the WHO limit for drinking water (50  $\mu\text{g/l}$ ) has been found in ground and surface water (Gibb *et al.*, 2000; WHO, 2011). Chromium VI is used in industrial welding, chromate plating, dyes and pigments, leather tanning, wood preservation and in anti-corrosive cooking systems and boilers (Sarin *et al.*, 2006). Chromium is present mostly in the oxidised state III and VI. Chromium III is inert; however, it may cause ulcers and respiratory tract injuries among industrial workers and has been shown to be teratogenic (Byrne *et al.*, 2008; Tchounwou *et al.*, 2012). Chromium VI in contrast to Cr III may target the liver and kidneys causing toxicity within these organs (Ahmad *et al.*, 2006; Tchounwou *et al.*, 2012). The manufacturing industries are the largest environmental sources of Cr VI, as Cr VI is released into the environment as a result of metal processing, leather tannery, chromate production, stainless steel welding as well as ferrochrome and chrome pigment production (Sarin *et al.*, 2000; Ricordel *et al.*, 2010). Metallurgical refractory and chemical industries

mainly release Cr VI into the air and water. However, occupational exposure has been a major concern because of the high risk of Cr VI-induced diseases (Occupational Safety and Health Administration; 2006). Non-occupational exposure occurs via ingestion of Cr III-coated food such as vitamins, water and via inhalation. The Cr III concentrations in food depend on the processing and packaging method. Workers in Cr VI related industries can be exposed to Cr VI concentrations twice as high as exposure levels of the general population (Tchounwou *et al.*, 2012). The lungs are the primary target for organ damage when Cr VI is inhaled (Gibb *et al.*, 2010). However, multi-organ toxicity, particularly organ failure in the kidneys, along with allergy and asthma as well as cancer of the respiratory tract in humans may also occur (Huvinen *et al.*, 2002; Caglieri *et al.*, 2005).

High doses of Cr VI have numerous health risks for individuals upon exposure and may cause irritation in the respiratory system via the conducting of the nasal cavity to the rest of the respiratory passages, resulting in breathing difficulties such a cough, fibrosis and asthma (Islam *et al.*, 2007). According to the IARC and a study by Quievryn *et al.*, (2002), Cr VI was confirmed to be carcinogenic within the nasal cavity and lungs. Exposure of Cr VI via inhalation may cause lung cancer. This is apparent in factories where welders are at the highest risk of exposure to Cr VI. The Occupational Safety and Health Administration established the safety limited of Cr VI as less than 5 µg of Cr VI per cubic meter of air and the US National Academy of Science established a daily intake of Cr at 50 – 200 µg in adults (Institute of Medicine, 2001; Occup Safety, 2006).

### **2.1.3 Mercury: Sources and associated disease**

Mercury is a transitional element and exists in three forms in nature: elemental, inorganic and organic, making it unique (Tchounwou *et al.*, 2012). Thus, environmental exposure is almost unavoidable due to these forms (Martin and Griswold, 2009). Elemental Hg is formed and released into the environment as Hg vapour at room temperature (Szczewski *et al.*, 2009). It is used in the electrical industry in switches, thermostats, batteries and in the industrial processes like soda production, nuclear reactions, and as an anti-fungal agent for wood processing (Sznoppek and Goonan, 2000; Pacyna *et al.*, 2010). The industrial usage of Hg declined between 1980 and 1994 as a result of federal bans placed on Hg (Wegner *et al.*, 2005; Pacyna *et al.*, 2010). Additionally, it is still being used as an additive in paint, pesticides and batteries (U.S. Environmental Protection Agency, 1999; Horowitz, *et al.*, 2014) and in South Africa, it is a by product of gold mining (Blaurock-Bush, 2010). Mercury is toxic to humans and causes severe alterations such as DNA mutation that activates oncogenesis, resulting in the transformation of normal cells into tumour cells (O'Connor, 2001; Onyido *et al.*, 2004).

Hg exposure includes all environmental pollutions, accidents like Hg spillage, food contamination, industrial and agriculture operations and occupational operations like coal burning power plants. The main source of exposure in humans was dental amalgam fillings and fish consumption (Tchounwou *et al.*, 2012). Mercury enters the water as a result of “gassing off” from the earth’s crust as well as via industrial pollution and is consequently absorbed by fish. Mercury consumed from fish includes methyl mercury (MeHg) that is highly lipid soluble and absorbed via the GIT (Arterburn *et al.*, 2006; Myers *et al.*, 2007). Methyl mercury is one of the most highly absorbed forms of Hg. Elemental Hg vapour is highly lipophilic and is absorbed through the lungs and the mucosa of the mouth and enters the blood, before rapidly passing through the cell membrane, entering the cytoplasm (Arterburn *et al.*, 2006). In the cytoplasm it is oxidised forming reactive  $Hg^{2+}$ . Most of the Hg absorbed is accumulated in the kidneys and excretion is very slow (Davidson *et al.*, 2004 and Tchounwou *et al.*, 2012).

Mercury is also used in agriculture as a fungicide that pollutes water and accumulates in sediment which is further metabolised by micro-organisms into stable MeHg which is extremely neurotoxic and teratogenic to humans (Clarkson and Magos, 2006; Grandejean *et al.*, 2010). Fungicides are absorbed in vegetables and fruits which increase human exposure (Tchounwou *et al.*, 2012). Mercury is transported by the blood and lymph and diffuses through tissues and is eliminated from the body after +/- 90 days after exposure. Previous studies indicated that both the inorganic and organic form of Hg accumulates over a period of time in the endocrine organs (e.g. pituitary gland and hypothalamus) (Martin and Griswold, 2009; Zhu *et al.*, 2014).

Exposure limits to Hg are 0.67 mg/ kg /day (Li *et al.*, 2008; Lui *et al.*, 2013). Diseases associated with Hg toxicity are not fully understood but the brain is one of the main target organs of toxicity although other organs are also affected to varying degrees (Jaishankar *et al.*, 2014). Mercury is known to disrupt cell membrane potential and interferes with calcium homeostasis. Since Hg binds to thiol groups readily, it can easily travel to the lungs through the circulatory system, causing bronchitis, asthma and short term respiratory problems (Jaishankar *et al.*, 2014). Mercury exposure can alter cellular structure as it damages tertiary and quaternary protein structures within the body (Ynalvez *et al.*, 2016). The integrity of the cellular structures is affected due to ROS formation (Mathew *et al.*, 2011). A study by Male *et al.*, 2013, has shown that Hg contamination as a result of gold mining in Indonesia had severe effects on the mine workers and local food sources. Mine workers displayed several health complications, including bronchitis and pulmonary fibrosis, whilst children displayed onset of Young’s syndrome, a condition specifically found in males, causing male infertility and damaging the airways in the lungs and inflammation of the sinuses (Clarkson and Magos, 2006; Male *et al.*, 2013),

## 2.2 Heavy metal toxicokinetics

Some heavy metals carry out essential biological functions; however, at higher concentrations it may exhibit oxidation or reduction properties (Jancic and Stosic, 2014) and can compete for protein binding sites displacing vital molecules or other essential metals. In addition, these metals can inhibit enzymatic activity and bind proteins and DNA (Yoshizuka *et al.*, 1991) and can also induce ROS formation via the Fenton reaction (Flora *et al.*, 2008).

Normally metals, within the safety limits are metabolised and excreted. However, over-exposure allows vascular recirculation and is transported to the liver (Damek-Poprawa and Sawicka-Kapusta, 2003). Once in the liver, the metals bind albumin inducing metallothioneins (MT) expression that is rich in cysteine residues and thiol groups (Jancic and Stosic, 2014). The albumin-heavy metal complex causes the expression of metal transcriptional factor-1 (MTF-1) (Figure 2.1).

Chronic exposure can lead to the disruption of cellular structural integrity via oxidative stress (Johri *et al.*, 2010), which reduces the concentration of metallothioneins and glutathione (GSH) levels ability, reducing the ability of a cell to respond to oxidative stress (Jancic and Stosic, 2014). The toxicokinetics of heavy metals are summarised in Figure 2.1.

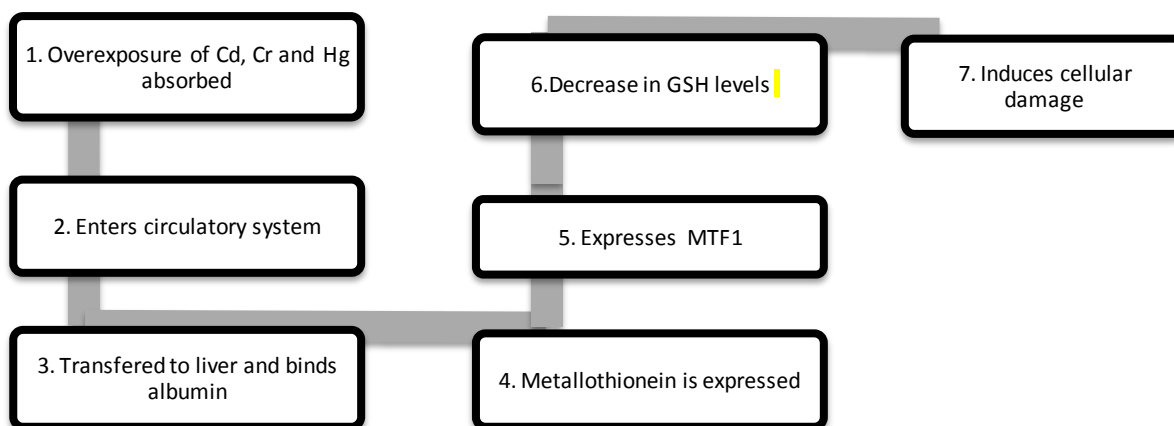


**Figure 2.1:** Flow diagram of the toxicokinetics of heavy metals (Adapted from Jancic and Stosic, 2014; Satarug *et al.*, 2003; Johri *et al.*, 2010).

### **2.2.1 GSH and the anti-oxidant pathway as targets of metal toxicity**

The role of GSH in the anti-oxidant pathway and redox cycle is to act as a catalyst. Glutathione acts as a regulator of intracellular redox homeostasis. GSH is either reduced (GSH) or oxidised [glutathione disulphide (GSSH)] and catalyses redox reactions by reversing the oxidation of the active thiols. In normal physiological conditions, GSH is reduced to the radical form within the nucleus, endoplasmic reticulum and mitochondria (Masella *et al.*, 2005). Another function of GSH is the involvement in defence mechanisms of the cell, in which the anti-oxidant binds to proteins and acts as a co-enzyme along several enzymes in the defence of the cell through the process of glutathionylation (Pompella *et al.*, 2003). The role of GSH is to act as scavenger, binding free radicals, or as a substrate that result in the detoxification of hydrogen peroxide ( $H_2O_2$ ). There are several tissue specific glutathione peroxidases (GPx) that also exhibits tissue specific functions including seleno-proteins that act against the oxidative reactions within the cell. The reaction occurs at the catalytic site of GPx as selenium is oxidised by  $H_2O_2$  forming a derivative selenic acid which is reduced via electron donor. GSH levels then decrease and GSSH levels (Masella *et al.*, 2005) shifting the cellular thiol redox status and activating oxidative response elements. The GSSH is secreted from the cell and degraded, in turn increasing the concentration of GSH. In a study by Suttorp *et al.*, (1986), the impairment of GSH pathways increased the possibility of endothelial cells within the lungs to be attacked by radicals. GSH in the lungs of patients with idio-pulmonary fibrosis (IPF) have reported reduced anti-oxidant status in the epithelial lining fluid and fibrotic foci observed (Suttorp *et al.*, 1986). Van Zandwijk *et al.*, (1995) investigated the crucial role that GSH plays in removing carcinogen species from cells thereby preventing the development of various cancers, particularly lung cancer (Traverso *et al.*, 2013).

Heavy metals such as Cd and Hg have electron sharing affinities resulting in covalent binding (Lloyd *et al.*, 1997) between the metals and sulfhydryl groups of proteins. Binding to GSH with the inhibition of antioxidant pathways, includes the effects on catalase, nicotinamide adenine dinucleotide phosphate (NADPH), GPx, glutathione reductase (GR), glutathione S-transferase and glutaminase 1 and 2 (Gorrine *et al.*, 2013). Depletion of GSH results in inefficient scavenging of the radical, increased levels of  $H_2O_2$  and ROS leading to increase intracellular levels of free radicals which is often associated with damage to cellular macromolecules leading to cell dysfunction (Stainslawski *et al.*, 2003; Townsend *et al.*, 2003). Gorrine *et al.*, 2013, showed in an *in vitro* based study that both Cd and Cr bind to GSH and inhibited antioxidant enzyme activity.

## **2.2.2 Role of metals in free radical formation**

Free radicals are small, diffusible molecules (Jones, 2008) containing one or more unpaired electrons in their atomic or molecular orbits (Halliwell and Gutteridge, 2007; Valk *et al.*, 2007) that are highly reactive. In mammals, free radical species are derived from oxygen ( $O_2$ ) and this is important since molecular oxygen (dioxygen) is a radical due to its electron configuration. Free radicals are involved in chain reactions such as an initiation of single free radical generation damage to multiple molecules (Figure 2.2) (Bartosz, 2010). These reactions are also highly selective and dependent on the radical concentration; delocalisation of the electrons and the bonds in the molecule with which the radical interacts (Brand *et al.*, 2004). Radicals that form and are relevant in metal toxicity are superoxide, hydroxyl and peroxy radicals and are described in greater detail below.

### **2.2.2.1 Superoxide generation in the mitochondria**

Addition of an electron to dioxygen forms Oxide ion ( $O_2^-$ ) which is an oxygenated radical that is produced by a number of enzymes through an auto-oxidation reaction and by non-enzymatic electron transfer reducing molecular oxygen ( $O_2$ ) (Cheresh *et al.*, 2013). Superoxide anion radicals are produced through a metabolic process or  $O_2$  activation which is considered the primary ROS. The primary ROS produced can further interact with molecules generating secondary ROS either through enzymes or metal catalysed processes (Valko *et al.*, 2005). Lung tissue is protected by antioxidant enzymes such as Superoxide dismutase (SOD) that converts  $O_2^-$  to  $H_2O_2$ . However, depletion of SOD results in the induction of lung disease through inflammation, causing structural damage (Kinnula and Crapo, 2003; Phaniendra, *et al.*, 2015) and is a major factor that influences disease progression within the lungs.

In the mitochondria, the mitochondrial electron transport chain supplies adenosine triphosphate (ATP), required for cellular energy production (Balaban *et al.*, 2005; Murphy, 2009) and mitochondrial superoxide is generated during electron transduction which if in excess, is associated with the pathophysiology of numerous diseases (Bartosz, 2010).

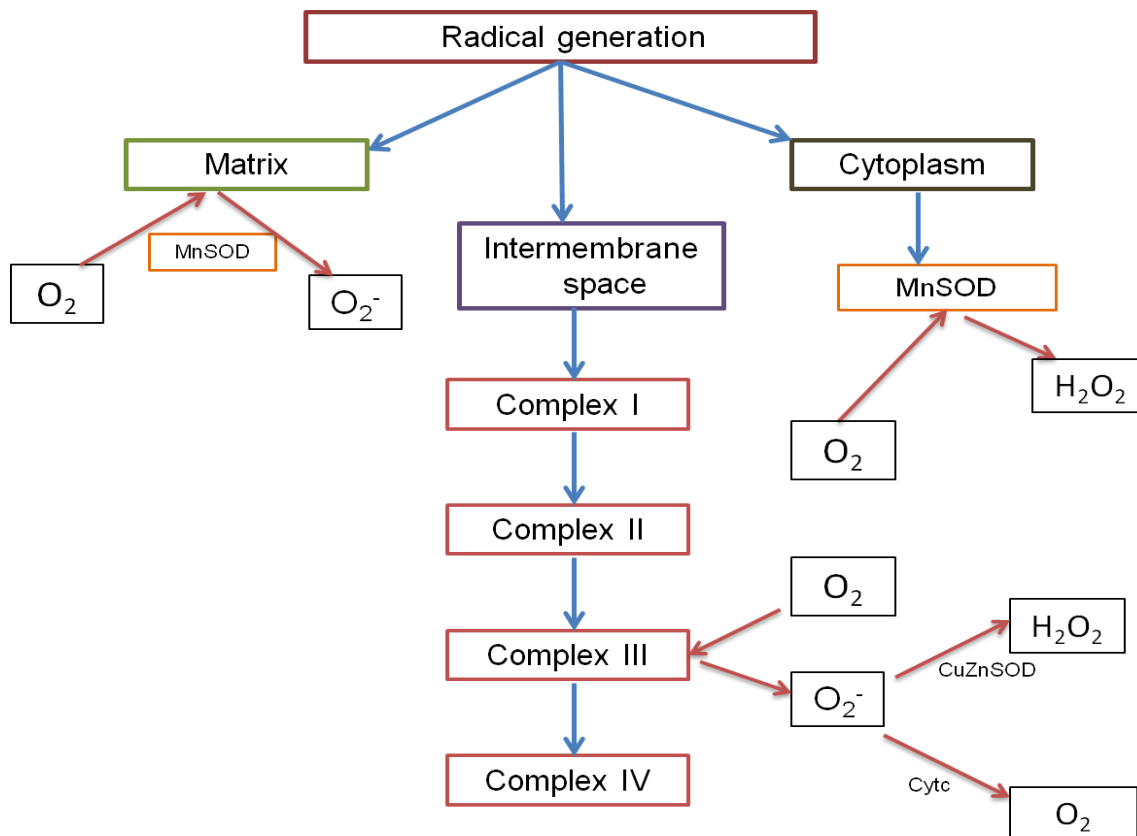


**Figure 2.2:** Diagrammatic representation of cellular ROS generation in the mitochondria (Adapted from Valko, 2005; Jomova and Valko, 2011).

Excessive mitochondrial derived ROS has been observed in the mediation of pulmonary fibrosis (Jomova and Valko, 2011). In the lungs, mitochondrial generation of  $H_2O_2$  by alveolar macrophages is caused by the exposure to lung irritants like asbestosis (Fubini and Hubbard, 2002). Reactive oxygen species formation by the mitochondria is necessary for normal cellular functioning and plays a role in maintaining low levels of free radicals through the anti-oxidant defence system; however, dysfunction within the mitochondria may lead to excessive ROS production. Superoxide is converted to  $H_2O_2$  by metallo-enzymes called SOD (Fridovich, 1995). Superoxide radicals ( $O_2^-$ ) may be reduced or can react with  $H_2O_2$  producing hydroxide ( $OH^-$ ). The membrane of the mitochondria contains SOD specifically with manganese (Mn) in its active site to eliminate the  $O_2^-$  that forms within its membrane. The formation of radicals is controlled by three mechanisms. Firstly, the compartment contains an isozyme (SOD containing Cu, Zn and Mn) also found within cells (Okado-Matsumoto and Fridovich, 2001). The intermembrane spaces that contain cytochrome c (Figure 2.2) is the second defence that has the ability to reduce  $O_2^-$  (Butler *et al.*, 1975) and can also regenerate  $O_2$  at the same time. Cytochrome c may also be reduced and transfer electrons to terminal oxidases (Figure 2.2). Due to mitochondrial dysfunction in the electron

transport chain, the mitochondria are uncoupled from the proton pump and the radicals ( $\text{H}_2\text{O}_2$  and  $\text{O}_2^-$ ) are released from the mitochondria into the cytosol.

### **2.2.2.2 Hydroxyl radical formation and the Fenton reaction**

The OH radical is a neutral form of the hydroxide ion. These radicals are highly reactive and dangerous with a short *in vivo* half-life of approximately  $10^{-9}$  seconds (Cheresh *et al.*, 2013). A characteristic of OH is that when it reacts with another molecule it forms other radical species. Hydroxyl radical formation is determined by the availability and location of metal ions that acts as a catalyst of the Fenton reaction (Figure 2.3). The Fenton reaction is an  $\text{O}_2$  transfer process involving the conversion of metals to yield free radicals through oxidation. Heavy metals act as catalysts of the Fenton reaction generating hydroxyl radicals via the reaction as shown in Figure 2.3. The radicals that are generated are superoxide anion radical ( $\text{O}_2^-$ ), hydrogen peroxide ( $\text{H}_2\text{O}_2$ ) and hydroxyl radical (OH).

- $M^{(n)} + \text{O}_2^- \rightarrow M^{(n-1)} + \text{O}_2$
- $2\text{O}_2^- + 2\text{H}^+ \rightarrow \text{H}_2\text{O}_2 + \text{O}_2$
- $M^{(n-1)} + \text{H}_2\text{O}_2 \rightarrow M^{(n)} + \text{HO} + \text{OH}^-$

**Figure 2.3:** Fenton reactions showing the generation of radicals due to heavy metal toxicity (Prousek, 2007).

Enhanced production of OH may cause the hyper proliferation of liver and lung tissue and injury through inflammation (Reuter *et al.*, 2010) by increasing the levels of the inflammatory factors and increasing cellular synthesis, leading to collagen fibrosis initiating acute lung disease (Todd *et al.*, 2012; Kularmi *et al.*, 2016).

## **2.3 Cadmium and oxidative stress**

Cadmium's routes of exposure include inhalation via the lungs and absorption via the intestines or the skin. The heavy metal binds to MT forming a Cd-metallothionein complex that is distributed to different organs and tissues and then reabsorbed within the kidney tubuli (Ohta and Cherian, 1991). Cadmium is mainly deposited in the kidneys, liver, pancreas and lungs (Seidal *et al.*, 1993). Cadmium itself is not capable of forming free radicals directly but indirectly it produces free radicals by using  $\text{O}_2^-$ , OH and nitric oxide (Waisberg *et al.*, 2003). The indirect formation of free radicals involves iron (Fe) as Cd

replaces Fe and Cu in different cytoplasmic and membrane proteins, the levels of unbound free or poorly chelated Fe or Cu increase and these metals can now act as catalysts of the Fenton reaction producing ROS (Figure 2.3). This mechanism is poorly understood but Cd is known to participate intracellularly, causing free radicals to induce damage mainly to the lungs, kidneys, bones and central nervous system (Jarup *et al.*, 1998; Jin *et al.*, 2002). The effect of Cd exposure via drinking water through oxidative stress shows a significant increase in lipoperoxides and malondialdehyde (MDA) and a decrease in SOD activity and GP<sub>x</sub> (Novelli *et al.*, 2000). Additionally, Cd is a potent human carcinogen in the lungs, prostate gland and the GIT (Zalups, 2003). Smoking synergistically increases the carcinogenic effects of Cd (Elinder *et al.*, 1976; Novelli *et al.*, 2000; Zalup, 2003). Uys, 2016 reported that Cd binds GSH and consequently depletes GSH and initiation of free radicals production occurs.

#### **2.4 Chromium and oxidative stress**

Chromium III is an essential dietary mineral that is required to potentiate insulin for glucose metabolism (Codd *et al.*, 2001). Cr III enters the cells via pinocytosis (Bagchi and *et al.*, 2001). Chromium VI is insoluble in water and is considered an occupational carcinogen at high doses compared to Cr III (Ding and Shi, 2002). Chromium VI is highly toxic and lung carcinogenicity requires chronic exposure over the daily limits of Cr (Wise *et al.*, 2002; Eastmond *et al.*, 2008; Beaver *et al.*, 2009). Oral administration of Cr VI results in the reduction of secretion of saliva from the salivary gland and gastric juices within the stomach (Sedman *et al.*, 2006). Chromium VI is absorbed via the intestines and reduced in the blood following a further reduction by the liver. In the lungs, Cr VI is reduced by GSH thus increasing the risk of lung cancer when Cr VI doses overwhelm the cellular defence mechanisms (Bagchi *et al.*, 2001). In red blood cells (RBC), the detoxification of Cr VI, reduces the oxidative stress and forms Cr-protein complexes. These complexes with different ligands do not leave the cells and move back into the cytoplasm. The rate of uptake of Cr VI is synchronised with the reduction of Cr VI to Cr III and the reduction process is through chelation that is not entirely safe, since free radicals are produced during this reaction (Cheung and Gu, 2007).

Ascorbate is most effective in the reduction of Cr VI in the cell but plays a dual role in Cr VI toxicity. Firstly it acts as a protective anti-oxidant outside and then as a pro-oxidative agent inside the cells (Stearns and Wetterhahn, 1997). The reduction of Cr VI with the use of ascorbate within the cells generates high levels of DNA adducts that lead to an increase in DNA mutations. Cr VI can be reduced by non-enzymatic reactions with cysteine and GSH;

however, for target tissue toxicity like the lungs, ascorbate is required and is the primary reducer (Liu *et al.*, 2007).

In the mitochondria, nicotinamide adenine dinucleotide phosphate (NADPH) reduces Cr VI and forms Cr III that is a stable state and binds more effectively to DNA than Cr VI (Blasiak *et al.*, 1999). Intermediate oxidation states of Cr also play a role in genotoxicity and carcinogenicity. Chromium species have the ability to produce ROS from both H<sub>2</sub>O<sub>2</sub> and lipid peroxide (Stohs *et al.*, 2001). The reduction of Cr VI produces numerous ROS including free radicals like OH<sup>·</sup>, singlet oxygen (O<sup>·</sup>) and O<sub>2</sub><sup>·-</sup>. These radicals are able to interact with DNA bases. Several types of DNA damage occur due to ROS generated as a result of exposure to Cr VI such as single strand breaks, DNA to DNA inter-strand crosslinks, DNA protein crosslinks, Cr-DNA adducts, oxidative nucleotide and chromosomal aberrations (Valko *et al.*, 2004). Pathways that are activated by Cr are the mitogen-activated protein (MAP) kinase signal transduction, nuclear factor (erythroid 2-related factor) (NF-κβ) and p53 (a gene that codes for protein that regulates cell cycle resulting in tumour suppression) which contribute the regulation of the cellular process including apoptosis (Bagchi *et al.*, 2001). The Cr VI-induced oxidative stress also triggers hypoxia signalling pathways that increases hypoxia-inducible factor 1-alpha (HIF-1α) and vascular endothelial growth factor (VEGF) protein levels (Shi and Dalal, 1990).

## **2.5 Mercury and oxidative stress**

Numerous *in vivo* and *in vitro* studies showed that the exposure to inorganic and organic Hg induces oxidative stress (Valko *et al.*, 2005). A high affinity between mercuric ions and thiols causes binding and depletion of intracellular thiols, particularly GSH, directly or indirectly, thereby inducing oxidative stress in tissue (Ercal *et al.*, 2001). Lund *et al.*, (1991) administered Hg as Hg (II) in rats, and found that Hg (II) caused the depletion of GSH and an increased H<sub>2</sub>O<sub>2</sub> formation and lipid peroxidation. Mercury (II) increases H<sub>2</sub>O<sub>2</sub> formation approximately 4-fold at the ubiquinone cytochrome b region and 2-fold at the nicotinamide adenine dinucleotide (NADH) dehydrogenase region, resulting in the depletion of mitochondrial GSH and increased H<sub>2</sub>O<sub>2</sub> which impairs the electron transport chains. The binding of a single Hg ion causes irreversible excretion of two GSH molecules. The release of Hg ions from GSH and cysteine complexes results in increased levels of free Hg ions which disturbs GSH homeostasis leading to cellular damage (Dalton *et al.*, 2004; Ortega-Villasante *et al.*, 2007). An increase in H<sub>2</sub>O<sub>2</sub> formation due to the increase in Hg (II) may lead to oxidative tissue damage such as lipid peroxide damage; making organs susceptible to Hg toxicity (Valavanidis *et al.*, 2006; Jomova and Valko, 2011). The effects of mercuric chloride on lipid peroxidation (LOP), GR, GP<sub>x</sub>, SOD and GSH levels in different organs of the mice were evaluated by Bas and Kalender, (2016). The results indicated that 28 day oral Hg

exposure enhanced lipid peroxidation in testes evaluated compared to Pb exposure. While MDA and antioxidant enzyme levels of the exposed groups were lower than the control, Hg was reported to induce toxicity within multiple organs and also causes histopathological changes in these organs.

## 2.6 Lungs as a target of heavy metal toxicity

The lungs form part of the respiratory system and the principle function of the lungs is to exchange O<sub>2</sub> and carbon dioxide (CO<sub>2</sub>) between inspired air and the blood (Meshcer, 2010). The lungs contain the respiratory bronchioles, alveolar ducts and alveoli. (Figure 2.4).

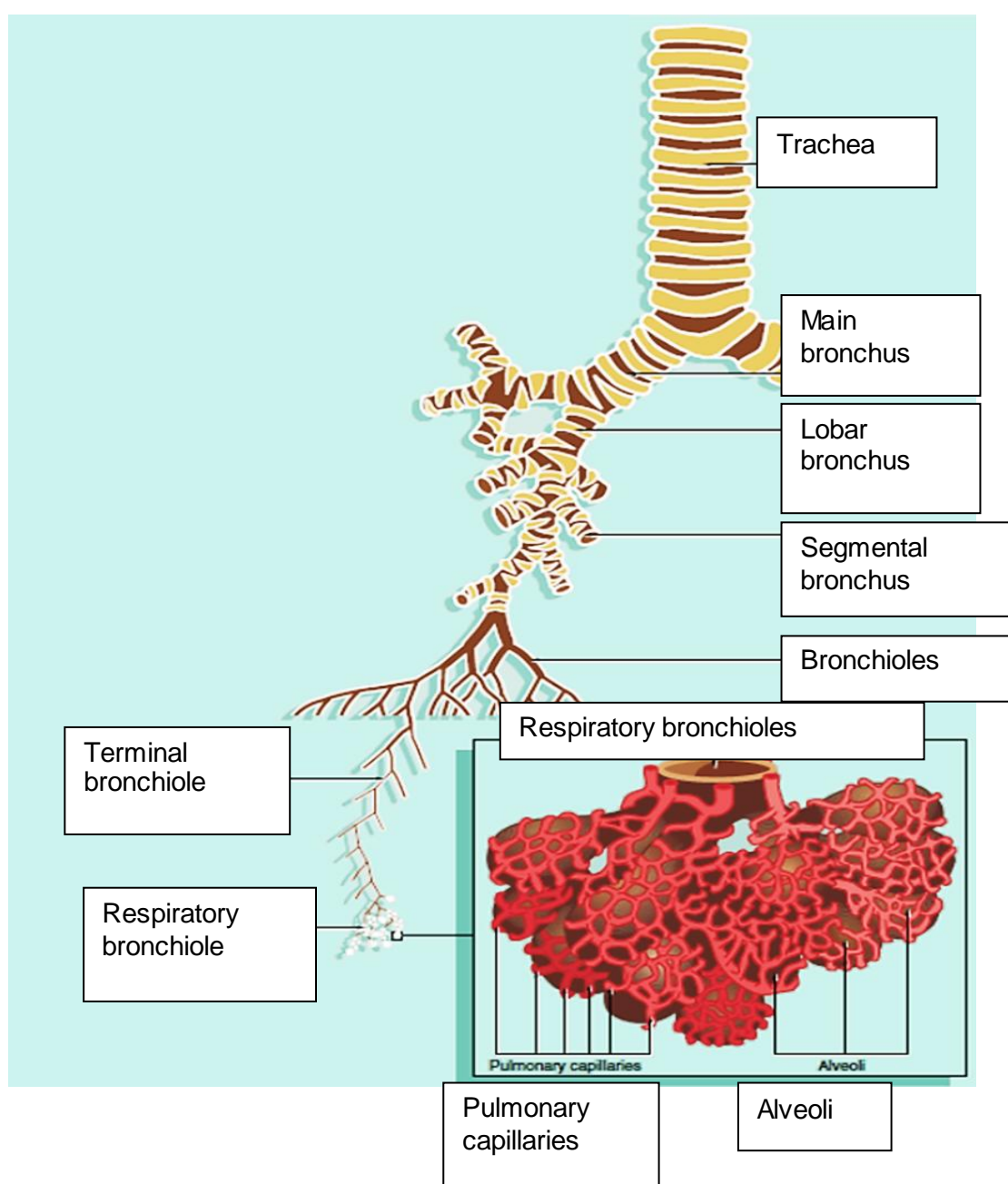


**Figure 2.4:** Representation of the bronchial tree of the lungs (Adapted from Gartner *et al.*, 2005).

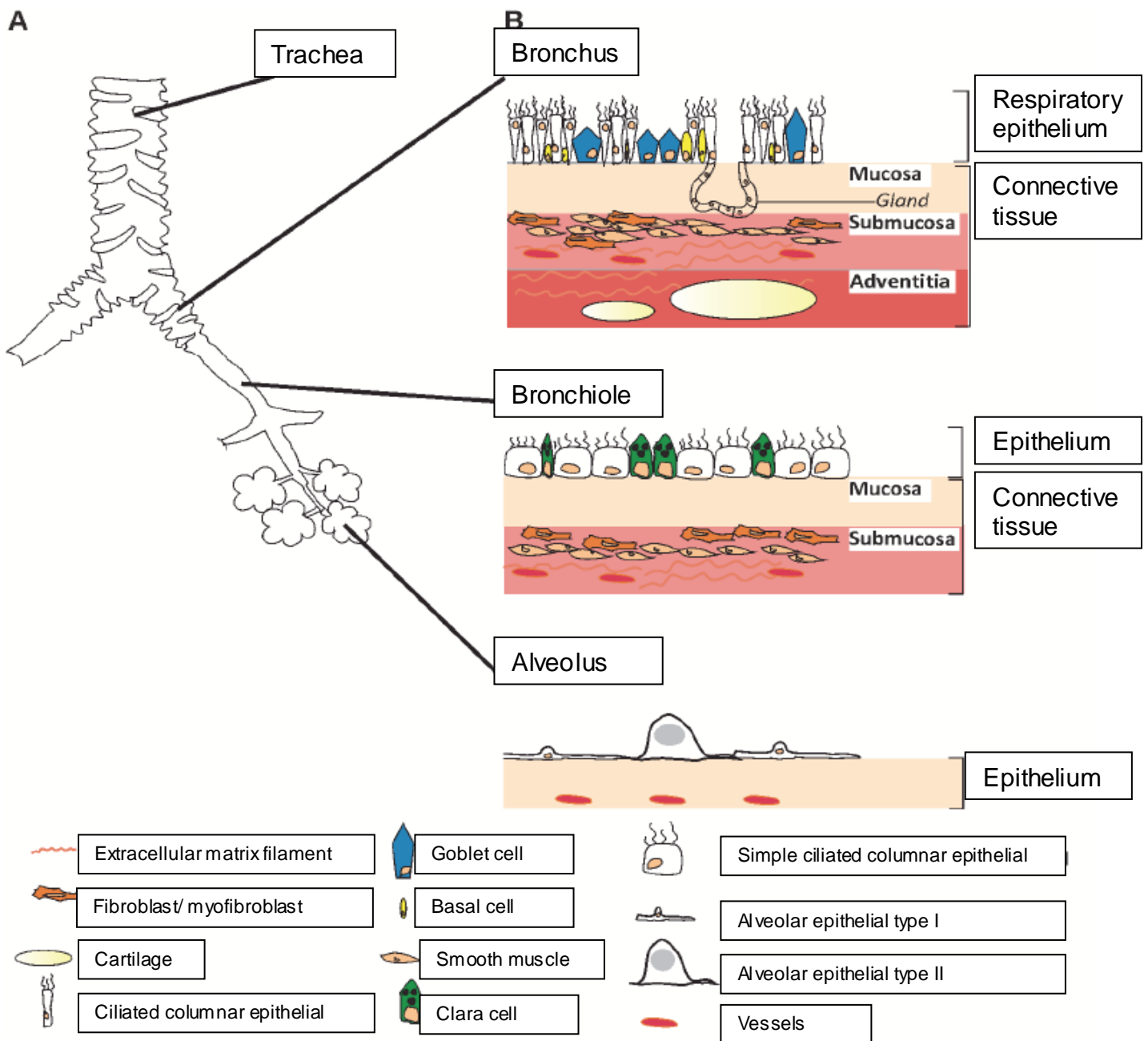


**Figure 2.5:** Representation of the bronchial tree and the lungs and cell types present in the epithelium and alveoli (Volckaert and De Langhe, 2014).

The bronchioles (Figure 2.5) are the intralobular airways, are 1 mm or less in diameter, consisting of a mucosal layer that lacks serous glands and cartilage (Meshcer, 2010). Ciliated columnar epithelium lines the bronchioli (Stevens and Lowe, 2005) and clara cells that are present in the epithelium, are mitotically active cells that secrete similar components to pulmonary surfactant that aids in multiple defensive functions (Meshcer, 2010) (Figure 2.5). These cells are most numerous in the terminal bronchioles, the smallest bronchioles

that are solely involved in air conduction. The terminal bronchiole then leads to the respiratory bronchioles where the epithelium changes to cuboidal, ciliated epithelium. The respiratory bronchioles then merge with the alveolar ducts containing the alveoli (Stevens and Lowe, 2005).

Alveoli are sac-like structures with a diameter of 200  $\mu\text{m}$  (Stevens and Lowe, 2005) and appear as small pockets that are open on one side. The inter-alveolar septum lies between two neighbouring alveoli (Gartner *et al.*, 2005) and consists of a connective tissue extra cellular matrix (ECM) containing elastic and collagen fibres with a large capillary network and are lined by highly attenuated simple squamous epithelium containing type I and type II alveolar cells (Gartner *et al.*, 2005; Meshcer, 2010). The structure of the alveolar wall is specialised to enhance diffusion between the internal and external environment (Meshcer, 2010).

Type I alveolar cells, also called alveolar pneumocytes or squamous alveolar cells are thin cells which cover approximately 95% of the alveolar surface and are responsible for gas exchange (Meshcer, 2010). These cells have a thin cytoplasm and form tight junctions with adjacent cells (Gartner *et al.*, 2005) (Figure 2.5). Type II alveolar cells, also known as type II pneumocytes or granular pneumocytes, are cuboidal cells that occur in groups of two or three along the alveolar surface. Type II alveolar cells rest on the basement membrane and are part of the epithelium (Gartner *et al.*, 2005). These cells have microvilli along their peripheral borders and form tight junctions with adjacent cells. Pulmonary surfactant is synthesised and stored in the lamellar bodies of the cytoplasm. Surfactant consists of phospholipids and four different types of proteins forming a tubular myelin network that spreads over the alveolar surface reducing tension in the alveoli (Gartner *et al.*, 2005).

Airway reflex responses such as coughing and sneezing are vital for the protection of the airway from chemicals and biological contaminants (Gu and Lin, 2010). An increase in type II collagen production is common in many diseases that lead to respiratory distress and is also associated with lung fibrosis. Respiratory distress is a life threatening disorder of the lungs caused by an increase filtration through the pulmonary capillaries (Meshcer, 2010).

### **2.6.1 Extracellular matrix proteins**

Fibrous components of connective tissue are secreted by fibroblasts and consist of collagen, reticular and elastin fibres. These fibres are distributed irregularly within the different types of connective tissue (Yurchenco *et al.*, 2003; Humphrey *et al.*, 2014).

Collagens are differentiated by their molecular composition, morphological characteristics, functions and pathologies and are grouped according to their structures and interacting subunits (Yurchenco *et al.*, 2003). Table 2.1 lists the different types of collagen, microscopic features and techniques used to identify the different types of collagen fibres, location and specific functions.

**Table 2.1: Collagen classification according to appearance, location in the body and main function. (Yurchenco *et al.*, 2003; Mesher, 2010).**

<u>Type</u>	<u>Optical features</u>	<u>Major location</u>	<u>Main function</u>
<b><u>Fibril forming collagen</u></b>			
I	Thick, highly PR* birefringement	Skin, tendon, bone and dentin	Resistance to tension
II	Loose aggregates of fibrils, PR birefringement	Cartilage and vitreous body	Resistance to pressure
III	Thin, weak PR birefringement and silver binding fibres	Skin, muscle, blood vessels and frequently together with type 1	Structural maintenance expansible organs
V	Frequently forms fibres with type I	Foetal tissue, skin, bones, placenta and most interstitial tissues	Resistance to tension
XI	Small fibres	Cartilage	Resistance to pressure
<b><u>Sheet forming collagen</u></b>			
IV	Detected by IHC*	All basal and external laminae	Support of epithelial cells: filtration
VII	Detected by IHC	Epithelial basement membranes	Anchors basal laminae to underlying reticular laminae
IX	Detected by IHC	Cartilage and vitreous body	Binds different proteoglycans associated with type II
XII	Detected by IHC	Placenta, skin and tendon	Interacts with type I collagen
XIV	Detected by IHC	Placenta and bone	Binds type I collagen fibrils with type V and XII and strengthen fibre

\*Picrosirius Red \*\*Immunohistochemistry

In collagen producing cells the initial procollagen  $\alpha$ -chains are formed within the rough endoplasmic reticulum (RER). The collagen family genes are large and many different chains of collagen have been identified, differing in length and in sequence. Within the endoplasmic reticulum (ER), three  $\alpha$  chains are selected, aligned and stabilised by disulphide bonds at their carboxyl terminal followed by folding as a triple helix resulting in a definite feature of collagen. The helix is exocytosed and cleaved to a rod like procollagen molecule that forms the basic subunits in which the fibres are assembled. The subunits are homotrimeric and all the chains identical or subunits are heterotrimeric with two or three chains have a different sequence. Different combinations of procollagen  $\alpha$  chains produce various types of collagen with different structures and function properties (Humphrey *et al.*, 2014).

Reticular fibres within the connective tissue of various organs consist mainly of collagen type III forming an extensive network of thin glycosylated fibres. The fibres are produced by

fibroblasts occurring within the reticular lamina of the basement membrane and surround adipocytes, smooth muscle, nerve fibres and small blood vessels (Humphrey *et al.*, 2014).

Elastin fibres are thinner in contrast to type I collagen, forming thin networks interspersed with collagen bundles in different organs subjected to bending and stretching. The fibres have a similar property to that of rubber which allows tissue to stretch, expand and return to original shape. Elastin fibres are a combination of fibrillin microfibrils that are embedded in a large mass of cross linked elastin. They are produced from ECM and are synthesis and secreted by fibroblast cells. Single genes are also involved in the production of mature elastin fibres that are produced by mature elastin protein (Rossetti *et al.*, 2011). Lysyl oxidase (LOX) is an enzyme that is involved in the production of elastin by inducing the cross-linking of elastin monomers of tropoelastin that were deposited and aligned by microfibrils (Kielty *et al.*, 2002; Kozel *et al.*, 2006). These components are secreted by fibroblasts and produce elastin in a step wise manner (Yurchenco *et al.*, 2003; Humphrey *et al.*, 2014).

Inhalation of heavy metals causes damage to the epithelium and the connective tissue of the lungs leading to diseases such as asthma, chronic obstructive pulmonary disease, emphysema, pulmonary fibrosis and cancer of the lungs. These will be discussed in the section to follow.

## **2.7 Diseases of the airways and associated exposure to heavy metals**

### **2.7.1 Asthma**

Asthma is a chronic inflammatory disease of the airways that is characterised by airway hyper-responsiveness to different stimuli, airflow obstruction and remodelling (Karaman *et al.*, 2011). South African population have estimated that 7.7% have asthma while industrialised countries have reported to have a prevalence of asthma ranging between 4% and 23%. The morbidity and mortality of this disease has increased over the years according to a study by Karaman *et al.*, (2011) with 1.5% of South Africans that die annually from asthma. The histopathology of the disease is associated with bronchial epithelial shedding, mucosal oedema and mucous plugging. This disease is associated with continuous inflammation within the airways and irreversible structural changes to the bronchial wall. Airway remodelling plays a prominent role in severe asthma. Chronic asthma includes sustained tissue eosinophilia, epithelial damage, sub-epithelial basement membrane thickness, sub-epithelial fibrosis and airway smooth muscle hypertrophy. Additionally, hyperplasia is observed due to the narrowing of the luminal airway with localisation of leukocytes such as

monocytes and mast cells infiltrating the surrounding tissue. Also, typically observed with chronic asthma is an increase in the endothelium of the capillaries, hyperplasia and shedding of the basal cells with squamous metaplasia of the epithelium and an increase in matrix deposition (Hamid, 2003). Exposure to metals Hg, Cd and Pb is associated with contamination of the physical environment increasing the risk of the development of asthma in children especially (Wu *et al.*, 2018).

## **2.7.2 Chronic obstructive pulmonary disease**

Chronic obstructive pulmonary disease (COPD) is a serious medical condition and is increasing worldwide (Murray and Lopez, 1996; American Thoracic Society; 2004). Additionally, 48 towns and major cities within South African have shown to have a 19% prevalence of COPD. The key cause is inflammation within the airways. Oxidative stress and defence system imbalance of the host may be the leading cause of COPD (Ichinose *et al.*, 2000). Examination of the histology of COPD, whereby the patients that smoked revealed a prominent increase in macrophage infiltration as a result of the COPD (Tetley, 2002). The disease is associated with the destruction of lung parenchyma with the inability to repair itself and resulting in emphysema with small structural changes to the small bronchi and the membranous bronchiole (Jeffery, 2001). Histopathology of COPD is characteristics by epithelial metaplasia and inflammation within the bronchial submucosa. The sub-epithelial basement membrane appears thicker with significant increase in fibroblasts. Additionally observed was the increase of mucosal thickness, with hypo-secretion from the tracheal bronchial submucosal glands along with mucous hyperplasia. Also noticeably is an increase of the size of capillary blood vessels within surrounding oedematous tissue (Jeffery, 1992). Inhalation of Cd and coal mine dust has been associated with the development of COPD in 3400 British mine workers (Cullinan, 2012).

## **2.8 Diseases affecting the alveoli**

### **2.8.1 Emphysema**

Emphysema is defined by the abnormal and permanent dilation of the distal air spaces of the terminal bronchioles (Hogg and Senior, 2002). Additionally, destructive alveolar walls and fibrosis are observed later resulting in respiratory insufficiency (Snider *et al.*, 1985; Suki *et al.*, 2003). The primary risk factors of emphysema are exposure to cigarette smoking (containing Cd) (Meshcer, 2010), environmental irritants and pollutants (Marcos *et al.*, 2015). The mechanism of the progression and development of emphysema is through anti-protease, oxidative stress and matrix remodelling (Di Petta, 2014). The disease progression itself is poorly understood and may be related to abnormal repair of the tissue after

inflammation has occurred. Met *et al.*, 2015, suggested that the mechanical forces and stress such as expiration is capable of physically rupturing the entire alveolar wall after initial damage. The remodelling of tissue following an injury results in the re-arrangement of the collagen fibres. This leads to stiffing of the fibrotic fibres due to collagen deposition within the lung tissue, thereby reducing the mechanical force within the alveolar wall resulting in rupture or reduced lung volume. Collagen is the load-bearing element along with elastin (Suki *et al.*, 2008). Under normal physiological conditions i.e. during breathing, collagen and elastin protects the lung from rupturing by facilitating lung expansion during inspiration. When heavy metals are absorbed, binding to MT occurs and it then leads to a degradation of collagen, replacing the degraded collagen with new collagen fibres by active remodelling. The newly remodelled fibres have a lower force and are mechanically defective (Suki *et al.*, 2003). The overall histopathological appearance of emphysema includes congested capillaries in the alveolar walls; alveolar permeability leads to disruption of the air blood barrier and the dilation of alveolar ducts and bronchioles containing fluid. Also, there is an increase in glandular material within the alveolar space and large air spaces are observed within the lungs which contain fluid. Lastly, macrophage- associated inflammation is also found in the lungs (Suki *et al.*, 2003). Exposure to metals such as Co, Cr and Ni have been associated with the development of emphysema and reduced lung function of workers in the metallic industry (Hamzah *et al.*, 2016).

### **2.8.2 Pulmonary fibrosis**

Idiopathic pulmonary fibrosis (IPF) is a progressive, fibrotic, interstitial lung disease of unknown aetiology (Mora *et al.*, 2006). The pathogenesis is partly understood (Selman and Pardo; 2003) but seems to be the result of abnormal wound repair and remodelling following epithelial damage (King *et al.*, 2011) (Table 2.2). It is a disorder that starts as alveolitis which then progresses to interstitial fibrosis (Raghu *et al.*, 2006). Histological observations found in pulmonary fibrosis are alveolar thickening with desquamation of the epithelium and interstitial inflammation with inflammatory cells near the area of fibrosis (Selman and Pardo, 2003; Kim *et al.*, 2006). There is also an increase of type II alveolar cells and loss of type I alveolar cells due to the cuboidalisation of the alveolar epithelium. In fibrotic areas of the lungs an increase in production of Th2 cytokine, high expression of growth factors, TGF- $\beta$  and matrix metalloproteinase-7, myofibroblast transformation and accumulation of alveolar macrophages is observed. These macrophages produce ECM and these cells may also affect the degradation of ECM by producing matrix metalloproteinases and their inhibitors (Selman and Pardo, 2003). The consequence is that an increase in Cd, Cr, Hg, Co, Pb and Ni metals are associated with the development of IPF in manufacturer workers especially mine steel workers (Cosgrove, 2015; Paolucci *et al.*, 2018).

### 2.8.3 Lung cancer

Lung cancer is the leading cause of cancer deaths (Jemal *et al.*, 2002) and worldwide it causes the death of over one million people per year (Parkin, 2001). Smoking is a major risk factor for lung cancer and approximately 10% of lung cancer deaths are associated with smoking (Santillan *et al.*, 2003) while the remainder may be due to exposure to different chemical and physical agents via different routes of exposure (Williams *et al.*, 1993). The incidence of squamous cell carcinoma (SQC), small cell cancer (SCLC) and large cell cancer (LGC) has decreased while the incidence of adenocarcinomas (ADC) has increased moderately (Khuder, 2001). Epithelial to mesenchymal transition (EMT) is an important biological process where epithelial cells lose their polarity and undergo a transition to mesenchymal cells, resulting in the cell to cell adhesion, reorganisation of the actin cytoskeleton and increase migratory characteristics (Shigematsu *et al.*, 2005).

The presence of irritants in cigarette smoke stimulates the destruction of the inter-alveolar septum, and impaired elastic fiber synthesis has been linked to squamous cell carcinoma, the principal tumour present in the lungs of cigarette smokers (Mescher, 2010). Chronic smoking induces the transformation of respiratory epithelium into stratified squamous epithelium which is an initial step in the differentiation of tumour cells (Mescher, 2010). Further histopathological changes associated with lung cancer are described in Table 2.2. Exposure to heavy metals such as Pb, Cd, Ni and Cr via inhalation and oral exposure is associated with an increased risk of developing lung cancer in mine workers and their families that live in surrounding areas of the mine (Fucic *et al.*, 2010).

**Table 2.2: Respiratory diseases of the lungs and associated histopathology**

<b><u>Diseases</u></b>	<b><u>Associated histopathology</u></b>	<b><u>References</u></b>
<b>Asthma</b>	<ul style="list-style-type: none"> <li>• Hyperplasia and shedding of basal cells with epithelium squamous metaplasia</li> <li>• Increase in capillary vessel penetration of endothelium</li> <li>• Immune cell infiltration – lymphocytes, monocytes and neutrophils</li> <li>• Tissue thickening and hyalinization</li> <li>• Increased matrix deposition</li> <li>• Increased smooth muscle mass</li> <li>• Increase in wall thickening of epithelium</li> <li>• Abnormalities in elastin</li> <li>• Sub-epithelial fibrosis</li> <li>• Adventitial thickening resulting in airway narrowing</li> </ul>	Bai <i>et al.</i> , 2005 Salvato, 1968

<b>COPD</b>	<ul style="list-style-type: none"> <li>• Epithelium basal cell hyperplasia</li> <li>• Increase in capillary blood vessels with surrounding tissue oedemas</li> <li>• Inflammatory cells infiltration - eosinophils and neutrophils</li> <li>• Tissue thickening and hyalinization</li> <li>• Increase in mucous acini with hyosecretion from the trachea-bronchial submucosal glands with mucous hyperplasia</li> <li>• Decrease in airway, increase wall muscle, fibrosis and airway stenosis</li> <li>• Enlargement of the bronchioles particularly smooth muscle</li> <li>• Lesions within the bronchiolitis resulting in the development of centrilobular emphysema</li> </ul>	Jeffery, 1992 Salvato, 1968
<b>Pulmonary fibrosis</b>	<ul style="list-style-type: none"> <li>• Alveolar septal thickening lined with cuboidal cells seen as cubodalisation of the alveoli</li> <li>• Inflammation and inflammatory cells particularly alveolar macrophages near sites of fibrosis</li> <li>• Fibrosis seen by the increase in collagen in bundles (transverse and longitudinal sections)</li> <li>• Increase of type II alveolar cells due to cubodalisation</li> <li>• Myofibroblast transformation</li> </ul>	Mora <i>et al.</i> , 2006 King <i>et al.</i> , 2011
<b>Emphysema</b>	<ul style="list-style-type: none"> <li>• Capillaries in alveolar walls are congested with many erythrocytes</li> <li>• Changes in alveolar permeability (the air blood barrier)</li> <li>• Glandular material within the alveolar space</li> <li>• Large air spaces containing fluid</li> <li>• Inflammation - macrophages</li> </ul>	Murray, 2011
<b>Lung cancer</b>	<ul style="list-style-type: none"> <li>• Increase of interstitial fibrosis, especially inter-alveolar septa</li> <li>• Squamous dysplasia</li> <li>• Spindle cells and heterogeneous</li> <li>• Atypical alveolar hyperplasia, atypical alveolar cuboidal cell hyperplasia</li> <li>• Bronchio-alveolar carcinoma are lesions located in the periphery of the lungs</li> </ul>	Brambilla <i>et al.</i> , 2001

## 2.9 Aim

The aim of this study was to investigate the effects of 28 days exposure to the heavy metals Cd, Cr and Hg alone and in combination at 1000 times the WHO limit of each metal in water, on the morphology of the lung tissue of Sprague-Dawley rats.

The aim of this study was achieved through the following research objectives:

- Determine the effects of the metals, Cd, Cr and Hg alone and in combination on the general morphology of the lung alveolar and bronchiole tissue using light microscopy with haematoxylin and eosin (H&E) staining.
- To evaluate the distribution and type of collagen in lung bronchiole and alveolar tissue as a result of exposure to Cd, Cr and Hg alone and in combination with

Picrosirius red (PR) staining and polarising light microscopy and further assess the birefringence of the fibres.

- To further evaluate elastin distribution within lung bronchiole and alveolar tissue as a result of exposure to Cd, Cr and Hg alone and in combination by using the Verhoeff van Geison staining (VvG).
- Lastly, to evaluate the effects of metals, Cd, Cr and Hg alone and in combination on the ultrastructure of the lung tissue with specific focus on nuclear membrane, condensation of heterochromatin, activation of mast cells and collagen and elastin fibre distribution using transmission electron microscopy (TEM).

## **Chapter 3: Materials and methods**

### **3.1 Materials**

Sodium hydroxide (NaOH) powder, sodium phosphate (NaH<sub>2</sub>PO<sub>4</sub>), sodium chloride (NaCl), powder, iron(III)chloride (FeCl<sub>3</sub>.6H<sub>2</sub>O), picric acid (C<sub>6</sub>H<sub>3</sub>N<sub>3</sub>O<sub>7</sub>), potassium aluminium sulphate (KAl(SO<sub>4</sub>)<sub>2</sub>.12H<sub>2</sub>O), sodium iodate (NaIO<sub>3</sub>), potassium iodine (KI), sodium thiosulfate (Na<sub>2</sub>S<sub>2</sub>O<sub>3</sub>.5H<sub>2</sub>O), Van Gieson's solution and Entellan mounting medium were of analytical quality and were obtained from Merck Chemicals, Modderfontein South Africa (SA). Sirius red dye powders (Direct red 80) were obtained from the Sigma-Aldrich Company, Atlasville, SA. Eosin yellow water soluble (standard stain), lead citrate, Quetol and thymol were obtained from British Drug House (BDH) Chemicals LTD, Poole England. Formaldehyde (FA) and glutaraldehyde (GA) was purchased from Sigma-Aldrich Company, Atlasville, SA. All consumables were obtained from Lasec, SA. A Leica RM2255 microtome (Kyalami, SA), Nikon Optiphod transmitted light microscope (Tokyo, Japan) and TEM (JEOL JEM 2100F) transmission electron microscope were used.

### **3.2 Study design**

48 male Sprague-Dawley rats weighing 200-250g were used in this study and were exposed to different metals alone and in combination for 28 days. Cadmium chloride (CdCl<sub>2</sub>) [Merck (Pty) Ltd, South Africa], potassium dichromate (K<sub>2</sub>Cr<sub>2</sub>O<sub>7</sub>) [Merck (Pty) Ltd, South Africa] and methylmercury chloride (MeHgCl<sub>2</sub>) [Merck (Pty) Ltd, South Africa] were dissolved in sterile water and administered to the rats via oral gavage. The animals were divided into seven experimental and one control group (Table 3.1). A diagrammatic representation of the study design is presented in Figure 3.1. The rats were exposed to 1000x the WHO limits as set by WHO for daily intake of these metals whereas (0.696 mg/kg Cd, 0.82 mg/kg Cr and 1.148 mg/kg Hg), metal dosage (µg/l) for an average person of 60.7kg, drinking 1.4l of water per day was calculated and converted using the dose equation of Reagan-Shaw, *et al.*, (2008) (Bartram and Howard 2003; Reagan-Shaw *et al.*, 2008; W.H.O. 2011). The concentration for human exposure was converted to the equivalent rat dosage. During the experimental period the weight of the animals were monitored and no differences were observed between the experimental groups and the control (results not shown).

**Human equivalent dosage (mg/kg) = Rat equivalent dosage (mg/ kg) \* (Rat Km/ Human Km).**

(\*K<sub>m</sub> factor for mouse is 3 while K<sub>m</sub> factor for human is 37)

The purpose of this model of sub-acute toxicity was to identify if the lungs are targets of Cd, Cr and Hg toxicity when consumed orally. The male Sprague-Dawley rats were terminated using isoflurane overdose. Lung tissue was harvested, dissected into smaller fragments and immediately fixed in 2.5% GAFA. Thereafter the standard light microscopy processing was followed.

**Table 3.1: Animal groups, metal dosages and the number of rats per group**

<b><u>Animal Groups</u></b>	<b><u>Dosage</u></b>	<b><u>Number</u></b>
<b>Control</b>	0.5 ml saline	6
<b>Hg</b>	1 mg/kg body weight	6
<b>Cd</b>	0.854 mg/kg body weight	6
<b>Cr</b>	0.854 mg/kg body weight	6
<b>Cd + Hg</b>	0.854 mg/kg + 1 mg/kg body weight	6
<b>Cr + Hg</b>	0.854 mg/kg + 1 mg/kg body weight	6
<b>Cr + Cd</b>	0.854 mg/kg + 0.854 mg/kg body weight	6
<b>Cd + Cr + Hg</b>	0.854 mg/kg + 0.854 mg/kg + 1mg/kg body weight	6
<b>Total</b>		<b>48</b>

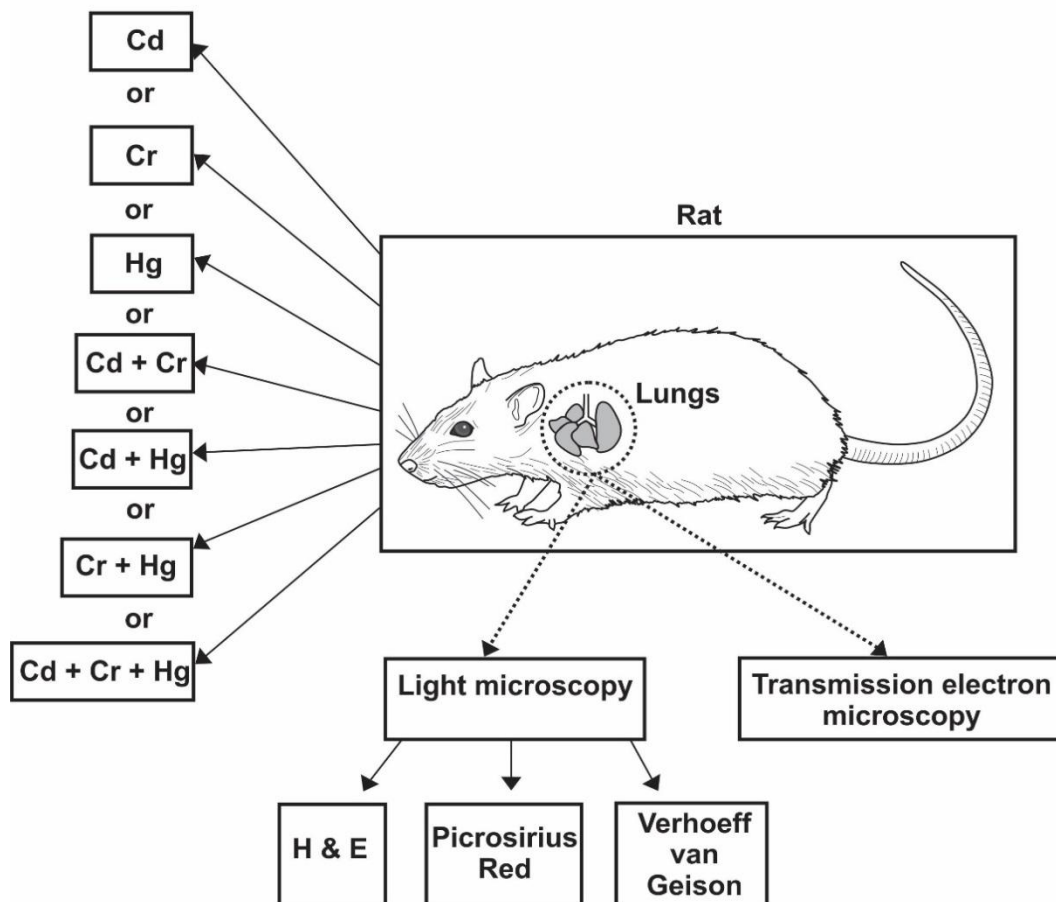


**Figure 3.1:** Schematic representation of the study objectives.

### **3.3 Light microscopy sample preparation**

The lung tissue was fixed in 2.5% GA/FA in 0.075 M sodium phosphate (8.1 mM Na<sub>2</sub>HPO<sub>4</sub>, 1.9 mM NaH<sub>2</sub>PO<sub>4</sub>·H<sub>2</sub>O, 0.137 mM NaCl, 3mM KCl, pH 7.4) buffer for an hour, rinsed three times in the same phosphate buffer for 15 minutes each before the tissue samples were dehydrated in 30%, 50%, 70%, 90% with three changes of 100% ethanol. The tissue samples were left overnight in 100% ethanol. The tissue was cleared of ethanol by placing the samples in 50% xylene in ethanol for 30 minutes, then 100% xylene for 2 hours. The tissue was then infiltrated with paraffin wax of increasing purity (30%, 70% and 100%) for one to two hours at 60°C. The samples were embedded in paraffin wax in grids and moulds and cooled at 4°C. Sections of 3 – 5 µm were made with a Leica RM 2255 wax microtome (Kyalami, SA).

### **3.4 Haematoxylin and eosin staining**

Haematoxylin and eosin (H&E) staining was used to evaluate general tissue morphology. Haematoxylin was used to stain the cell nucleus, RNA-rich portions of the cytoplasm, associated with the ribosomes and rough endoplasmic reticulum. Negatively charged eosin binds the positive residues of proteins such as lysine and stains the cytoplasm pink (Liigand *et al.*, 2016)

To achieve this, slides with the sections were cleared in xylene for five minutes to remove the paraffin wax. The slides were then placed in a series of descending ethanol concentrations to rehydrate the tissue. The series was started by placing the slide twice in 100% ethanol for two minutes, then the slides were placed in 90% EtOH for a minute and then in 70% EtOH for another minute. Before the slides were placed in the haematoxylin for five minutes it was rinsed in ddH<sub>2</sub>O for a minute. After the haematoxylin staining, the slides were rinsed with tap water and then placed into Scott's blue buffer solution for five minutes; this changed the reddish-purple colour of the haematoxylin into a purple-bluish colour, providing a contrast to Eosin. The tissue was then dipped in acidic ethanol where after it was counterstained by leaving it in eosin for five minutes, which stains the cytoplasm and collagen pink. After the eosin, the tissue was dipped in a series of ascending EtOH concentrations (70%, 90% and 100% EtOH) to dehydrate the tissue and ensure that excess dye is removed. Finally, the slides were dipped in xylene before the coverslip was mounted using Entellan and then viewed with a light microscope.

### **3.5 Picro-Sirius Red staining**

Changes to collagen structure are associated with fibrosis or degeneration of the collagenous matrix (Junqueira *et al.*, 1979) often observed in a condition such as idiopathic pulmonary fibrosis (Kauf *et al.*, 1994). Direct red 80 or Sirius red is a poly azo dye and is used to stain all types of collagen with yellow and green birefringence of fibres (Dapson *et al.*, 2011). PR stains collagen and with a polarised light, the collagen fibres are seen to be birefringent due to their molecular arrangement (Borges *et al.*, 2007). Thin fibres are viewed as green to yellow and have a weaker birefringence while thick fibres present with yellow-orange to orange-red colours and have a stronger birefringence (Velindala *et al.*, 2014). The difference in colours and birefringence intensities may occur in the same tissue sample and this is caused by the distinct patterns of physical aggregation of collagen fibres (Junqueira *et al.*, 1979). Collagen molecules react easily with anionic dyes, as collagen is rich in glycine, proline, alanine and glutamic acids (Hirschberg *et al.*, 1999).

To prepare PR stain, 0.5 g Sirius red dye was weighed out and dissolved in 500 ml of aqueous solution of picric acid. Acidified water was used for washing. As described in H&E method (Section 3.4), the tissue was de-waxed and rehydrated, followed by staining in haematoxylin for 8 minutes and rinsed in running tap water for 10 minutes. The samples were stained in PR solution for one hour and then washed twice with acidified water. The tissue was then dehydrated three times in 100% ethanol and then cleared in xylene. The samples were visualised using a light microscope with a polarising filter.

### **3.6 Verhoeff van Gieson stain**

In the previously described PR stain, type III collagen and elastin have a similar green birefringence under polarised light, making it difficult to differentiate between the two connective tissue types. The Verhoeff van Geison (VvG) stain is an elastin specific stain which allows for the identification of elastic fibres and visualisation of any changes to their structure. Using this stain and comparing it to the PR images allowed for a better differentiation between collagen type III and elastin in the tissue and improve on the accuracy of histological results. The VvG stain is a regressive dye composed of haematoxylin, ferric chloride and iodine (Kazlouskaya *et al.*, 2013). Differentiation is achieved by using excess mordant ions, in this case  $\text{FeCl}_2$ . The mordant has a positive charge and has a high affinity to the dye that is negatively charged thus attracting the dye to the excess amounts of mordant used in the solution, forming an iron-haematoxylin complex (McCullen, 1969). The elastic tissue has a strong affinity to the iron-haematoxylin complex and retains the dye longer than the other tissue structures (Kazlouskaya *et al.*, 2013) resulting in a deep black staining of elastin. The elastin-specific staining aids in the determination of tissue elastin atrophy within the lung tissue, often observed in loss of elastic fibres associated with different lungs diseases (emphysema). With increasing age and damaged induced by metals, splitting and fragmentation of elastin can also be observed within the lung tissue (McCullen, 1969).

To prepare the VvG working solution, different types of solutions are required to be made before the adding them together to make the VvG working solution. The first solution is 5% alcoholic haematoxylin and was prepared by weighing out 5 g of haematoxylin and dissolving the haematoxylin in 100 ml of 100 % EtOH. The second solution is 10 % aqueous  $\text{FeCl}_3$  and was freshly made each time before staining the lung tissue by weighing out 10 g  $\text{FeCl}_3$  and dissolving the weighed out ferric chloride in 100 ml of  $\text{dH}_2\text{O}$ . The Weigert's iodine

solution consists of the following dry reagents: 2 g of  $KI_2$ , 1 g of  $I_2$ , followed adding the dry reagents in 100 ml of  $dH_2O$ . The VvG working solution consists of 20 ml of 5% alcoholic haematoxylin, 8 ml of  $FeCl_3$  and 8 ml of Weigert's iodine solution. The solution is a jet-black colour. The staining required the tissue be deparaffinised and hydrated in  $dH_2O$  followed by staining in the VvG working solution for an hour. The tissue was then rinsed with tap water for 6 seconds followed by the tissue being differentiated in 2% of  $FeCl_3$  (consisting of 10 ml of 10 %  $FeCl_3$  and 50 ml of  $dH_2O$ ) for 6 seconds. The slides were then rinsed with water and treated with 5 % of aqueous  $Na_2S_2O_3 \cdot 5H_2O$  for 1 minute. The tissue was washed with water and counterstained with Van Gieson's solution for 6 seconds followed in 95 % EtOH, twice in 100 % EtOH and cleared in xylene twice. The samples were visualised using a light microscope. Elastic fibres appear black and collagen stains pink.

### **3.7 Transmission electron microscopy**

A limitation of light microscopy is that it provides only information on general cellular structure and provides no detailed information on organelle and membrane structure (Williams, 1996). Transmission electron microscopy contains a hot tungsten filament emitting electrons and an anode that has a small hole through which electrons moves at high speed. These filaments and the anode make up the electron gun (LeBeau JM *et al.*, 2008). A beam is converged onto the specimen by electromagnetic condenser lenses and an image is formed by the subtractive action of the sample. Some electrons are scattered from the atoms of the object and the pattern of electron loss generates the image pattern (Williams, 1996). The image is magnified by three electromagnetic lenses that are diffraction, intermediate and projection lenses (Hansen *et al.*, 2001).

Transmission electron microscopy was used to confirm the results obtained with LM evaluation and to determine the ultrastructural effects of exposure with specific focus on cellular morphology and collagen and elastin distribution. Samples were fixed in 2.5 % FA/GA for 1 hour followed by rinsing with PBS 3 times for 15 minutes and secondary fixation in 0.2 M Osmium tetroxide for 1 hour. The samples were rinsed again 3 times in buffer for 15 minutes each within the fume hood. Thereafter, the samples were dehydrated in a series of increasing ethanol concentrations [30%, 50%, 70%, 90% and 100% (3 times)] for 15 minutes each. The samples were left overnight in 100% EtOH after which the samples were infiltrated first with 30% Quetol resin in EtOH for 30 minutes, 60% Quetol resin in EtOH for 30 minutes and 100% Quetol resin for 4 hours. The samples were polymerised for 39 hours, and sectioned using an ultramicrotome (Reichert-Jung Ultracut E). The samples were contrasted with aqueous uranyl acetate for 2 minutes and Reynold's lead citrate for 5 minutes and viewed with a TEM (JEOL JEM 2100F).

### 3.8 Statistical considerations

This observational qualitative study of eight animal groups, consisting of the control and seven heavy metal exposed groups (Table 3.1), aimed to describe the general structure (H&E staining), fibrosis (PR staining) and elastic fibre formation (VvG staining) in tissue using LM. Furthermore, the effects on the internal cellular structures were evaluated with TEM. The changes in tissue structure in the exposed groups were compared with the control group. Six rats were included in each group and for each of the three stains, two slides from each rat were analysed. Two grids for each animal were analysed for TEM. The sample sizes were adequate as the study was done using a homogenous animal population.

For comparative purposes a scoring system was used, where the degree of change was evaluated and the parameters that were evaluated were the extent of inter-alveolar septum thickening, disruption/ displacement of smooth muscle, the presence of BALT, epithelial desquamation and cellular debris within the bronchiole, increased displacement/ distribution of collagen type III to type I, degree of disruptions in elastic fibres and collagen, nuclear membrane disruption, heterochromatin condensation and mast cell activation. Where (-) is none; (+) minimal, (++) mild and (+++) severe based on the degree of change.

**Table 3.2: Rat groups, number per group and sections/slides stained**

Animal groups	Rats per group	Number of sections/slides			
		H&E stain	PR stain	VvG stain	TEM
Control	6	12	12	12	12
Cd	6	12	12	12	12
Cr	6	12	12	12	12
Hg	6	12	12	12	12
Cr + Cd	6	12	12	12	12
Cd + Hg	6	12	12	12	12
Cr + Hg	6	12	12	12	12
Cd + Cd + Hg	6	12	12	12	12
<b>Total</b>	<b>48</b>	<b>96</b>	<b>96</b>	<b>96</b>	<b>96 grids*</b>

\*1 grid= 10 images, 96 grids= 96 \*10 = 960 images

### **3.9 Ethical considerations**

The samples used in this study were obtained from two previously approved animal studies with Animal Ethics Committee (AEC) approval numbers H009/15 (Annexure 2) and H007/15. The current study was approved by the AEC (H004/17). Approval was also obtained from the Research Ethics Committee of the Faculty of Health Sciences, University of Pretoria 423/2017 (Annexure 1).

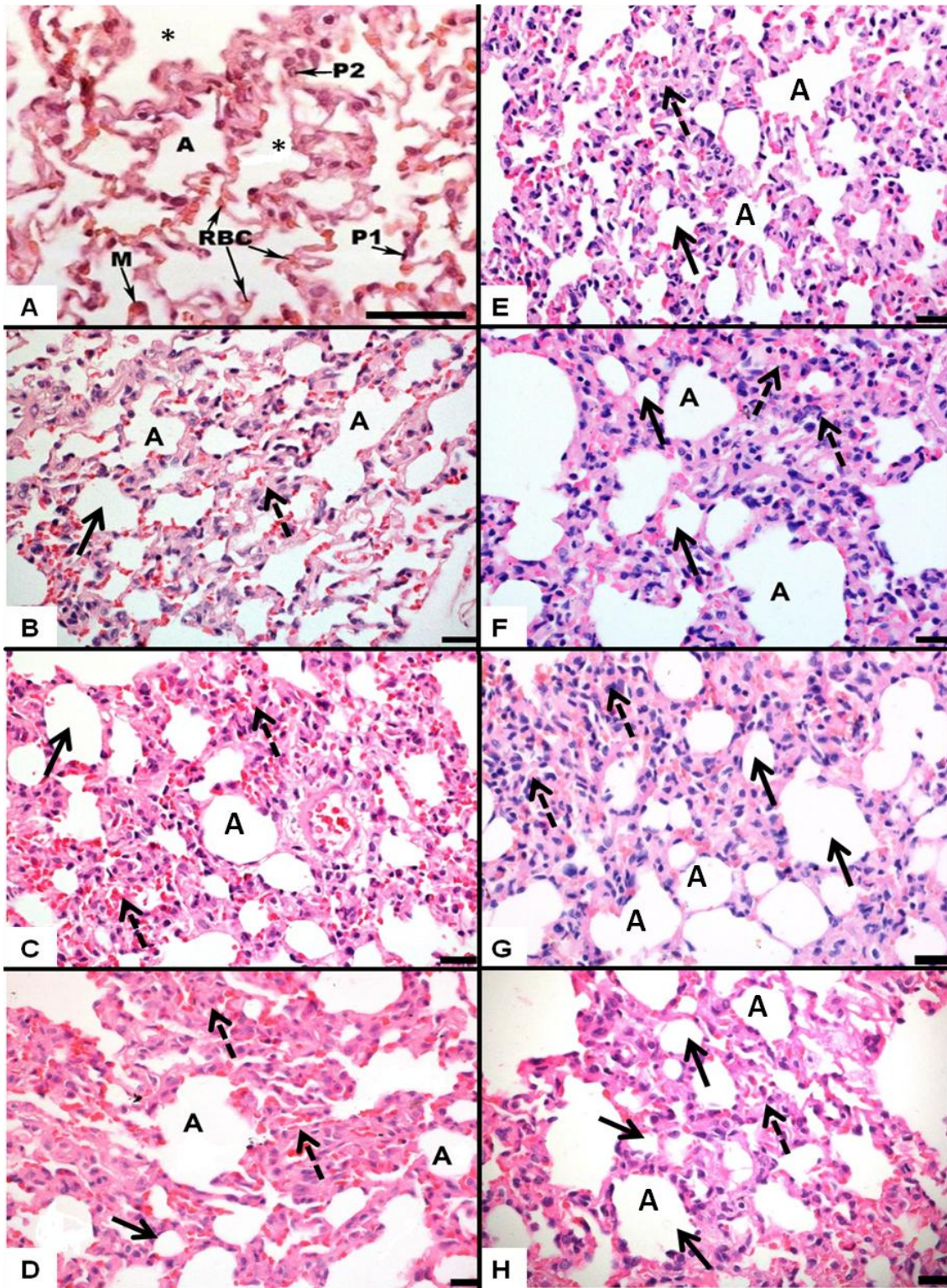
## **Chapter 4: Results**

Heavy metal exposure has become an increasing concern in the mining community of South Africa (Blaurock-Busch, 2010). Heavy metals leech into water sources as a result of the by-product of mining (Blaurock-Busch, 2010; Blaurock-Busch *et al.*, 2010). The chapter further examines the effects of Cd, Cr and Hg alone and in combination in lung tissue using various stains with light microscopy and transmission electron microscopy. Zhu *et al.*, (2014), mention the additive, synergistic and agonist effects of heavy metal combination, however, no literature is available on the combination effects of heavy metals in lung tissue until now. The general morphology and ultrastructure of control and exposed groups were evaluated with light microscopy and transmission electron microscopy (TEM).

### **4.1 General morphology of the alveoli and bronchiole tissue**

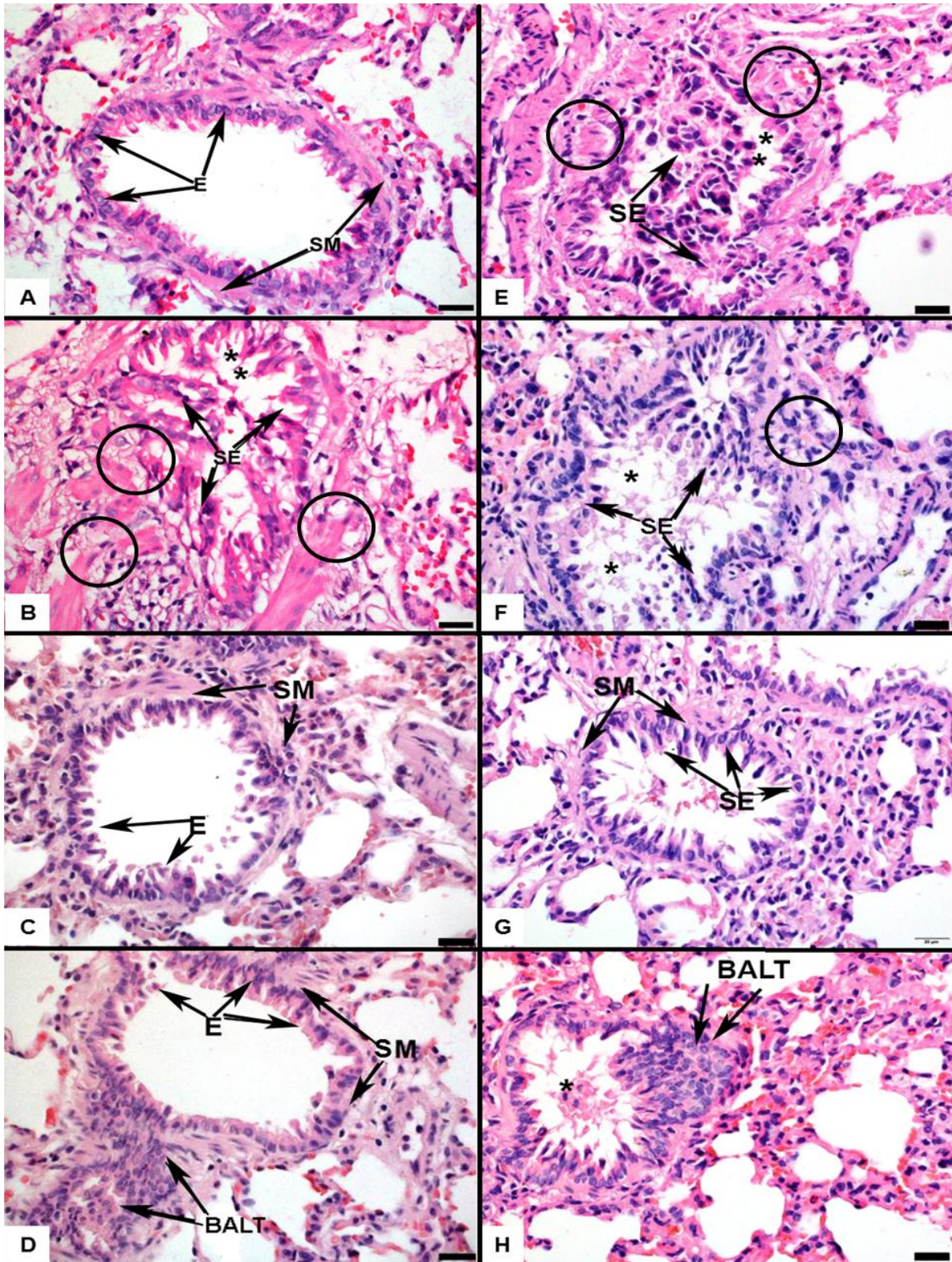
H&E staining was used to investigate the general structure of the alveoli and bronchiole tissue.

Figure 4.1 is a comparison of the general structure and arrangement of the alveoli between the control (Figure 4.1 A) and experimental groups (Figure 4.1 B - H). In Figure 4.1 A, well defined alveolar spaces (A) can be seen with thin epithelial walls, fine interstitium (asterisk) and along the alveolar wall are capillaries containing RBC, all forming the air-blood barrier and respiratory membrane. Pneumocyte type I (P1) and II (P2) also form part of the alveolar walls. Figure 4.1 B - H is representative of the lung tissue of rats exposed to the heavy metals alone and in combination (Cd, Cr, Hg and double and triple combinations). Figure 4.1 B - D are representative of the Cd, Cr and Hg single metal exposure groups respectively and Figure 4.1 E - H is representative of the combination groups. In all metal exposed groups, a thickening of the intra-alveolar space (black arrow) can be seen with an increased thickening of inter-alveolar septa (black dashed arrows) and cell nuclei. The presence of RBC (light pink cells) is more pronounced along the alveolar wall and surrounding the alveolar spaces in the exposed groups compared to the control and is most obvious in the single metal exposed groups (Figure 4.1 B - D). The single metals (Cd; Cr and Hg), double combination of heavy metals (Cd + Cr; Cr + Hg and Cd + Hg) and triple combination of heavy metals (Cd + Cr + Hg) show very little to no differences of the alveoli, the exposure of single, double and combination of the heavy metals. The exposure of heavy metals single, double and triple combination have apparent structural changes to the alveoli and the changes appear to be constant regardless of the single exposure or between combination groups.



**Figure 4.1:** General structure of the alveoli. A: Control; B: Cd; C: Cr; D: Hg; E: Cr + Cd; F: Cd + Hg; G: Cr + Hg and H: Cd + Cr + Hg. Label A: alveolar spaces; Label P1: Type I pneumocyte; Label P2: type II pneumocyte; Label RBC: red blood cells; Label M: alveolar macrophage. \*fine interstitium; Black arrow: thickening of intra-alveolar space; Dashed arrow: thickening of inter-alveolar septa. Scale bar in A = 50  $\mu$ m and B - H = 20  $\mu$ m.

Figures 4.2 A - H are micrographs representing the bronchiole structure of the control (Figure 4.2 A) and exposed groups (Figure 4.2 B - H). Figure 4.2 A shows the typical structure of a bronchiole with an intact epithelial lining (E) and a regular arrangement of smooth muscle (SM) surrounding the bronchiole. Figure 4.2 B, E, F and H (asterix) show desquamation of the epithelium resulting in cellular debris within the bronchioles, and stratification of the bronchiole epithelium, (indicated by SE). Also, the smooth muscle (black circle) surrounding the bronchioles in the Cd (Figure 4.2 B) and Cd + Cr exposed groups (Figure 4.2 B, E and F) appears to have an irregular displacement, and additional connective tissue surrounding the smooth muscle can be seen as an indication of possible fibrosis. In the Hg and Cd + Cr + Hg exposed groups (Figure 4.2 D and H), the infiltration of inflammatory cells was observed by the presence of bronchus associated lymphoid tissue (BALT). These changes mentioned was not observed in the control samples or any of the other exposed groups (Cd; Cr; Cd + Cr; Cd + Hg and Cr + Hg). The alveoli surrounding the bronchioles had a thickening of intra-alveolar spaces and prominent influx of RBC, similar to what can be seen in Figure 4.1.



**Figure 4.2:** General bronchioles structure. A: Control; B: Cd; C: Cr; D: Hg; E: Cr + Cd; F: Cd + Hg; G: Cr + Hg and H: Cd + Cr + Hg. Label E: bronchial epithelium; Label SM: Smooth muscle; Label SE: stratification of epithelium; Label BALT: Bronchus associated lymphoid tissue. \*: desquamated epithelial cells. Black circle: smooth muscle disruptions (Scale bars = 20  $\mu$ m).

## **4.2 PR Stain: Collagen distribution and deposition in alveoli and bronchiole tissue**

PR staining was performed to investigate changes of collagen deposition within the lung tissue. With polarised light, the PR stain allows for the differentiation between thick (Type I) and thin (Type III) collagen fibres having a yellow – green and an orange – red birefringence respectively. Figure 4.3 A - H are micrographs of the alveoli stained with PR and viewed with polarised light.

An evaluation of the alveolar spaces revealed differences in the type and the distribution of the collagen fibres between the control (Figure 4.3 A) and exposed (Figure 4.3 B - H) groups. As seen in Figure 4.3 A, the control sample had pale regular type III collagen fibres (green birefringence) that are arranged more loosely; indicative of the presence of the elastin and collagen fibres. Similar pale type III collagen fibres were present in Figure 4.3 B, C, E, F and H. However, in Figure 4.3 B and C, fibres appeared denser and thicker; that is due to the thickening of the intra-alveolar spaces observed in Figure 4.1. In contrast the fibres in Figure 4.3 D and G, have a bright orange-red birefringence, noticeable type I collagen fibres, associated with increased collagen fibre deposition. The alveolar space appears to be irregular due to the thickening of the inter-alveolar septa as was also seen in Figure 4.1 with the H&E staining. The Cd + Cr (Figure 4.3 E), Cd + Hg (Figure 4.3 F), and Cd + Cr + Hg (Figure 4.3 H) combination groups appeared to have a brighter green- orange birefringence while Cr + Hg (Figure 4.3 G) had a brighter red-orange birefringence observed.

Further evaluation of the bronchioles revealed differences between the control (Figure 4.4 A) and the exposed groups (Figure 4.4 B-H). The control group, Figure 4.4 A, had a pale regular type III collagen fibre distribution (green birefringence). No similarities between the control and exposed groups were observed. Figure 4.4 B, C and E, have brighter yellow – green fibre distribution and appeared thicker and denser due to the thickening of the inter-alveoli space. However, Figure 4.4 D, F, G and H had a brighter red- orange irregular placement of type I collagen fibres that were arranged more densely with an increase in collagen fibre deposition. The similarities between the exposed groups showed that the increased thickening of the intra-alveolar space and inter-alveolar septa resulted in an increased collagen deposition and distribution of the bronchioles. The arrangement is thicker and denser than seen in the control.

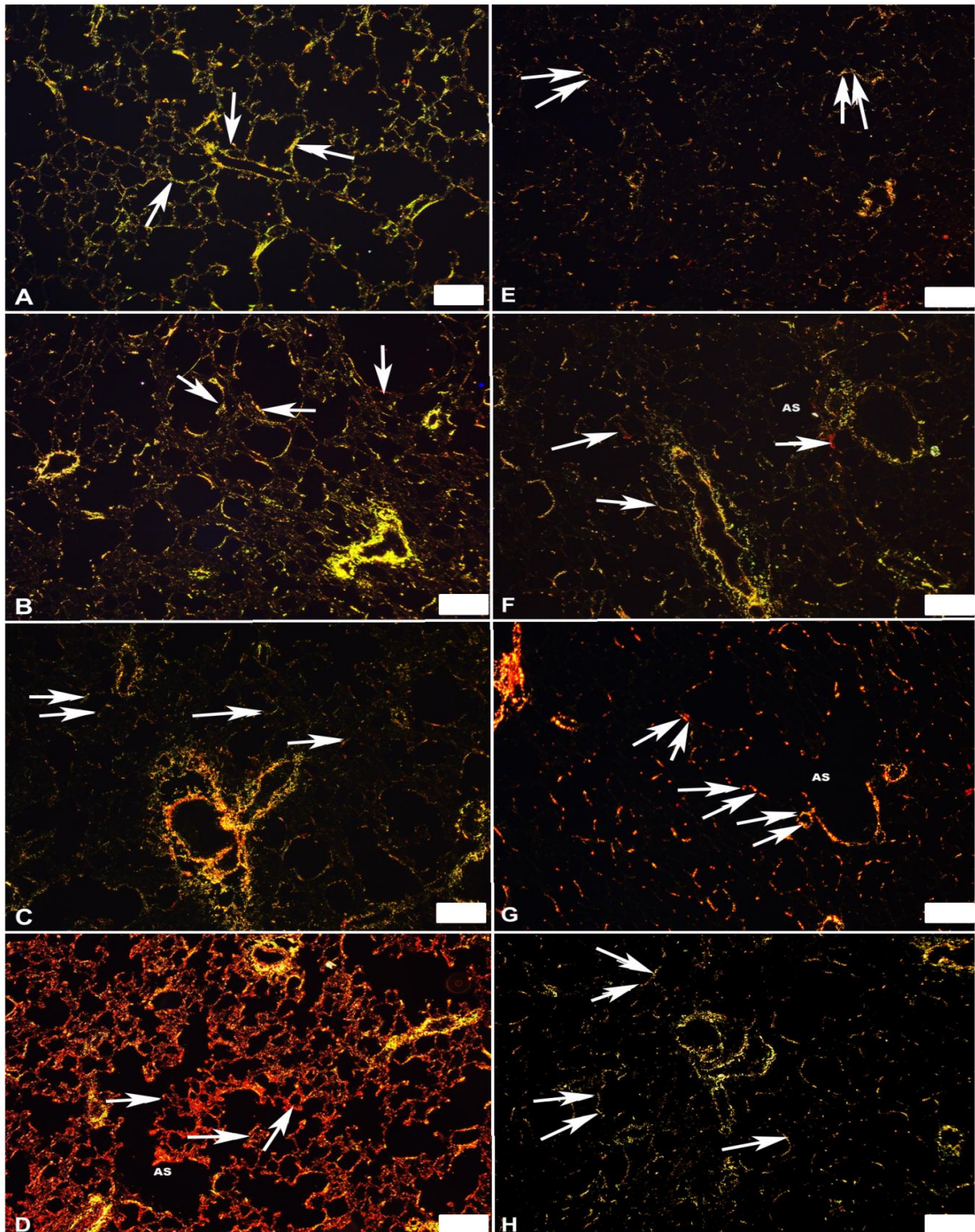


**Figure 4.3:** Polarised light micrographs of the alveoli from the exposed groups. A: Control; B: Cd; C: Cr; D: Hg; E: Cr + Cd; F: Cd + Hg; G: Cr + Hg and H: Cd + Cr + Hg. Each arrow indicates either thin (Type III) collagen or shows colour changes indicative of fibre thickness increase of type I collagen deposition. AS: Alveolar space. Scale bars = 50  $\mu$ m.

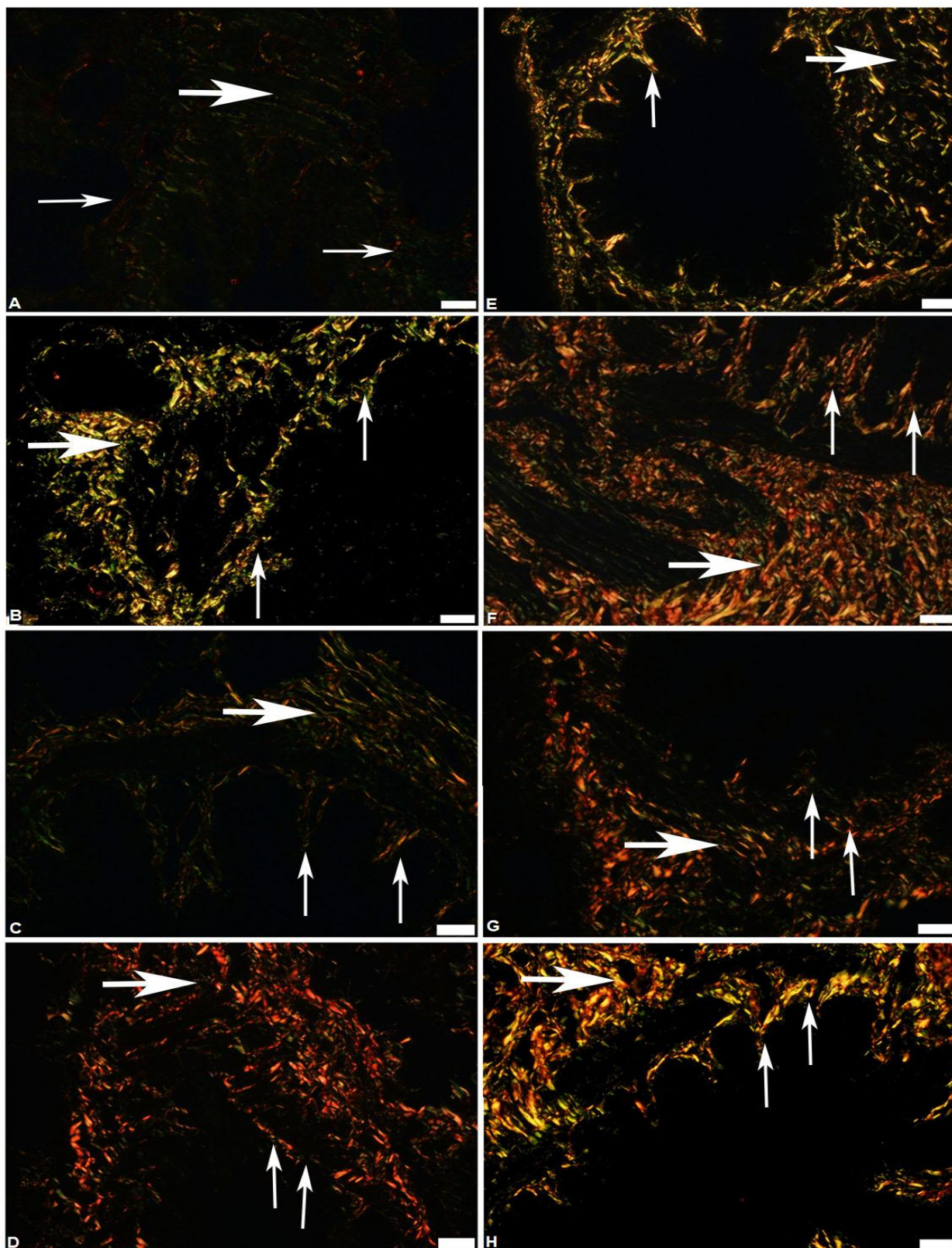


**Figure 4.4:** Polarised light micrographs of the bronchioles from A: Control; B: Cd; C: Cr; D: Hg; E: Cr + Cd; F: Cd + Hg; G: Cr + Hg and H: Cd + Cr + Hg. Thicker arrows indicate fibre alteration surrounding the smooth muscle of the bronchiole and thinner arrows show altered fibres in the basement membrane of the bronchioles. Scale bar = 50  $\mu$ m.

### **4.3 Verhoeff van Gieson Stain: Elastin deposition and distribution in the alveoli and bronchioles**

Besides collagen the connective tissue of the lung also contains elastic fibres and with PR staining it is not possible to distinguish between the various types of collagen fibres and elastic fibres. Therefore, the Verhoeff van Gieson (VvG) stain is an elastin specific stain that was used for the evaluation of elastin fibre distribution within the alveolar spaces and bronchioles.

Figures 4.5 A - H are micrographs of the alveolar structures stained with VvG. The alveoli between the control (Figure 4.5 A) and exposed (Figure 4.5 B - H) groups were compared. In Figure 4.5 A, the control, the alveoli have defined alveolar spaces while all the exposed groups showed a thickening of the intra-alveolar spaces as observed in Figure 4.1 with the H&E stain as well, however since VvG stain is specific to elastin there were minimal to mild differences in the distribution and disruption of elastin fibres between the exposed groups to heavy metals within the alveolar spaces except Hg and Cd + Cr + Hg. Figure 4.5 B - D the examination of elastin (black arrows) and collagen fibres (red arrows) are similar to the control (Figure 4.5 A) with no apparent differences between the exposed groups except the single exposure of Hg and the triple combination of heavy metals.

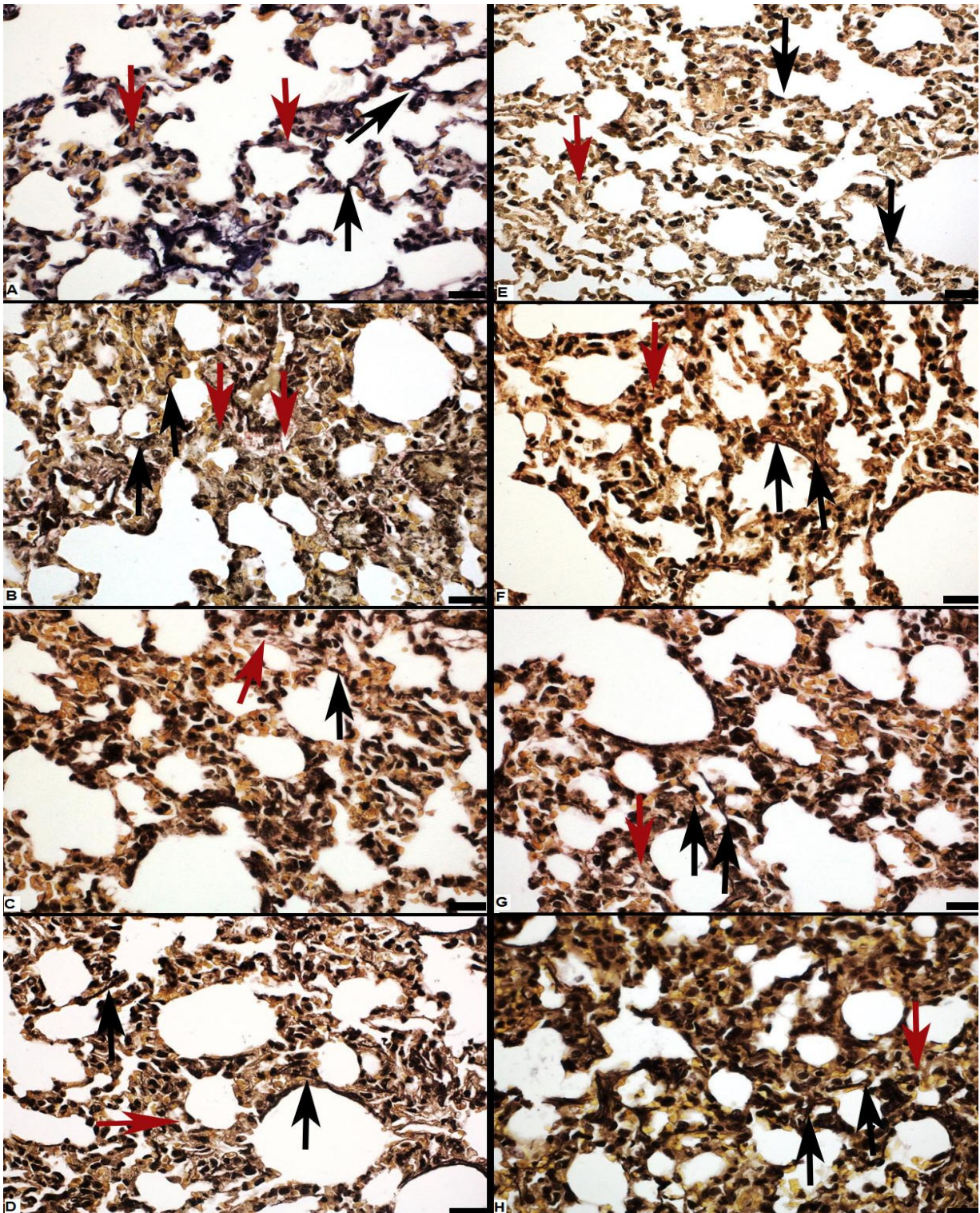


**Figure 4.5:** Structure of the alveoli and the air-blood barrier. A: Control; B: Cd; C: Cr; D: Hg; E: Cr + Cd; F: Cd + Hg; G: Cr + Hg and H: Cd + Cr + Hg. Black arrows: elastic fibres; red arrows: collagen. Scale bars = 20  $\mu$ m.

The examination of the arrangement and distribution of elastin and collagen fibres in the bronchioles (Figure 4.6 A – H) were assessed and differences were observed between the control (Figure 4.6 A) and exposed groups (Figure 4.6 B – H). The control had a wavy but continuous layer of elastin fibres on the basement membrane while the exposed groups (Figure 4.6 B - H) revealed disruptions of the elastic fibres that are discontinuous with the lining of the basement membrane as indicated by the black arrows. The collagen (red arrows) content stained in pink, are more prominent in the exposed groups compared the control, particularly in Cd exposed group. The presence of smooth muscle was observed in Figure 4.6 B, C, D, E, F and H. BALM was observed to infiltrate the bronchioles in Figure 4.6 C, D, F and H (indicated by the black circles).

Evaluation of the arrangement and distribution of elastin and collagen fibres in the bronchioles (Figure 4.6 A - H) on higher magnification (Figure 4.7 A - H) revealed differences between the control and exposed groups. In the control group elastin was observed as a wavy layer in the basement membrane. The elastic fibres (black arrows) in the exposed groups (Figure 4.7 B - H) appeared irregular and discontinuous with the basement membrane of the epithelial lining of the bronchioles, in contrast to the control (Figure 4.7 A). The elastic lamina of the exposed groups are disrupted and delineated from the bronchioles basement membrane especially in the Cd exposed group (Figure 4.7 B). The collagen content (Figure 4.7 B – H) (stained pink) surrounding the bronchioles are observed to be increased compared to the control. Increased presence of collagen was observed in the Cd exposed group. The presence of smooth muscle fibres and long oval nuclei can be observed in Figure 4.7 B, C, E, F and H; however, it is more prominent in 4.7 F and H.

A summary of the histological findings are shown in Table 4.1 below. Of the single metals, Hg was the most toxic. Cd + Hg were the most toxic of the double metal combinations while Cd + Cr + Hg were slightly more toxic.

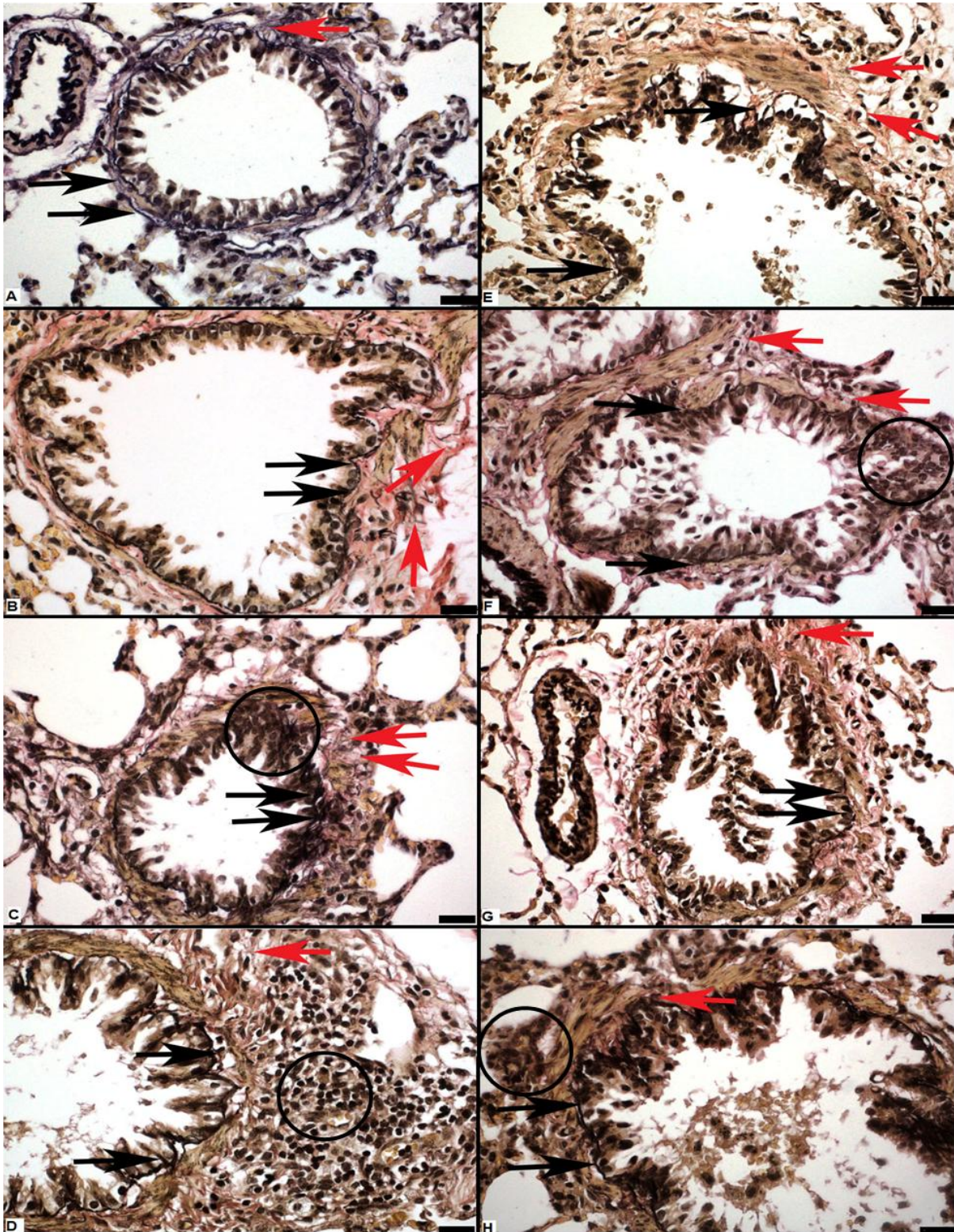


**Figure 4.6:** Structure of the bronchioles in A: Control; B: Cd; C: Cr; D: Hg; E: Cr + Cd; F: Cd + Hg; G: Cr + Hg and H: Cd + Cr + Hg. Smooth muscle staining pink surrounds the bronchioles in exposed groups with an increase in collagen is indicated by the red arrows and disruption of elastin surrounding the smooth muscle is indicated by the black arrows. Black circles indicated the presence of BALT. Scale bars = 20  $\mu$ m.

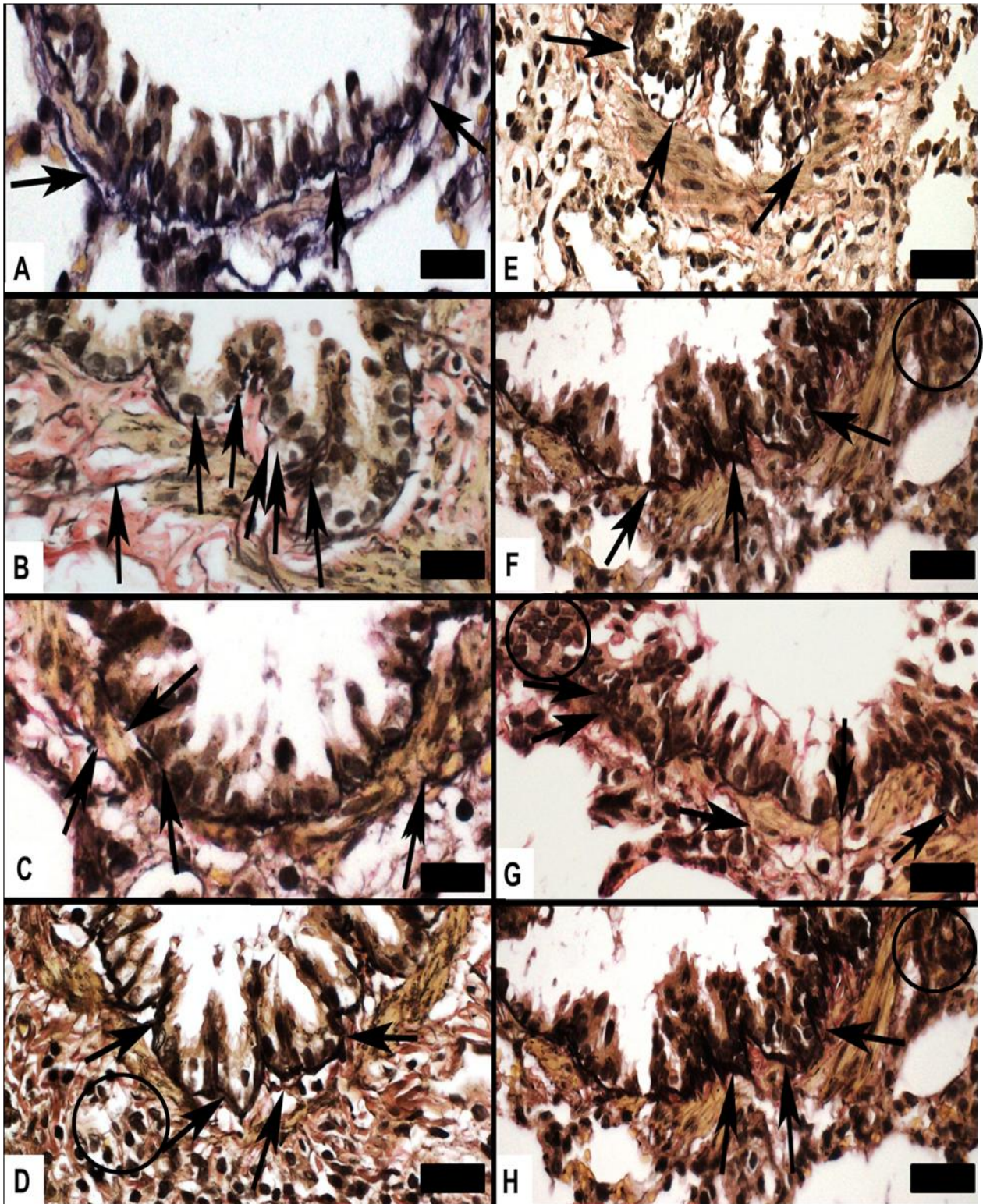


**Figure 4.7:** Magnified images of regions of the bronchioles A: Control; B: Cd; C: Cr; D: Hg; E: Cr + Cd; F: Cd + Hg; G: Cr + Hg and H: Cd + Cr + Hg. Black arrows: Disruption of elastin fibres; Black circle: BALT. Scale bars = 20  $\mu$ m.

**Table 4.1:** Summary of the histological changes observed

Group	Intra-alveolar space thickening	Disruption/displacement of smooth muscle	Presence of BALT	Epithelial desquamation and cellular debris within the bronchiole	Increased displacement/distribution of collagen type III to type I	Disruptions in elastic fibres and collagen
Control	-	-	-	-	-	-
Cd	++	+++	++	+++	++	+
Cr	++	+	++	-	++	+
Hg	+++	++	+++	++	+++	++
Cd + Cr	+	++	++	+++	+++	+
Cd + Hg	+++	+++	++	+++	++	+
Cr + Hg	++	++	-	+++	++	+
Cd + Cr + Hg	++	+++	+++	+++	++	++

Key – None; + minimal, ++ mild and +++ severe

#### **4.4 Transmission electron microscopy**

Transmission electron microscopy was used to evaluate membrane morphology, organelle structure and the distribution of collagen and elastin in the lung tissue of the control and exposed groups.

Type II pneumocytes with typical features (cuboidal in shape, resting on the basement membrane and lamellar bodies within the cytoplasm) were identified in each section. The structure of the nuclei of the control (Figure 4.8 A and B) and exposed groups (Figure 4.8 C, D, E, F, G and H and Figure 4.9 C, D, E, F, G and H) were compared. Pneumocytes from the control group had a centrally placed nucleolus and heterochromatin (Figure 4.8 A and B, white arrow head) that was evenly distributed within the nucleus. In all the exposed metal groups (Figure 4.8 C, D, E, F, G and H and Figure 4.9 C, D, E, F, G and H), the nucleolus was not easy to identify or was surrounded by condensed heterochromatin.

The nuclear membrane in the control group had a typical bilayer (black arrow). The exposed groups (Figure 4.8 C, D, E, F, G and H and Figure 4.9 C, D, E, F, G and H) revealed a detachment of the nuclear membrane (black arrows). The degree of nuclear detachment varies between exposed groups. The combination groups (Figure 4.9 C, D, E, F, G and H) had a higher degree of detachment compared to single metal exposed groups (Figure 4.8 C, D, E, F, G and H).

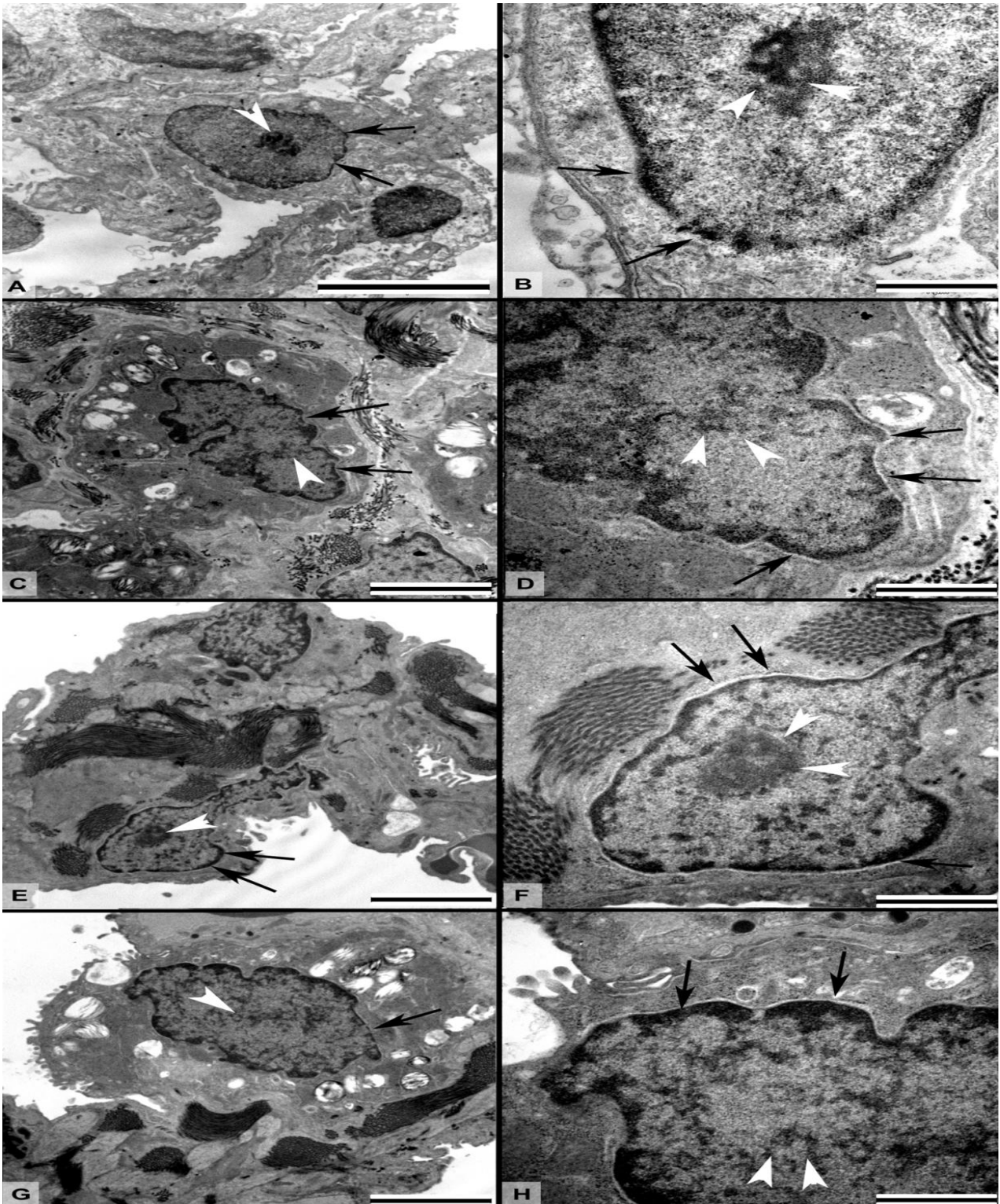


**Figure 4.8:** TEM micrographs of lung tissue from the control and Cd, Cr and Hg exposed groups, showing Type II pneumocytes and the effects of exposure on nuclear membrane integrity (black arrows) and chromatin condensation (white arrow heads). A and B: Control; C and D: Cd; E and F: Cr; G and H: Hg. B, D, F and H are at a higher magnification. A = 6 $\mu$ m, B = 12 $\mu$ m, C, E and G = 10 $\mu$ m, D, F and H = 20 $\mu$ m.

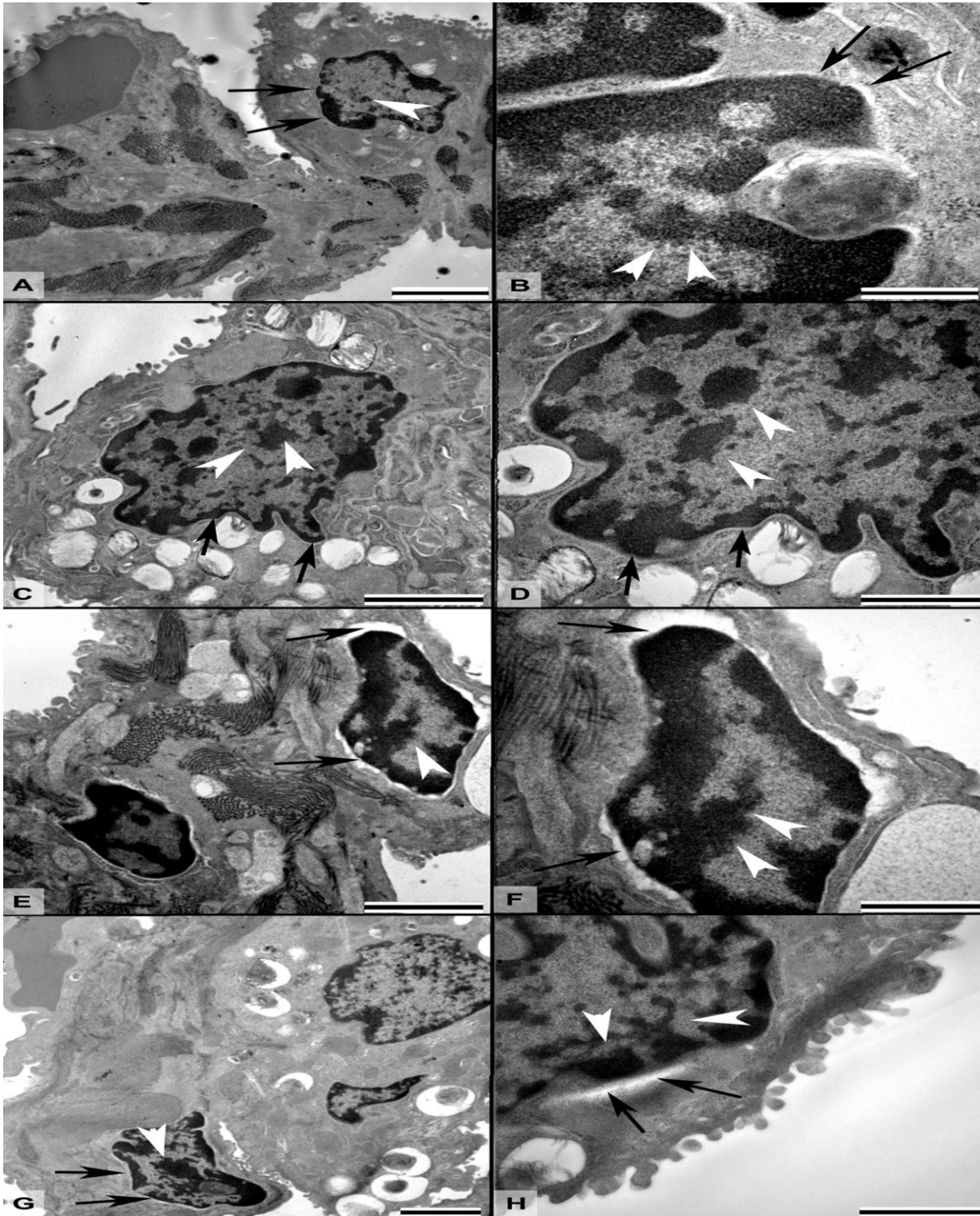


**Figure 4.9:** TEM micrographs of lung tissue from the Cd + Cr, Cd + Hg, Cr + Hg and Cd + Cr + Hg groups showing Type II pneumocytes and the effects of exposure on nuclear membrane integrity (black arrows) and chromatin condensation (white arrow heads). A and B: Cd + Cr; C and D: Cd + Hg; E and F: Cr + Hg; G and H: Cd + Cr + Hg. B, D, F and H are at a higher magnification. A, C, E and G = 10  $\mu$ m, B, D, F and H = 20 $\mu$ m.

The distribution of the collagen and elastin bundles in the control group (Figure 4.10 A) was compared with that of the exposed groups (Figure 4.10 B - H). Fine and few collagen (black arrow) and elastic fibres (white arrow) were observed in control group (Figure 4.10 A). In all metal exposed groups a dramatic increase in the presence of collagen fibril bundles (Figure 4.10 B - H, black arrows) was observed. In addition, the arrangement was irregular as was observed for the Cd exposed group (Figure 4.10 B). The arrangement of the collagen fibres in the collagen bundles was more loosely arranged in the Hg exposed group (Figure 4.10 D). A similar arrangement of collagen was also observed in the combination groups. Compared to the control group, elastin fibre distribution was increased in all the exposed groups (Figure 4.10 B – H, white arrow heads).

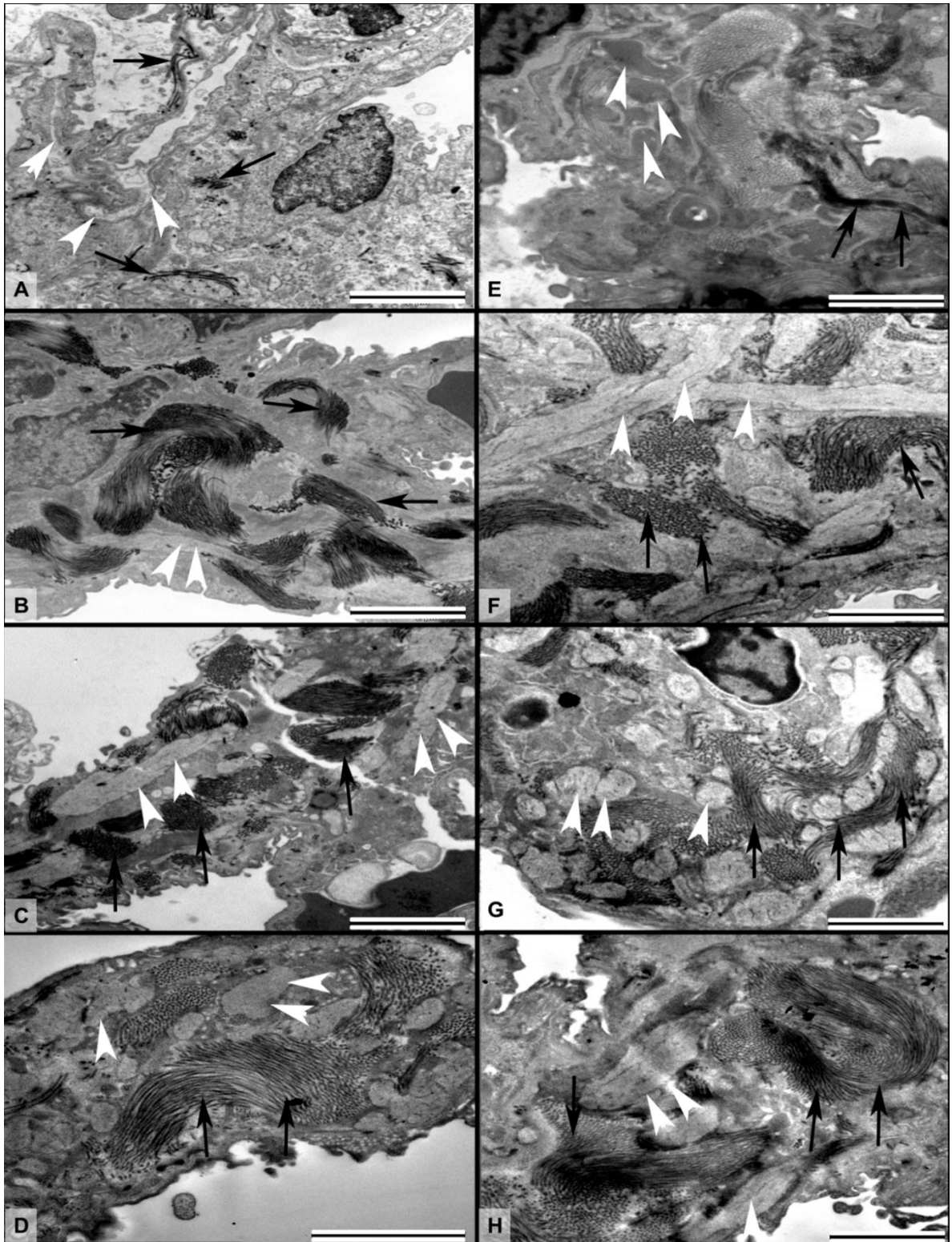


**Figure 4.10:** TEM micrographs of the lung tissue of the control and exposed groups showing fibrotic changes and associated increase in collagen (black arrow) and elastin (white arrow heads) fibre distribution. A: Control; B: Cd; C: Cr; D: Hg; E: Cd + Cr; F: Cd + Hg; G: Cr + Hg and H: Cd + Cr + Hg. A, B, C, E, F, G and H = 20 μm, D= 2μm.

TEM was further used to examine the mast cells and the release of large dense granules from mast cells (black arrows and large circle) and secondary granules (smaller circles). Mast cells are associated with increased inflammation and the development of fibrosis (Caruntu *et al.*, 2014). Mast cells were identified based on the presence of large dense granules in the cytoplasm. Mast cells were not observed in the control samples analysed (Figure 4.11 A) but were present in the exposed groups (Cd; Cr; Hg; Cd + Hg and Cd + Cr + Hg) (Figure 4.11 B – F). The mast cells were found in close association with fibroblasts (Figure 4.11, Black circles) or intracytoplasmic environment/ nucleus (Figure 4.11, Black circles). TEM examined the presences of the mast cells with thier distinct electron densities shown in Figure 4.11 B – F of the exposed groups. Figure 4.11 B – F indicate the presences of activated mast cells due to the exposure of heavy metal or activation or partial degranulation based on the exposure of heavy metals. Single and combination of heavy metal exposure showed the presences of secondary granules (small circles) that emitted an outer light electron density compared to the denser electron density inside within. This was particularly seen in exposed group of Cd alone and in combination of Cd + Hg.

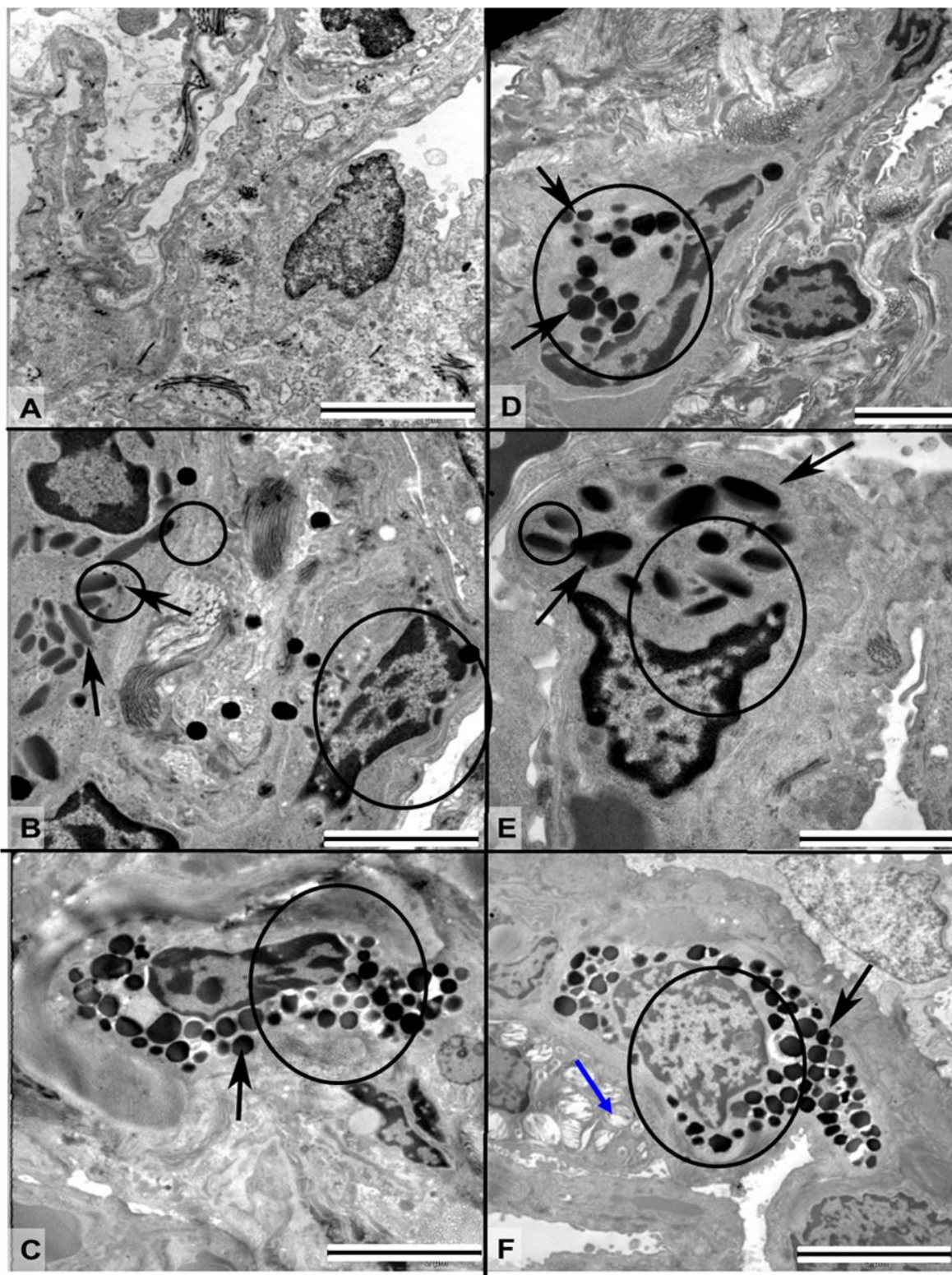


**Figure 4.11:** TEM micrographs showing mast cells (black arrows) within the lung tissue A: Control; B: Cd; C: Cr; D: Hg; E: Cd + Hg; and F: Cd + Cr + Hg. (Blue arrow: Mitochondria, large circles: large dense granules from mast cells and small circles: secondary granules). A, B, C, E and F = 20  $\mu\text{m}$ , D = 2  $\mu\text{m}$ .

A summary of the ultrastructural analyses are shown in Table 4.2. Of the single metals, Hg was the most toxic. Cd + Hg were the most toxic of the double metal combinations while Cd + Cr + Hg were slightly more toxic.

**Table 4.2:** Summary of ultrastructural changes in lung tissue after heavy metal exposure

	Nuclear membrane detachment	Increase in collagen bundles	Increase in elastin bundles	Disruptions in elastic fibres and collagen	Presence of mast cells	Activated mast cells
Control	-	-	-	-	-	-
Cd	++	+++	+	+++	+++	++
Cr	++	+++	++	+++	+++	+
Hg	++	+++	++	+++	+	++
Cd + Cr	+++	+	+	-	-	-
Cd + Hg	+++	++	+++	+++	+	+
Cr + Hg	+++	++	++	-	-	-
Cd + Cr + Hg	++	+++	++	+++	+++	+

Key – None; + minimal, ++ mild and +++ severe

## **Chapter 5: Discussion**

The aim of this study was to investigate the effects of 28 days exposure to the heavy metals Cd, Cr and Hg alone and in combination at 1000 times the WHO limit of each metal in water, on the morphology of the lung tissue of male Sprague-Dawley rats. In other studies, the concentrations that are used are selected from previous studies, however, in the current study the selected dosages were based on several fold lower concentrations of the lethal dosage 50 (LD50) in rats that is 0.854 mg/ kg, 14.22mg/ kg and 0.854 mg/kg for Cd, Cr and Hg respectively (Regan-Shaw *et al.*, 2014). In the present study, concentrations based on the established WHO limits for drinking water were selected. These were then converted to the equivalent dosages in rats. This method takes into account factors such as differences in absorption, metabolism, the route of exposure and combination of exposure of heavy metals.

Many studies have evaluated the effects of aerosol pollutants on the respiratory system (Ristovski *et al.*, 2011; Martins *et al.*, 2015; Guan *et al.*, 2016; Lakey *et al.*, 2016), however only a few studies have investigated the effects of metals on the respiratory system if taken orally. This model of sub-acute toxicity provides an opportunity to determine whether, following oral intake of these metals in water, the lungs are a target of toxicity.

The metal levels evaluated were selected to be 1000 times the WHO limit for drinking water and is relevant as these levels are comparable to groundwater levels found in the Ratchathani province of Thailand where the average As, Cd, Cr, Hg, Ni, Pb and Zn were found to exceed average concentrations (Wongsasuluk *et al.*, 2014). Several heavy metals levels in South Africa were also measured and according Blaurock-Bush (2010), reported no available sources on the maximum amount of Hg allowed in drinking water. However, the South African water quality guides (1996) have indicated the intake of Cd should not exceeds 50 mg/ kg daily, daily dose of Hg should not exceed 20 000 mg/ kg and no information is provided for Cr. Thailand water concentrations of Cd, Cr and Hg were found to be an average of  $16.66 \pm 18.52$  µg/l. This compared to water levels in Africa (Nigeria and South Africa) were the levels of Cd, Cr and Hg were reported to 0.09 - 14.78 µg/l; 9.27 - 327.29 µg/l and 0.1 - 8.09 µg/l respectively (Olujimi *et al.*, 2016). This is much lower than the average that was reported in Thailand and observed within the averages found in South Africa (Fatoki and Awofolu, 2003). The industrial workers that are continually exposed to the heavy metals at average concentration still develop various respiratory diseases such as asthma, COPD, lung cancer and fibrosis (Jarup, 2003; Jaishankar *et al.*, 2014; Anyanwu *et al.*, 2018).

The rats in this study provide an opportunity to evaluate the effects of these metals when administered orally on the lungs. Light microscopy, with H&E staining showed thickening of the intra-alveolar space and inter-alveolar septa, infiltration of inflammatory cells, desquamation of epithelium and cellular debris within bronchioles as well as the pronounced presence of RBC along the alveoli and bronchioles with the most severe effects observed for Cd, Hg, Cd + Hg, Cr + Hg and Cd + Cr + Hg.

Roberts *et al.*, (2013) observed similar histopathological changes after the exposure of Cd was evaluated in rats where 5 nm particles of Cd were administered orally for 28 days. Tissue necrosis and hypertrophy within the lungs caused alveolar septal thickening. Additionally observed were the presence of macrophages along the bronchioles and infiltrated in the inter-alveolar septa (Roberts *et al.*, 2013).

Beaver *et al.*, (2009) investigated the association of lung injury, inflammation and proliferation of cells after repetitive exposure to chromate (50 µL of dose of Cr VI via intranasal treatment) on female BALB mice for 28 days. Chronic exposure to chromate resulted in inflammation of the alveolar and interstitial spaces with significant increase of lymphocytes and macrophages. Also, degenerative changes and sloughing of the epithelial cells were noticed. The study by Goldoni *et al.*, (2008) measured the lung tissue for levels of Cr in exhaled breath condensates (biomarker of Cr exposure) of the pulmonary tissue of 15 patients; the results obtained showed an absence of the monolayer lining of the lung tissue due to cellular stratification.

Mercury mediated ROS formation causes destabilisation and disintegration of the cell membranes, mainly caused by lipid peroxidation (Celikoghi *et al.*, 2015). In a study conducted on 48 rats for 28 days, the authors assessed if vitamin E and sodium selenite protected against mercury chloride (100 mg/kg oral) induced lung toxicity. Hg was observed to cause an increase in inter-alveolar septal thickening, degeneration of bronchiole epithelium and infiltration of inflammatory cells as well as haemorrhage and oedema of the alveoli. Most of the observations are similar to the present study. Yoshida *et al.*, (1999) found similar effects after exposure to 6.6 and 7.5 mg/kg of Hg vapour to null mice over 3 days. The results reported extensive pulmonary damage of the alveolar structure, influx of inflammatory cells and haemorrhaging. A conducted by Soussa *et al.*, (2013) with an oral exposure to Hg in female rats for 28 days, reported the presence of fibrosis and inflammatory cell infiltration. Additionally, it appears oedematous with thinner inter-alveolar septa. Effects of Hg on the lungs have largely been described as a result of exposure to Hg vapour via inhalation. Occupational or accidental exposure to Hg vapour has been shown to

lead to acute respiratory failure (Rowens *et al.*, 1991; Moromisato *et al.*, 1994; Lim *et al.*, 1998; Asano *et al.*, 2000; Smiechowicz *et al.*, 2017) pulmonary oedema and acute interstitial pulmonary fibrosis (Jaeger *et al.*, 1979).

Alveolar epithelial cells are important in maintaining the integrity and fluid balance of the lungs, therefore the epithelial lining of the airway serves as a protective barrier and is extremely sensitive to injury. Damage can result in the loss of selectively permeability, allowing water, ions and macromolecules to move across into the lungs (Gonzales *et al.*, 2015). The earliest sign of damage is noticed by thinning epithelium and an increase in inflammation. The alveolar cells are normally covered with a thin protective fluid; surfactant that is rich in antioxidants (Tang *et al.*, 2005; Behndig *et al.*, 2006). Type II pneumocytes and endothelial cells fuse with the basement membrane. This is strengthened by type IV collagen fibres to form the air-blood barrier (ABB) (Kindlen, 2003), thereby ensuring selective permeability. Several studies have observed macrophages present in the ABB and have noticeably increased in the number of phagosomes and lysosomes (Zelikoff *et al.*, 1993; Tátrai *et al.*, 1998, Fortoul *et al.*, 2005; Kaczynska *et al.*, 2011). Balogun *et al.* (2014) identified that toxicity of the alveolar cells within the lungs and fibrosis, hyperplasia of alveolar, necrotic cells with influx of inflammatory cells after the exposure of paint fumes.

Czekaj *et al.*, (2002) investigated the morphological changes in lungs of pregnant rats exposed to cigarette smoke (1500 mg/kg of Cd) for 3 weeks. The authors observed significant decreases in the height of the respiratory bronchiole epithelium particularly, thickening of the intra-alveolar spaces and inter-alveolar septa, squamous epithelium metaplasia, cysts lining the epithelium and inflammatory granulomas present. Ibramin *et al.*, (2016), administered Cr VI 3mg and 9mg/ 100kg of base water orally. Within the 30 days of the experiment, the lung tissue was assessed and the authors found an enlargement of the bronchioles, hyperplasia of the epithelium and infiltration of inflammatory cells near the lumen of the bronchioles. Lu *et al.*, (2010) investigated the ability of MeHg to induce type II pneumocyte damage using the human lung invasive carcinoma cell line (CI1-0) (2.5 and 5µM for 72 hours) and International cancer research (ICR) mice for 28 days (0.2 mg/kg per day of MeHg). After exposure to MeHg, cell viability was decreased while MDA and ROS levels were increased in the lung tissue. MeHg also caused a decrease in the levels of surfactant proteins and several sites of lung fibrosis were identified.

Fortoul *et al.*, (2005) assessed the effects of Cd and Pb alone and in combination on the bronchiolar structure of lungs in mice. Morphological analysis of the tissue samples after exposure showed flattened and decreased bronchiolar cells mainly in the Cd group as well

as in the combination group. Also observed was an increase in cell proliferation in the lungs and this study suggested that the inhalation of the metals enhanced the proliferation of the cells to regrow the bronchiolar wall (seen as tissue repair mechanism). In contrast to the present study, the combination had a similar effect on the structure of the tissue as the single exposed groups. However, with each combination group, the severity of damage increased compared to the control. Each combination also acted as a synergist or antagonist resulting in various degrees of damage to the tissue in each combination. The study was vital as it provided the link that oral exposure may result in health risks. Additionally, the effects of the combinations of the heavy metals are not adequately researched. Additionally, Zhu *et al.*, (2014) assessed the oral exposures to Pb and As alone and in combination and reported no difference between the effects of the single and combination of exposures in lungs of female Sprague-Dawley rats. Synergistic and antagonistic interactions have been reported in other studies (reviewed by Zhu *et al.*, 2014). The histological results of the current study showed that there is an increase in the degree of tissue alterations after exposure to combinations of the heavy metals.

Collagen is an ECM protein that maintains the integrity of lung tissue and provides structural support for lung cells involved in gas exchange and actively regulates lung function in homeostatic and pathological conditions. Persistent exposure to harmful chemicals or pollutants causes the activation of monocytes and alveolar macrophages, releasing protease resulting in damage to the components of ECM in alveolar septa (MacNee, 2005). The development of different lung diseases such as asthma, COPD, emphysema, lung cancer and pulmonary fibrosis is due to the damage of the alveolar cells. In addition, increase degradation of the ECM components promotes connective tissue remodelling that may result in lung fibrosis. Type VI collagen is deposited early within the lungs and is often associated with lung fibrosis. Kasper *et al.*, (2004) examined and confirmed the presence of type I collagen fibres in Wistar rats after a 3 day exposure to 0.3mg/ kg of CdCl<sub>2</sub> via aerosol fumes which indicates the development of fibrosis. The type I fibres were mostly deposited in the inter-alveolar septa and increased deposition and synthesis of a single collagen type often results in structural abnormalities of the connective tissue. An increase in type I collagen synthesis (shown in Figure 4.4) is indicative of fibrosis that due to heavy metal exposure of Cd, Hg and Cd + Hg (Arbi, 2014). Miller and Hook, (1990), also reported morphological dysfunction of type II pneumocytes that showed the separation of the phospholipid layer and the distribution of the surfactant cells in the alveolar epithelium was discontinuous.

El-Refaiy and Eissa (2012) administered vitamin C (Vit C) and Zn to rats after the exposure to 3mg/kg Cd orally for 90 days. Histological observations reported that Vit C is a strong

antioxidant with the ability to reduce the damage done by ROS. However, it was found within the study that Zn has a stronger affinity to free radicals than Vit C, reducing ROS. The results after 8 weeks of exposure to Cd showed signs of histopathological changes such as oedema, thickening of the inter-alveolar septa, and enlargement of the alveolar spaces, aggregation and infiltration of lymphocytes which, in contrast to the control group, showed no changes in the tissue.

Both light- and electron microscopy in the present study confirmed the presence of accumulation of type I collagen fibres. These fibres appeared more dense and thicker as it can be seen in the thickening of the inter-alveolar septa and intra-alveolar space. The similarities between the exposed groups showed an increased thickening of the inter-alveolar septa, bronchiole epithelium hyperplasia and an increased collagen deposition and distribution of the bronchioles in the overall lung tissue. The arrangement is thicker and denser than seen in the control especially for Cd, Hg, Cd + Hg and Cd + Cr and Hg. The elastic fibres in the connective tissue observed showed no apparent changes in the alveolar structure but appeared irregular and discontinuous with the basement membrane of the epithelial lining of the bronchioles of the exposed groups. The elastic lamina were disrupted and delineated from the bronchioles basement membrane. An increased presence of collagen was noticed surrounding the bronchioles of Hg; Cd + Cr; Cd + Hg; Cr + Hg and Cd + Cr + Hg.

TEM examined Cd, Cr and Hg alone and in combination on the morphology of type II pneumocytes. These cells have been previously reported to have damage to the ultrastructure after exposure of heavy metals with an increased detachment of the nuclear membrane was observed. The heterochromatin was condensed and the nucleoli were not visible. This effect was the greatest for Cd + Cr, Cd + Hg, Cr + Hg and Cd + Cr + Hg. The consequent nuclear membrane damage and heterochromatin condensation indicates altered cellular functioning, that may lead to disease. Associated with the type II pneumocytes were mast cells which normally are found in the interstitial space together with inflammatory cells such as macrophages, basophils and eosinophils. Degranulation of mast cells results in the release of histamine and attraction of other granulocytes (neutrophils, basophils and eosinophils). These inflammatory mediators cause the release of vasoactive amines and peptides, eicosanoids and pro-inflammatory cytokines. While chronic inflammation is mediated by nitrogen species, proteases and other reactive oxygen species may lead to tissue injury. Increased inflammation is associated with diseases such as asthma, pulmonary fibrosis, emphysema and COPD (Lee and Yang, 2013; Lotvall *et al.*, 2010; Proud and Leigh, 2011).

Apparent changes in the lungs after heavy metal exposure were observed in all the exposed groups overall (Cd; Cr; Hg; Cr + Cd; Cd + Hg; Cr + Hg and Cd + Cr + Hg). These alternations suggest that oxidative stress plays a role through in the inflammatory process.

Numerous studies (Zelikoff *et al.*, 1993; Tátrai *et al.*, 1998; Fortoul *et al.*, 2005) tested the toxicity of Pb in pulmonary tissue of rats and the results obtained indicated an increase in inflammatory cells, reduction of phagocytic activity of the cells in the lungs and necrosis of the ciliated bronchiolar epithelium. In a previous study by Kaczynska *et al.*, (2011), the authors found that after exposure to Pb, the acute effects observed were pathogenic alterations of the lung tissue with enhanced inflammation, injury to the surfactant cells leading to the impairment of the production of surfactant and increased production of fibrotic connective tissue. Additionally, the presences of the several collagen and elastin fibres were noted in the interstitium. Thinning of the alveolar septa was observed; this is evident in the pathology of emphysema.

This study appears, after an extensive evaluation of the literature, to be the first study that investigates the effect of Cd, Cr and Hg alone and in combination on the ultrastructure of lung tissue by assessing the distribution of collagen and elastic fibres.

The clinical implications of heavy metal exposure include asthma, chronic bronchitis and potentially COPD - these are summarised in Figure 5.1. In Figure 5.1, the overall mechanisms of action of the three metals are hypothesised affecting each structure of lung tissue resulting in respiratory diseases. Cd, Cr and Hg induce oxidative damage to the epithelium and pneumocyte type II cells. This promotes inflammatory cell infiltration via the blood and pro-inflammatory factors to be secreted activating BALT influx, mast cells and other lymphocytes to promote the activation of TGF- $\beta$  either by the inflammatory state or by YAP1 and lysyl oxidase. TGF- $\beta$  enhancement promotes the synthesis of collagen type I fibre and fibronectin, disrupting smooth muscle, leading to fibrosis and elastosis of the lung tissue. Continuation of the inflammatory process due to the heavy metal exposure causes airway remodelling, smooth muscle contractibility and elastic recoil. This is observed in the histopathology of asthma and COPD.

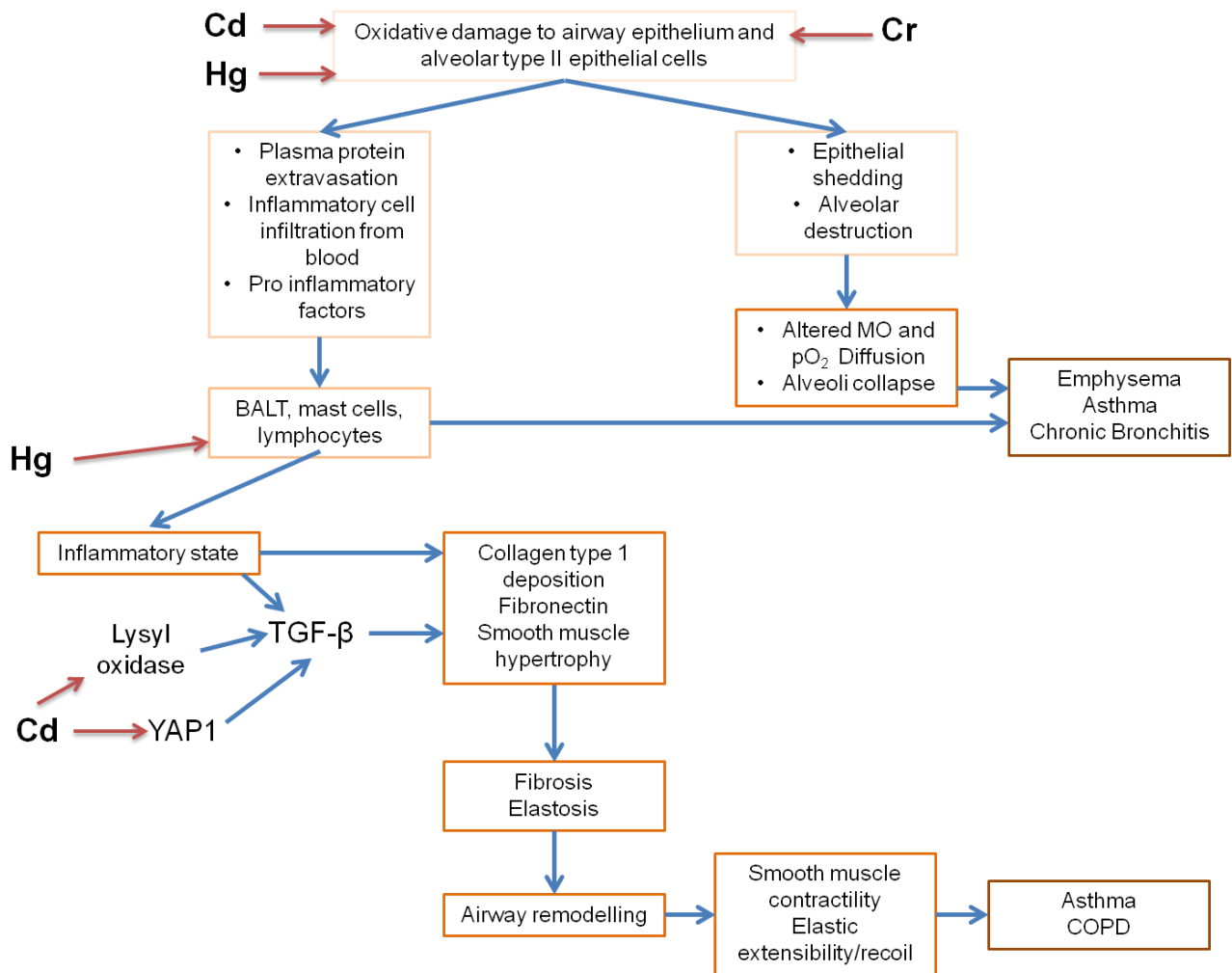


**Figure 5.1:** Flow diagram of the hypothesised method of action of Cd, Cr and Hg on lung tissue, contributing to lung pathologies associated with asthma, chronic bronchitis, COPD and pulmonary fibrosis. Adapted from Salvato, 1968; Jeffery, 1992; Bai *et al.*, 2005; Valko, 2005; Martin and Griswold, 2009; Johri *et al.*, 2010; Jomova and Valko, 2011; King *et al.*, 2011; Tchounwou *et al.*, 2012; Traverso *et al.*, 2013; Jaishankar *et al.*, 2014).

Heavy metals such as Cd, Cr and Hg have been reported to cause oxidative stress (Jaishankar *et al.*, 2014) and the extent of this effect may determine the extent of damage observed in the experimental groups compared to the control. Oxidative stress and the formation of the OH, O<sub>2</sub><sup>-</sup> and ROO radicals are associated with membrane damage. Injury to the nuclear membrane was observed following exposure to the heavy metals Cd, Cr, Hg, Cd + Cr, Cd + Hg, Cr + Hg, Cd + Cr + Hg and this may be the result of ROS generation. ROS has a pro-inflammatory effect, leading to the migration of mast cells, basophils and eosinophils into regions of cellular damage. Inflammatory cells activate the innate pathway of inflammation and initiates increased collagen and elastin production by fibroblasts. Continuous exposure of heavy metals results in chronic inflammation that may result in pulmonary fibrosis. Pulmonary fibrosis leads to hypoxia, as the fibrosis increases the extracellular portion of the barrier resulting in insufficient gas exchange. Likewise Lag *et al.*,

(2009) investigated the effects of Cd induced inflammatory responses in Type 2 epithelial cell-enriched cultures and alveolar macrophages from rat lungs cells relevant for lung toxicity. Fibroblasts were activated at higher concentration of Cd (7  $\mu$ M) compared to lower concentrations of Cd (3-6  $\mu$ M). An exposure of 7  $\mu$ M of Cd was examined to increase inflammatory process by the upregulation of chemokines and their receptors (IL-6 and IRL1). However, no visible effects of inflammatory process were observed at lower concentrations. From the present study, in accordance with the dosages of exposure set by WHO; the lung tissue had profound effects on the ultrastructure of the lungs. Lag *et al.*, (2009) further reported that real time PCR revealed the significant increase of pro-inflammatory factors and cytokines, with enhanced fibroblast secretory factors. Bakshi *et al.*, (2008), conducted an *in vitro* experiment with gold nanoparticles (Au NP) and showed that these particles have the ability to be embedded within pneumocytes II and decreased the surfactant ability to reduce surface tension. The dysfunction in surfactant function increases the resistance and pressure of the airways as cells and gases such as RBC and O<sub>2</sub> move across the alveolar epithelium causing damage to the alveolar cells (Zhao *et al.*, 2010). Heavy metal exposure induces free radical production and oxidative stress contributes to the observed structural changes in the lung tissue. Increased fibrosis is due to collagen and elastin fibre deposition and due to fibroblast activation in an attempt to repair the alveolar epithelium. The extent of fibrosis observed in the current study was dependent on the heavy metal type and combination with other metals. Exposure to Hg alone and Hg combinations were observed to induce more fibrotic changes than Cr and Cd alone. This fibrosis may be a result of inflammation as indicated by the presence of inflammatory cells such as mast cells found in Cd, Cr and Cd + Cr + Hg exposed lung tissue (Table 4.2). The activation of inflammatory cells such as macrophages initiates a pro-fibrotic environment and was observed in Cd; Cr; Hg; Cd + Hg; and Cd + Cr + Hg exposed groups and initiated the development of lung fibrosis (Akers *et al.*, 2000).

Increased accumulation of ROS and associated inflammation is linked to the development of fibrosis (Reuter *et al.*, 2010; Gobe and Crane, 2012; Sanchez-Valle *et al.*, 2012). Metals such as Cd, Cr and Hg alone and in combination act as catalysts of the Fenton reaction and may result in the accumulation of ROS. Binding of these metals to thiol groups can result in the depletion of GSH and consequently the disruption of the antioxidant pathways. Increased ROS causes an increase in inflammation and an increased infiltration of inflammatory cells into the respiratory tissue (Valavanidis *et al.*, 2013; Vattanasit *et al.*, 2013). In addition, Hg induces BALF formation, with influx of inflammatory cells while Cd is known to induce the suppression of apoptotic cells and the cell cycle (Nwokocha *et al.*, 2011). Inflammatory cell mediated TGF- $\beta$  production promotes the synthesis of collagen and the deposition of

collagen along the alveoli. Enhanced smooth muscle hypertrophy was also observed. Increase in deposition and distribution of collagen and elastin fibres may then cause fibrosis or elastosis causing airway remodelling, smooth muscle contractility and elastic recoil overall. The overall histopathology observed is similar to asthma and COPD.

Inflammation is a vital process carried by the immune system and the main function is cellular and tissue protection. However, excess inflammation is potentially harmful as during the process of destroying microbes may also injure healthy tissue. Inflammation is mediated by several regulators and pro-inflammatory molecules (MacNee, 2001; Mall *et al.*, 2004) Mast cells play an important role in acute inflammation which releases stored mediators like histamine. Chronic inflammation often results in inflammatory diseases such as asthma, autoimmune diseases, and cancer. Exposure to heavy metals has led to increased levels of oxidative stress and inflammation associated with upregulation of cytokines and growth factors inducing the production of type I collagen fibres. Increased levels of markers of inflammation have been observed in industrial workers (Assad *et al.*, 2018). Oral or aerosol exposure to heavy metals results in an increase presence of alveolar macrophages and neutrophils observed as tissue inflammation (Pappas, 2011).

The evaluation of the histological changes of the lung tissue observed in this study after exposure to the heavy metals compared to the histopathological alterations of diseases listed in Table 2.1, revealed that the changes observed in the present study are primarily consistent with that of asthma (Bai *et al.*, 2005) including intra-alveolar space thickening, hyperplasia of bronchiolar epithelium, infiltration of BALT and noticeable changes in the presence of collagen and elastin fibres. In the bronchioles, the triple metal combination caused an increase in collagen type I deposition which is associated with the development of asthma (Bai and Knight, 2005). Therefore, damage to the lung tissue is a function of dosage, duration, heavy metal type and combination with other metals that results in direct structural changes to the tissue and indirect induction of inflammation and increased collagen and elastin deposition.

## **Chapter 6: Conclusion**

The reason for the current study was an increasing concern regarding the effects of daily exposure to heavy metals as part of mixtures containing different types of metals at different concentrations and exposure depending on the duration of exposure - it can be acute, sub-acute or chronic. Safety limits have been established for acute exposure and the effect of long-term exposure to low concentrations of metals as part of mixtures is unknown. Aerosol exposure to heavy metals is often associated with disease, particularly respiratory diseases such as COPD, asthma, emphysema and cancer (Ross and Murray, 2004). In addition, communities living close to mining and industrial areas are also often exposed to these heavy metals via their water supply. Little is known regarding the effects of oral exposure to low levels of heavy metals found in water used for drinking, food preparation, washing and the irrigation of crops. The aim of this study was, therefore, to investigate the effects of Cd, Cr and Hg alone and in combination, in a sub-acute model of exposure on the lung tissue of Sprague Dawley rats with specific focus on cellular morphology and ultrastructure as well as the distribution of collagen and elastin.

Light microscopy was used to examine the general morphology of the lung tissue and included the assessment of the alveoli and bronchioles as well as the distribution of collagen and elastin. In the exposed groups (Cd, Cr and Hg, alone and in combination), compared to the control, an increase in thickening of intra-alveolar space with a decrease in the alveolar volume was observed. Desquamation of the epithelial lining of the bronchioles with increased cellular debris, presence of BALT near the bronchioles of the exposed groups and an increase in RBC was observed. An increase in collagen production and distribution, as well as displacement of the elastin and smooth muscle fibres was observed. Cadmium and Hg had the greatest effect on alveolar structure while Hg and Cd + Cr + Hg had the greatest effect on the bronchiole structure.

Transmission electron microscopy was used to assess cellular morphology, and also to evaluate the presence and distribution of collagen and elastin. Compared to the control, heavy metal exposure caused nuclear membrane detachment, and an increase in the deposition of collagen and elastin. Specifically, Hg and Cd exposure in the lungs caused an increase in the deposition of collagen and elastin. The structure of the alveolar epithelium was assessed and an increased presence of mast cells was observed specifically for Cd; Cr; Hg; Cd + Hg; and Cd + Cr + Hg.

The effects of single heavy metal exposure including Cd, Cr and Hg have been thoroughly researched and the effect of these metals on several organs has been documented (Sharma

*et al.*, 1991; Russell *et al.*, 1994; Ross and Murray, 2004; Fortoul *et al.*, 2005; Molokwane *et al.*, 2008; Mishra, 2009). Heavy metals have been reported to interact and produce synergistic toxic effects (Silins and Hogberg, 2011). Synergistic or additive effects may result in the accumulation of ROS and oxidative stress (Valavanidis *et al.*, 2013) resulting in an increase in inflammation, thereby initiating or promoting disease development in the lungs (Knaapen *et al.*, 2004; Valavanidis *et al.*, 2013). In the present study, the concentrations of heavy metals were not the focus but rather outcome of the standard levels of the heavy metals underlined by WHO contributing to the observed effect within the lungs. An example as observed in the present study, exposure to Hg alone causes the same amount of damage as Cd + Cr + Hg which has a higher total metal concentration.

### **6.1 Limitations to the study**

This study has provided preliminary data on the effect of Cd, Cr and Hg alone and in combination on the morphology of lung tissue. Sprague Dawley rats were exposed to 1000X the WHO limits of each metal. The relative rat dosage was calculated, differences in absorption and metabolism can cause differences in the levels of metals in rats compared with humans. In addition, the levels of each metal in the lung tissue were not determined. A limitation of this study was that no quantitative data was generated on the levels of ROS, GSH and inflammatory markers. Although an inflammatory effect was observed, it is not known if this was mediated by the innate (macrophages, neutrophils and eosinophils) or humoral (B-cells, T-cells) immune response and this creates room for further investigation.

### **6.2 Future perspectives**

In the present study a single dosage of each metal was used in the double and triple combinations. Future studies can investigate several concentrations of each heavy metal to evaluate the effects produced within the lung tissue. The concentration of each metal in the lungs of the rats can be correlated with metal levels in the lung biopsy tissue of patients suspected to be exposed to these metals. The levels of ROS, GSH and antioxidant enzymes can be determined in frozen rat lung tissue using standard colorimetric and enzymatic methods. Although, PR staining does show an increase in the deposition of collagen types, IHC can be used to distinguish between the different types of collagen fibres (Table 2.1). The distribution of lysyl oxidase, TFG- $\beta$  and YAP in the lung tissue of exposed rats can be determined also with Immunohistochemistry (IHC) or enzyme-linked immunosorbent assay (ELISA) methods. Lastly, the detection of specific markers of mast cells, eosinophils, basophils, macrophages, or B-cell and T-cells can be used to identify the immune specific inflammatory pathways that are involved.

## **Chapter 7: References**

Adam M. [Internet]. ICP-MS analysis of toxic elements (heavy metals) in 100 municipal water samples from across the United States. NSJ. (Updated June 2013; cited 05 June 2017). Available from: <http://naturalsciencejournal.org/ICP-MS-Analysis-100-Municipal-WaterSamples.html>.

Ahmad SA, Khatun F, Sayed MH, *et al.* 2006. Electrocardiographic abnormalities among arsenic-exposed persons through groundwater in Bangladesh. *J. Health Popul Nutr.* 24(2):221-227.

American Thoracic Society. [Internet]. European Respiratory Society task force. Standards for the diagnosis and management of patients with COPD. (Updated 2005 September 8, cited on the 25 November 2018). Available from: <http://www.thoracic.org/go/copd>.

Anderson RA. 2000. Chromium in the prevention and control of diabetes. *Diabetes Metab.* 26(1): 22-27.

Anyanwu BO, Ezejiofo AN, Igweze Zn and Orisakwe OE. 2018. Heavy metal mixture exposure and effects in developing nations: An update. *Toxics.* 6(4):65-69.

Arbi S. 2014. Exploratory descriptive study of the support tissue in keloids. University of Pretoria: MSc study.

Arruti A, Fernández-Olmo I and Irabien A. 2012. Evaluation of the contribution of local sources to trace metals levels in urban PM<sub>2.5</sub> and PM<sub>10</sub> in the Cantabria region (Northern Spain). *J Environ Monit Assess.* 12(7): 1451-1458.

Arterburn LM, Hall EB and Oken H. 2006. Distribution, interconversion and dose response of n-3 fatty acids in humans. *Am J Clin Nutr.* 83(6):1467-1476.

Asano S, Eto K and Kurisaki E. 2000. Acute inorganic mercury vapor inhalation poisoning. *Pathol Int.* 50(3): 169-174.

Assas N, Sood A, Campen MJ, *et al.* 2018. Metal induce pulmonary fibrosis. *Current Environment Health Reports.* 5(4): 486-498.

Athanazio R. 2012. Airway disease: similarities and differences between asthma, COPD and bronchiectasis. *Clinics (Sao Paulo).* 67(11): 1335-1343.

Awofolu OR, Mbolekwa Z, Mtshemla V, *et al.* 2005. Levels of trace metals in water and sediment from Tyume River and its effects on an irrigated farmland. *AJOL*. 331(1): 87-94.

Bagchi D, Bagchi M and Stohs SJ. 2001. Chromium (VI)-induced oxidative stress, apoptotic cell death and modulation of p53 tumor suppressor gene. *Mol Cell Biochem*. 222(1-2): 149-158.

Bai TR and Knight DA. 2005. Structural changes in the airways in asthma: observations and consequences. *Clin Sci (Lond)*. 108(6): 463-477.

Bakshi MS, Zhao L, Smith R, *et al.* 2008. Metal nanoparticle pollutants interfere with pulmonary surfactant function in vitro. *Biophysic J*. 94(3):855-868.

Balaban RS, Nemoto S and Finkel T. 2005. Mitochondria, oxidants, and aging. *Cell*. 120(4): 483-495.

Balogun WG, Ibrahim RB, Ishola AO, *et al.* 2014. Histological changes in the lungs of adult wistar rats following exposure to paint fumes. *Anat J Afri*. 3(2): 329-335.

Bartosz G. 2008. Reactive oxygen species: destroyers or messengers. *Biochem Pharm*. 77(3):1303-1347.

Bartram HG and Howard G. 2003. Effective Monitoring of Small Drinking-water Supplies in Providing Safe Drinking-water in Small Systems, Cotruvo A, Craun G and Hearne N. 1<sup>st</sup> Eds. CRC Press, Boca Raton, USA, pp: 353-365.

Bas H and Kalender S.2016. Antioxidant status, lipid peroxidation and testis, histoarchitecture induced by lead nitrate and mercury chloride in males rats. *Braz Arch Boil Technol*. 59: 1-9

Beaver LM, Stemmy EJ, Constant SL, *et al.* 2009. Lung injury, inflammation and Akt signalling following inhalation of particulate hexavalent chromium. *Toxicol Appl Pharmacol*. 235(1):47-56.

Begum M and Huq SMI. 2016. Heavy metals contents in soils affected by industrial activities in a southern district of Bangladesh. *Bangladesh J Sci Res*. 29(1): 11-17.

Behndig A, Brown JL, Mudway I, *et al.* 2006. Airway antioxidant and inflammatory responses to diesel exhaust exposure in healthy humans. *Eur Respir J*. 27(2): 359-365.

Bertin G and Averbeck D. 2006. Cadmium: cellular effects, modifications of biomolecules, modulation of DNA repair and genotoxic consequences (a review). *Biochimie*. 88(11): 1549-1559.

Blasiak J, Trzeciak A, Malecka-Panas E, *et al.* 1999. DNA damage and repair in human lymphocytes and gastric mucosa cells exposed to chromium and curcumin. *Teratog Carcinog Mutagen*. 19: 19-31.

Blaurock-Busch E. 2010. Environmental exposure and the toxicity of metals: The South African vs Global problems. *Environ Exposure Toxic Metals*. 2010:1-17

Blaurock-Busch E, Friedle A, Godfrey M, *et al.* 2010. Metal exposure in children of Punjab, India. *Clin Med Insights Ther*. 2: 655-661.

Borges LF, Gutierrez PS, Marana Sebastia HRC, *et al.* 2007. Picrosirius-polarization staining method as an efficient histopathological tool for collagenolysis detection in vesical prolapse lesions. *Micron*. 38: 580-583.

Brambilla E, Travis WD, Colby TV, *et al.* 2001. The new World Health Organisation classification of lung tumours. *Eur Respir J*. 18: 1059-1068.

Brand MD, Affourtit C, Esteves TC, *et al.* 2004. Mitochondrial superoxide: production, biological effects and activation of uncoupling proteins. *Free Radic Biol Med*. 37(6): 755-767.

Butler J, Jayson GG and Swallow AJ 1975. The reaction between the superoxide anion radical and cytochrome c. *BBA*. 408: 215-222.

Byrne JD and Baugh JA. 2008. The significance of nanoparticles in particles induced pulmonary fibrosis. *MJM*. 11(1): 43-50.

Cagliari A, Goldoni M, Acamoia O, *et al.* 2005. The effect of inhaled chromium on different exhaled breath condensate biomarkers among chrome-plating workers. *Environ Health Perspect*. 114(4): 542-546.

Cairncross E, Kisting S, Liefferink M, *et al.* 2013. Case study on Extractive industries prepared for the lancet commission on global governance, report from South Africa. 1-54.

Caruntu C, Boda D, Musat S, *et al.* 2014. Stress induced mast cell activation in glabrous and hairy skin. *Mediators Inflamm*. 2014:105950-105959.

Celikoglu E, Aslanturk A and Kalender Y. 2015. Vitamin E and sodium selenite against mercuric chloride induced lung toxicity in the rats. *Braz Arch Technol.* 58(4): 587-594.

Cheresh P, Kim SJ and Tulasiram S, *et al.* 2013. Oxidative stress and pulmonary fibrosis. *Biochim Biophys Acta.* 1832: 1028-1040.

Cheung KH and Gu JD. 2007. Mechanism of hexavalent chromium detoxification by microorganisms and bioremediation application potential: A review. *Int Biodeterior Biodegrad.* 59(1): 8-15.

Clarkson TW and Magos L. 2006. Overview of the clinical toxicity of mercury. *Clinical Biochem: Int J Lab Med.* 48(4): 257-268.

Codd R, Dillon CT, Levina A, *et al.* 2001. Studies on the genotoxicity of chromium: from the test tube to the cell. *Coord Chem Rev.* 108:1-9.

Cosgrove MP. 2015. Pulmonary fibrosis and exposure to steel welding fumes. *Occup Med.* 65(9): 706-712.

Cullinan P. 2012. Occupation and chronic obstructive pulmonary disease (COPD). *Br Med Bull.* 104(1): 143-161.

Czekaj P, Pałasz T, Lebda-Wyborny G, *et al.* 2002. Morphological changes in lungs, placenta, liver and kidneys of pregnant rats exposed to cigarette smoke. *Int Arch Occup Environ Health.* 75: 27-35.

Dalton TP, Chen Y, Schneider SN, *et al.* 2004. Genetically altered mice to evaluate glutathione homeostasis in health and disease. *Free Radic Biol Med.* 37(10): 1511-1526.

Dapson RW, Fagan C, Kiernan JA, *et al.* 2011. Certification procedures for Sirius red F3B (CI 35780 and Direct red 80). *Biotech Histochem.* 86(3): 133-139.

Davidson PW, Myers GJ and Weiss B. 2004. Mercury exposure and child development outcomes. *Pediatrics.* 113(3): 1023-1029.

Dillon SJ, Tang M, Carter WC and Harmer MP. 2007. Complexion: A new concept for kinetic engineering in material science. *Acta Materialia.* 55(18):6208-6218.

Di Pette A. 2014. Histopathological characteristics of pulmonary emphysema in experimental model. *Einstein.* 12(3): 382:383-388.

Ding M and Shi X. 2002. Molecular mechanisms of Cr (VI) induced carcinogenesis. *Oxygen/Nitrogen Radicals: Cell Injury Dis Mol Cell Biochem*: 37: 293-300.

Durand JF. 2012. The impact of gold mining on the Witwatersrand on the rivers and karst system of Gauteng and North West Province, South Africa. *J Afr Earth Sci*. 68(15): 24-43.

Eastmond DA, MacGregor JT and Sleisinki RS. 2008. Trivalent chromium: Assessing the genotoxic risk of an essential trace element and widely used human and animal nutritional supplement. *Crit Rev Toxicol*. 38(3):569-575

Elinder CG, Lind B, Kjellstrom T, *et al*. 1976. Cadmium in kidney cortex, liver, and pancreas from Swedish autopsies. Estimation of biological half time in kidney cortex, considering calorie intake and smoking habits. *Arch Environ Health*. 31(6): 292-302.

El-Refaiy I and Eissa F. 2012. Protective effects of ascorbic acid and zinc against cadmium induced histopathological, histochemical and cytogenetic changes in rats. *Communicata Scientiae*. 3(3): 162-180.

Ercal N, Gurer-Orhan H and Burns N.A. 2001. Toxic metals and oxidative stress Part I: mechanisms involved in metal induced oxidative damage. *Curr Top Med Chem*.1: 529-539.

Fatoki OS and Awofolu R. 2003. Levels of Cd, Hg and Zn in some surface waters from the Eastern Cape Province, South Africa. *AJOL*. 29(4): 375-380.

Flora SJS, Mittal M and Mehat M. 2008. Heavy metals induce oxidative stress and its possible reversal by chelation therapy. *Indian J Med Res*. 128(4): 501-523.

Fortoul TI, Moncada-Hernandez S, Saldivar-Osorio L, *et al*. 2005. Sex differences in bronchiolar epithelium response after the inhalation of lead acetate. *Toxicol*. 207: 323-330.

Fortoula TI, Saldivar L, Espejel-Mayab G, *et al*. 2005. Inhalation of cadmium, lead or its mixture effects on the bronchiolar structure and its relation with metal tissue concentrations. *Environ Toxicol Pharmacol*.19: 329-334.

Fridovich I.1995. Superoxide radical and superoxide dismutases. *Annu Rev Biochem*.64: 97-112.

Fubini B and Hubbard A. 2002. Reactive oxygen species (ROS) and reactive nitrogen species (RNS) generation by silica in inflammation and fibrosis. *Free Radic Biol Med*. 34(12): 1507-1516.

Fucic A, Gamulin M, Ferencic Z, *et al.* 2010. Lung cancer and environmental chemical exposure: A review of our current state of knowledge with reference to the role of hormones and hormone receptor as an increase risk factor for developing lung cancer in man. *Toxicol Pathol.* 38: 849-855.

Gartner LP, Hiatt JL and Strum JM. 2005. *Cell Biology and Histology*. 5th ed. Philadelphia, USA. Lippincott Williams and Wilkins. pp 210-217.

Gibb HJ, Lees PSJ, Pinsky PF, *et al.* 2000. Lung cancer among workers in chromium chemical production. *Am J Ind Med.* 38(2): 115-126.

Godt J, Scheidig F, Grosse-Siestrup C, *et al.* 2006. The toxicity of cadmium and resulting hazards for human health. *J Occup Med.* 1(22): 1-6.

Goldoni M, Caglieri A, Corradi M, *et al.* 2008. Chromium in exhaled breath condensate and pulmonary tissue of non-small cell lung cancer patients. *Int Arch Occup Environ Health.* 81(4): 487-493.

Gonzales JN, Lucas R and Verin AD. 2015. The acute respiratory distress syndrome: Mechanisms and perspective therapeutic approaches. *Austin J Vasc Med.* 2(1):1009-1032.

Gorrini C, Harris I and Mak TW. 2013. Modulation of oxidative stress as an anticancer strategy. *Nat Rev Drug Disc.* 12: 931-947.

Grandjean P, Satoh H, Murata K, *et al.* 2010. Adverse effects of methylmercury: Environmental health research implication. *Environ Health Persp.* 118(8): 1137-115.

Gu Q, and Lin RL. 2010. Heavy metals zinc, cadmium and copper stimulate pulmonary sensory neurons via direct activation of TRPA1. *J Appl Physiol.* 108: 891-897.

Guan WJ, Zheng XY, Chung KF and Zhong NS. 2016. Impact of air pollution on the burden of chronic respiratory disease in China: time for urgent action. *The Lancet.* 388(10054):15-21.

Halliwell B and Gutteridge JMC. 2007. *Free Radicals in Biology and Medicine*. 4<sup>th</sup> Eds. Oxford University Press, pp: 205-215.

Hamid Q. 2003. Gross pathology and histopathology of asthma. *Journal Allergy Clin Immunol.* 111(2): 431-432.

Hamzah NA, Tamrin SBM and Ismail NH. 2016. Metal dust exposure and lung function deterioration among steel workers: an exposure-response relationship. *Int J Occup Environ Health*. 22(3): 224-232.

Hansen TW, Wagner JB, Hansen PI, Dhal S, *et al.* 2001. Atomic resolution *in situ* transmission electron microscopy of a promoter of a heterogenous catalyst. *Science*. 294(5546): 1508-1510.

Hirschberg A, Sherman S, Bucher A, *et al.* 1999. Collagen fibres in the wall of odontogenic keratocysts: a study with picosirius red and polarizing microscopy. *J Oral Path Med*. 28(9): 410-412.

Hogg J and Senior R. 2002. Chronic obstructive pulmonary disease c2: Pathology and biochemistry of emphysema. *Thorax*. 57(9): 830-834.

Horowitz HM, Jacob DJ, Amosell HM, *et al.* 2014. Historical mercury release from commercial products: global environment implications. *Environ Sci Technol*. 48(17): 1042-10250.

Huff JM, Lunn RM, Waalkes MP, *et al.* 2007. Cadmium-induced cancers in animals and in humans. *Int J Occup Environ Health*. 13(2): 202-212

Humphrey JD, Dufresne ER and Scharzt MA. 2014. Mechanotransduction and extracellular matrix homeostasis. *Nat Rev Mol Cell Biol*. 15: 802-812.

Huvinen M, Uitti J, Oksa P, *et al.* 2002. Respiratory health effects of long term exposure to different chromium species in stainless steel production. *Occup Med*. 52(4): 203-212.

Ibrahim ZI, Ahmed JA and Chelab KG. 2016. Histopathological evaluation of pulmonary effects of sodium dichromate CR VI in rats. *J Agri Vet Sci*. 9(4):13-17.

Ichinose M, Sugiura H, Yamagata S, *et al.* 2000. Increase in reactive nitrogen species production in chronic obstructive pulmonary disease airways. *ATS J*. 162(2): 81-96.

Il'yasova D. 2005. Cadmium and renal cancer. *Toxicol Appl Pharmacol*. 207(2):179-186.

Institute of Medicine (IOM). 2001. Dietary Reference Intakes for Vitamin A, Vitamin K, Arsenic, Boron, Chromium, Copper, Iodine, Iron, Manganese, Molybdenum, Nickel, Silicon, Vanadium, and Zinc. Food and Nutrition Board, Institute of Medicine. National Academy Press, Washington, DC. pp 309-321.

International agency for research on cancer. 2012. IARC monographs on the identification of carcinogenic hazards to humans: Chemical agents and related Occupations. 100F:1-567.

Islam LN, Nabi AHM, Rahman N, *et al.* 2007. Association of respiratory complication and elevated serum immunoglobulins with drinking water arsenic toxicity in humans. *J Environ Sci Health, Part A.* 42(12): 1804-1813.

Jaishankar M, Tseten T, Anbalagan N, *et al.* 2014. Toxicity, mechanism and health effects of some heavy metals. *Interdiscip Toxicol.* 7(2): 60-72.

Jancic SA and Stosic B. 2014. Cadmium effects on the thyroid gland. *Vitamin Horm.* 94: 392-425.

Jarup L. 2003. Hazards of heavy metal contamination. *Br Med Bull.* 68(1):167-182.

Jasinski SM. 2012. The materials flow of mercury in the United States. *USBM Inform Circular.* 9412: 1-10.

Jeffery P. 2001. Inflammation and remodelling in the adult and child with asthma. *Pediatr Pulmon.* 32(21): 3-16.

Jeffery PK. 1992. Histological feature of the airways in asthma and COPD. *Respir.* 59(1): 13-16.

Jemal A, Thomas A, Murray T, *et al.* 2002. Cancer Statistics. *CA Cancer J Clin.* 52:23-47.

Jin T, Nordberg M, Frech W, Dumont X, *et al.* 2002. Cadmium biomonitoring and renal dysfunction among a population environmentally exposed to cadmium from smelting in China. *BioMetals.* 15(4): 397-410.

Johri N, Jacquillet G and Unwin R. 2010. Heavy metal poisoning: the effects of cadmium on the kidney. *BioMetals.* 23(5):783-792.

Jomova K and Valko M. 2011. Advances in metal induced oxidative stress and human disease. *Toxicol.* 283:65-87.

Jones DP. 2006. Extracellular redox state: refining the definition of oxidative stress in aging. *Rejuvenation Res.* 9: 169-181.

- Junqueira LC, Bignolas G and Brentani RR. 1979. Picrosirius staining plus polarization microscopy, a specific method for collagen detection in tissue sections. *Histochemistry*. 11(4): 447-455.
- Kaczynska, K, Walski M and Szereda-Przestaszewska M. 2011. Ultrastructural changes in lung tissue after acute lead intoxication in the rat. *J Electron Microsc (Tokyo)*. 60:289-294.
- Karaman M, Ayyidliz ZA, Firinci F, *et al.* 2011. Effects of curcumin in lung histopathology and fungal burden in a mouse model of chronic asthma and oropharyngeal candidiasis. *Arch Med Res*. 42: 79-87.
- Kasper M, Seidel D, Knels L, *et al.* 2004. Early signs of lung fibrosis after in vitro treatment of rat lung slices with CdCl<sub>2</sub> and TGF-β<sub>1</sub>. *Histochem Cell Biol*. 121(2): 131-140.
- Kauf E, Dawczynski H, Jahreis G, *et al.* 1994. Sodium selenite therapy and thyroid hormone status in cystic fibrosis and congenital hypothyroidism. *Biol Trace Elem Res*. 40(3): 247-253.
- Kazemipour M, Ansari M, Tajrobehkar S, *et al.* 2008. Removal of lead, cadmium, zinc and copper from industrial wastewater by carbon developed from walnut, hazelnut, almond, pistachio shell and apricot stone. *J Hazard Mater*. 150(2): 322-327.
- Kazlouskaya V, Malhotra S, Lambe J, *et al.* 2013. The utility of elastin Verhoeff Van Gieson staining in dermatopathology. *J Cutan Pathol*. 40: 211-255.
- Khelifi R and Hamza-Chaffai A. 2010. Head and neck cancer due to heavy metal exposure via tobacco smoking and professional exposure: A review. *Toxicol Appl Pharmacol*. 248(2): 71-88.
- Khuder SA. 2001. Effects of cigarette smoking on major histological types of lung cancer: a meta-analysis. *Lung Cancer*. 31(3): 139-148.
- Kielty CM, Sherratt MJ and Shuttleworth CA. 2002. Elastic Fibres. *J Cell Sci*. 115(Pt 14):2817-2828.
- Kim DS, Park JH, Park BK, Lee JS, *et al.* 2006. Acute Exacerbation of idiopathic pulmonary fibrosis: frequency and clinical features. *Eur Respir J*. 27: 143-150.
- Kindlen S. 2003 *Physiology for Health Care and Nursing*. 2<sup>nd</sup> ed Churchill Livingstone, London; pp 125-138.

King TE, Pardo A and Selman M. 2011. Idiopathic pulmonary fibrosis. *Lancet*. 378(9807): 1949-1961.

Kinnula VL and Crapo JD. 2003. Superoxide dismutases in the lung and human lung diseases. *Am J Respir Crit Care Med*. 167(12):1600-1619.

Knaapen M, Bornm PJA, Ablrecht C, *et al*. 2004. Inhaled particles and lung cancer: Part A, Mechanisms. *Int J Cancer*. 100(6): 799-809.

Kozel BA, Rongish BJ, Czirok A, *et al*. 2006. Elastic fiber formation: a dynamic view of extracellular matrix assembly using timer reporters. *J Cell Physiol*. 207:87-96.

Kulkarni T, O'Reilly P, Antony VB, *et al*. 2016. Matrix remodelling in pulmonary fibrosis and emphysema. *Am J Respir Cell Mol Biol*. 54(6):751-760.

Lag M, Rodionov D, Ovrevk J, *et al*. 2010. Cadmium induced inflammatory response in cells relevant for lung toxicity: Expression and release of cytokines in fibroblast, epithelial cells and macrophages. *Toxicol Lett*. 193(3): 252-260.

Lakey PSJ, Berkemeier T, Tong H, *et al*. 2016. Chemical exposure-response relationship between air pollutants and reactive oxygen species in the human respiratory tract. *Sci Rep*. 6: 32916-32922.

Langard S, Andersen A and Ravnstad J. 1990. Incidence of cancer among ferrochromium and ferrosilicon workers: An extended observation periods. *Occupat Environ Medic*. 47(1): 14-19.

LeBeau JM, Findlay SD, Leslie JA, *et al*. 2008. Quantitative atomic resolution scanning transmission electron microscopy. *Phys Rev J*. 100(20): 260-261.

Lee IT and Yang CM. 2013. Inflammatory signalings involved in airways and pulmonary diseases. *Mediators Inflamm*. 2013. 1-13.

Leem AY, Kim SK, Chang J, *et al*. 2015. Relationship between blood levels of heavy metals and lung function based on the Korean National Health and Nutrition Examination Survey IV–V. *Int J Chron Obstruct Pulmon Dis*. 10: 1559-1570.

Li N, Xia T and Nel AE. 2008. The role of oxidative stress in ambient particulate matter-induced lung diseases and its implications in the toxicity of engineered nanoparticles. *Free Radic Biol Med*. 44: 1689-1699.

- Liigand P, Kaupmees K and Kruve A. 2016. Ionization efficiency of doubly charge ions formed from polyprotic acids in electrospray negative mode. *J Am Society Mass Spectro.* 27(7): 1211-1218.
- Lim HE, Shim JJ and Lee, SY. 1998. Mercury inhalation poisoning and acute lung injury. *Korean J Int Med.* 13(2): 127–130.
- Liu Y, Wang X, Zeng G, *et al.* 2007. Cadmium-induced oxidative stress and response of the ascorbate–glutathione cycle in *Bechmeria nivea* (L.) Gaud. *Chemosphere.* 69(1): 99-107.
- Lloyd RV, Hanna PM and Mason RP. 1997. The origin of the hydroxyl radical oxygen in the Fenton reaction. *Free Radic Biol Med.* 22: 885-888.
- Lodovici M and Bigagli E. 2011. Oxidative stress and air pollution exposure. *J Toxicol.* 2011:1-9.
- Lovtall J, Akdis CA, Bacharier LB, *et al.* 2011. Asthma endotypes: A new approach to classification of diseases entities within the asthma syndrome. *J Allergy Clin Immunol.* 127(2): 355-360.
- Lu TH, Chen CH, Lee MJ, *et al.* 2010. Methylmercury chloride induces alveolar type II epithelial cell damage through an oxidative stress-related mitochondrial cell death pathway. *Toxicol Letters.* 194(3):70-78
- Lui X, Song Q, Tang Y, *et al.* 2013. Human health risk assessment of heavy metals in soil–vegetable system: A multi-medium analysis. *Sci Total Environ.* 436: 530-540.
- Lund BO, Miller D and Woods JS. 1991. Mercury-induced H<sub>2</sub>O<sub>2</sub> production and lipid peroxidation in vitro in rat kidney mitochondria. *Biochem Pharmacol.* 42(11): 181-187.
- MacNee W. 2001. Oxidative stress and lung inflammation in airways disease. *Eur J Pharma.* 429(1): 195-207.
- Male YT, Reichelt-Brushette AJ, Pocock H, *et al.* 2013. Recent mercury contamination artisanal gold mining on Buru Island Indonesia: Potential future risks to environmental health and food safety. *Mar Pollut Bull.* 77(1-2): 428-433.
- Mall M, Grubb BR, Harkema JR, *et al.* 2004. Increase airway epithelial Na<sup>+</sup> absorption produces cystic fibrosis like lung diseases in mice. *Nat Med.* 10:487-493.

Mamuya SHD, Bratveit M, Mashalla Y, *et al.* 2007. High prevalence of respiratory symptoms among workers in the development section of a manually operated coal mine in a developing country: A cross sectional study. *BioMed Central*. 2458: 7-17.

Marcos JV, Munoz-Barrutia A, Ortiz-de-Solorzano C, *et al.* 2015. Quantitative assessment of emphysema severity in histological lung analysis. *Ann Biomed Eng*. 43(10): 2515-2529.

Martin S and Griswold W. 2009. Human health effects of heavy metals. *Center Hazard Sub Res*.15: 1-6.

Maseki J, Annegarn HJ and Spiers G. 2017. Health risk posed by enriched heavy metals (As, Cd and Cr) in airborne particles Witwatersrand gold tailings. *J S Afri Inst Min Metall*. 117: 663-670.

Masella R, Di Benedetto E, Vari R, *et al.* 2005. Novel mechanisms of natural antioxidant compounds in biological systems involvement of glutathione and glutathione-related enzymes. *J Nutritional Biochem*. 16(10): 577-586.

Mathew B.B, Tiwari A and Jatawa S.K. 2011. Free radicals and antioxidants: A review. *J Pharm Res*. 4(12): 4340-4343.

Matins V, Minguillon MC, Moreno T, *et al.* 2015. Depositon of aerosol particles from a subway microenvironment in the human respiratory tract. *J Aerosol Sci*. 90:103-113.

Mayans J.D, Laborda R and Nunez A.1985. Hexavalent chromium effects in motor activity and some metabolic aspects of Wistar albino rats. *Biochem Physiol*. 83(1): 191-195.

McCullen K.S. 1969. Vascular pathology of homocysteinemia: Implications for the pathogenesis of arteriosclerosis. *Homocysteinemia*. 56(1): 111-128.

Mescher AL. 2010. *Juqueira's Basic Histology*, 12th ed, McGraw Hill Companies, USA. pp 375-394.

Miller BE and Hook GE.1990. Hypertrophy and hyperplasia of alveolar type II cells in response to silica and other pulmonary toxicants. *Environ Health Perspect*. 85:15-23.

Mora AL, Torres-Gonzalez E, Rojas M, *et al.* 2006. Activation of alveolar macrophages via the alternative pathway in herpesvirus-induced lung fibrosis. *AJRCM*. 35(4): 466-473.

Moromisato, DY, Anas, NG and Goodman, G. 1994. Mercury inhalation poisoning and acute lung injury in a child. Use of high-frequency oscillatory ventilation. *Chest*. 105(2): 613-615.

Murray JF. 2011. Pulmonary oedema: pathophysiology and diagnosis. *Int J Tuberc Lung Dis.* 15(2): 155-160.

Murry CJ and Lopez AD. 1996. Global health statistic: A compendium of incidence, prevalence and mortality estimates for over 200 conditions. *Science.* 274: 739-744.

Myers GJ, Davidson PW and Strain JJ. 2007. Nutrient and methyl mercury exposure from consuming fish. *JN.* 137(12): 2805-2808.

Naicker K, Cukrowska E and McCarthy TS. 2003. Acid mine drainage from gold mining activities in Johannesburg, South Africa and environs. *Environ Pollut.* 122: 29-40.

Nawrot TS, Staessen JA, Roels HA, *et al.* 2010. Cadmium exposure in the population: from health risks to strategies of prevention. *BioMetals.* 23(5): 769-782.

Novelli JLVV, Novelli ELB, Manzano MA, *et al.* 2000. Effect of tocopherol on superoxide radical and toxicity of cadmium exposure. *Inter J Environ Health Res.* 10: 125-134.

Nwokocha CR, Nwokocha MI, Owu DU, *et al.* 2011. Estimation of absorbed cadmium in tissue of males and females albino rats through different routes of administration. *Nig J Physio Sci.* 26: 097-101.

O'Connor JM. 2001. Trace elements. *Biochem Soc Trans.* 29(2): 354-358.

Occupational Safety and Health Administration (OSHA), Department of Labor. 2006. (Occupational Exposure to Hexavalent Chromium). Final rule Fed Regist. 71: 10099-10385.

Occupational Safety and Health Administration (OSHA). 1998. Occupational Safety and Health Standards, Toxic and Hazardous Substances. Code of Federal Regulations. 29 CFR 1910.1000.

Occupational Safety and Health Administration Cadmium. [Accessed December 19, 2017]. Available from: <https://www.osha.gov/Publications/3136-08R-2003-English.html#contents>.

Odeyemi C, Latinwo LM, Badisa VLD, *et al.* 2018. Modulation of cadmium induced apoptotic, cancer and inflammation related cytokines by diallyl disulfide in rat liver cells. *Ann Toxicol.* 1(1):1-8.

Ogunbileje JO, Nawgiri RS, Anetor JI, *et al.* 2014. Particles internalization, oxidative stress apoptosis and pro-inflammatory cytokines in alveolar macrophages exposed to cements dust. *Environ Toxicol Pharmacol.* 37(3): 1060-1070.

Ohta H and Cherian MG. 1991. Gastrointestinal adsorption of cadmium and metallothioneins. *Toxicol Appl Pharmacol.* 107(1): 63-72.

Okado-Matsumoto A and Fridovich I. 2001. Subcellular distribution of superoxide dismutases (SOD) in rat liver: Cu, Zn-SOD in mitochondria. *J Biol Chem.* 276: 38388-38393.

Olujimi OO, Ajayi OL and Oputu OU. 2016. Toxicity assessment of olusosun and igando leachates using the African catfish (*clarias gariepinus*) as bioindicator species part I. *Life Sci.* 18(3):693-701.

Omrane F, Gargouri I, Khadhraoui M, *et al.* 2018. Risk assessment of occupational exposure to heavy metals mixtures: a study protocol. *BMC Public Health.* 18(314):1-11.

Onydio I, Norris AR and Buncl E. 2000. Biomolecule, mercury interactions: modalities of DNA base, mercury binding mechanism remediation strategies. *Chem Rev.* 104: 5911-5929.

Ortega-Villasante C, Hernández LE, Rellán-Álvarez R, *et al.* 2007. Rapid alteration of cellular redox homeostasis upon exposure to cadmium and mercury in alfalfa seedlings. *New Phytol.* 176(1): 269-305.

Ouyang L, Shi Z, Zhao S, *et al.* 2012. Programmed cell death pathways in cancer: a review of apoptosis, autophagy and programmed necrosis. *Cell Proliferat.* 45(6): 487-498.

Pacyna EG, Pacyna JM, Sundseth K, *et al.* 2010. Global emission of mercury to the atmosphere from anthropogenic sources in 2005 and projections to 2020. *Atmos Environ.* 44(20): 2487-2499.

Paolucci G, Folletti I, Toren K, *et al.* 2018. Occupational risk factors for idiopathic pulmonary fibrosis in southern Europe: a case control Study. *BMC Pulm Med.* 18: 75

Pappas RS. 2011. Toxic elements in tobacco and in cigarette smoke: Inflammation and sensitization. *Metallomics.* 3(11):1181-1198.

Parkin D.M. 2001. Cancer burden in the year 2000: The global picture. *Europ J Can.* 37:4-66.

Patra RC, Rautray AK and Swarup D. 2011. Oxidative stress in lead and cadmium toxicity and its amelioration. *Veter Med Int.* 2001: 1-9

Perez-Campana C, Gomez-Vallejo V, Puigivilla M, *et al.* 2013. Bio-distribution of different sized nanoparticles assessed by positron emission tomography: a general strategy for direct activation of metal oxide particles. *ACS Nano.* 7(4): 3498-3505.

Pesch B, Haerting J, Ranft U, *et al.* 2000. Occupational risk factors for renal cell carcinoma: agent-specific results from a case-control study in Germany. *J Epidemiol.* 29(6): 1014-1024.

Phaniendra A, Jestadi DB and Periyasamy L. 2015. Free radicals: Properties, sources, targets and their implications in various disease. *Indian J Clin Biochem.* 30(1):11-26.

Pompella A, Visvikis A, Paolicchi A, *et al.* 2003. The changing faces of glutathione, a cellular protagonist. *Biochem Pharmacol.* 66: 1499-503.

Proud D and Leigh R. 2011. Epithelial cell and airways diseases. *Immunol Rev.* 242(1):186-204

Prousek, J. 2007. Fenton chemistry in biology and medicine. *Pure Appl Chem.* 79: 2325-2338.

Quiévryn G, Messer J and Zhitkovich A. 2002. Carcinogenic chromium (VI) induces cross-linking of vitamin C to DNA in vitro and in human lung A549 cells. *Biochem.* 41: 3156-3167.

Raghu G, Weycker D, Edelsberg J, *et al.* 2006. Incidence and prevalence of idiopathic pulmonary fibrosis. *AJRCCM.* 174(7): 810-816.

Reagan-Shaw S, Nihal, M and Ahmad N. 2008. Dose translation from animal to human studies revisited. *FASEB J.* 22(3):659-661.

Reuter S, Gupta SC, Chaturvedi MM, *et al.* 2010. Oxidative stress, inflammation and cancer: How are they linked? *Free Radic Biol Med.* 49(11):1603-1616.

Ricodela C, Darchenb A and Hadjiev D. 2010. Electrocoagulation-electroflotation as surface water treatment for industrial uses. *Sep Purif Technol.* 74: 342-347.

Ristovski ZD, Miljevic B, Surawsko NC, *et al.* 2011. Respiratory health effects of diesel particulate matter. *Respirology.* 17(2): 201-212.

Robert JR, Antonini JM, Porter DW, *et al.* 2013. Lung toxicity and biodistribution of Cd/Se-ZnS quantum dots with different surface functional groups after pulmonary exposure in rats. *Particle Fibre Toxicol.* 10:26-35.

Ros JPM and Slooff W. 1987. Integrated criteria document on cadmium; Bilthoven. National Institute of Public Health and Environmental Protection (Report No. 758476004).

Ross MH and Murray J. 2004. Occupational respiratory disease in mining. *Occup Med.* 54(5): 304-310.

Rowens B, Guerrero-Betancourt D and Gottlieb CA. 1991. Respiratory failure and death following acute inhalation of mercury vapor. A clinical and histologic perspective. *Chest.* 99(1): 185–190.

Russell WJ, Matalon S and Jackson RM. 1994. Manganese superoxide dismutase expression in alveolar type II epithelial cells from nonventilated and hypoperfused lungs. *Am J Respir Cell Mol Biol.* 11: 366-371.

Salvato G. 1968. Some histological changes in chronic bronchitis and asthma. *Thorax.* 23(2): 168-172.

Santillan AA, Camargo CA and Colditz GA. 2003. A meta-analysis of asthma and risk of lung cancer (United States). *Cancer Causes Control.* 14: 327-334.

Sarin V, Singh TS and Pant KK. 2006. Thermodynamic and breakthrough column studies for the selective sorption of chromium from industrial effluent on activated eucalyptus bark. *Bioresour Technol.* 97(16): 1986-1993.

Sarkar A, Ravindran G and Krishnamurthy V. 2013. A brief review on the of cadmium toxicity; from cellular to organ level. *Int J Biotech.* 3:17-36.

Satarug S, Baker JA, Urbenjapol S, *et al.* 2003. A global perspective on cadmium pollution and toxicity in non-occupationally exposed population. *Toxicol Letters.* 137(1): 65-83.

Sedman RM, Beaumont J, McDondal TA, *et al.* 2006. Review of the evidence regarding the carcinogenicity of hexavalent chromium in drinking water. *J Environ Sci Health, Part C.* 24(1): 155-182.

Seidal K, Jorgensen N, Elinder CG, *et al.* 1993. Fatal cadmium-induced pneumonitis. *Scand J Work Environ Health.* 19(6): 429-431.

Selma M and Pardo S. 2003. Cigarette smoke exposure potentiates bleomycin-induced lung fibrosis in guinea pigs. *Am J Physiol Lung Cell Mol Physiol*. 285(4): 949-956.

Sharma G, Sandhir R, Nath R, *et al.* 1991. Effects of ethanol on cadmium uptake and metabolised of zinc and cooper in rats exposed to cadmium. *J Nutr*.121: 87-91.

Shi X and Dalai NS. 1990. On the hydroxyl radical formation in the reaction between hydrogen peroxide and biologically generated chromium (V) species. *Arch Biochem Biophys*. 277: 342-350.

Shigematsu H, Lin L, Takahashi T, *et al.* 2005. Clinical and biological features associated with epidermal growth factor receptor gene mutations in lung cancer. *J Nat Cancer Instit*. 97(5): 339-346.

Shrivastava VK and Sathyanesan AG.1988. Effects of cadmium chloride on thyroid activity of the female Indian palm squirrel, *Funambulus pennanti*. *Environ Contam*. 40: 268-272.

Singh A, Mehta SK and Gaur JP. 2007. Removal of heavy metals from aqueous common freshwater filamentous algae. *World J Microbiol Biotechnol*. 23: 1115-1127.

Singh N, Gupta VK, Kumar A and Sharma B. 2017. Synergistic effects of heavy metals. *Frontiers Chem*. 5(70): 1-9.

Smiechowicz J, Skocynska A, Nieckula-Szarc A, *et al.* 2017. Occupational mercury vapour poisoning with a respiratory failure, pneumomediastinum and severe quadriparesis. *SAGE Open Med Case Rep*. 5:1-4.

Snider GL. 1985. Distinguishing among asthma, chronic bronchitis and emphysema. *Chest*. 87: 35-39.

Department of Water affairs and forestry. 1996. South African water quality Guidelines. 1:1-190.

Soussa E, Shalaby Y, Maria AM, *et al.* 2013. Evaluation of oral tissue response and blood levels of mercury released from dental amalgam in rats. *Arch Oral Biol*. 58(8)-981-988.

Stearns DM and Wetterhahn KE.1997. Intermediates produced in the reaction of Cr(VI) with dehydroascorbate causes single-strand breaks in plasmid DNA. *Chem Res Toxicol*.10: 271-278.

Steven J and Lowe A. 2005. Human Histology. 4<sup>th</sup> ed. Mosby Ltd: Philadelphia, USA. pp 167-185

Suki B, Lutchen KR and Ingenito EP. 2003. On the progressive nature of emphysema: roles of proteases, inflammation, and mechanical forces. *Am J Respir Crit Care Med.* 168: 516-521.

Suttorp N, Toepfer W and Roka L. 1986. Antioxidant defense mechanisms of endothelial cells cycle versus catalase. *Am J Physiol.* 251(5): 671-680.

Sznoppek JL and Goonan TG. 2000. The material flow of mercury in the economies of the United States and the world. *US Geological Survey Circular.* 1-19.

Szyczewski P, Siepak J, Niedzielski P, *et al.* 2009. Research on heavy metals in Poland. *Pol J Environ Stud.* 18(5): 755-768.

Tajudeen Y, Okpuzor J and Fausat AT. 2011. Investigation of general effects cement dust to clear the controversy surrounding its toxicity. *Asian J Sci Res.* 4(4): 315-325.

Tang K, Wagner PD, and Baker AB. 2005. Effects of alveolar dead-space, shunt and V/Q distribution on respiratory dead-space measurements. *BJA.* 95(4): 538-548.

Tátrai E, Náráy M, Brózik M, *et al.* 1998. Combined pulmonary toxicity of diethyldithiocarbamate and lead oxide in rats. *J Appl Toxicol.* 18: 33–37.

Tchounwou PB, Yedjou CG, Patlolla AK, *et al.* 2012. Heavy metals toxicity and the environment. *NIH.* 133-164.

Terzano C, Di Stefano F, Conti V, *et al.* 2010. Air pollution ultrafine particles: toxicity beyond the lung. *Eur Rev Med Pharmacol Sci.* 14: 809-821.

Tetley TD. 2002. Macrophages and the pathogenesis of COPD. *Chest.* 121(5):156S-159S

Todd N, Luzina IG and Atamas SP. 2012. Molecular and cellular mechanisms of pulmonary fibrosis. *Fibrogenesis Tissue Repair.* 5(1):11-86.

Townsend DM, Tew KD and Tapiero H. 2003. The importance of glutathione in human disease. *Biomed Pharmacother.* 57(3-4): 145-155.

U.S. Environmental Protection Agency. 1999. Integrated Risk Information System (IRIS) on Mercuric chloride. National Center for Environmental Assessment, Office of Research and Development, Washington, DC.

Valavanidis A, Vlachogianni T, Fiotakis K, *et al.* 2013. Pulmonary oxidative stress, inflammation and cancer: Respirable particulate matter, fibrous dusts and ozone as major causes of lung carcinogenesis through reactive oxygen species mechanisms. *Int J Environ Res Public Health.* 10(9): 3886-3907.

Valavanidis A, Vlahogianni T, Dassenakis M, *et al.* 2006. Molecular biomarkers of oxidative stress in aquatic organisms in relation to toxic environmental pollutants. *Ecotoxicol Environ Saf.* 64(2): 178-189.

Valko M, Izakovic M, Mazur M, *et al.* 2004. Role of oxygen radicals in DNA damage and cancer incidence. *Mol Cell Biochem.* 266: 37-56.

Valko M, Morris H and Cronin MTD. 2005. Metals, toxicity and oxidative stress. *Curr Med Chem.* 12: 1161-1208.

Van Zandwijk N. 1995. N-Acetylcysteine (NAC) and glutathione (GSH): Antioxidant and chemopreventive properties, with special reference to lung cancer. *J Cell Biol.* 22: 24-32.

Velindala S, Gaikwad P, Ella KKR, *et al.* 2014. Histochemical analysis of polarizing colours of collagen using Picro Sirius red staining in oral submucous fibrosis. *J Int Oral Health.* 6(1): 33-38.

Venter C, Oberholzer HM, Cumming FR, *et al.* 2017. Effects of metals cadmium and chromium alone and in combination on the liver and kidney tissue of male Sprague Dawley rats: An ultrastructural and electron energy loss spectroscopy investigation. *Microsc Res Tech.* 80(8): 878-888.

Volckaert T and De Langhe S. 2014. Lung epithelial stem cells and their niches: FGF10 takes center stage. *Fibro Tissue Repair.* 7:8-16.

Wegner P, Kleinstauber G and Baum F. 2005. Long-term investigation of the degree of exposure of German peregrine falcons (*Falco peregrinus*) to damaging chemicals from the environment. *J Ornithol.* 146: 34-54.

WHO/UNICEF.2011. Drinking Water: Equity, Safety and Sustainability. WHO/UNICEF, Geneva, Switzerland.

Williams DB. 1996. Transmission electron Microscope. Springer Science and Business Media, New York. Chapter 1:1-15. pp159-167.

Wise JP, Wise SS and Little JE. 2002. The cytotoxicity and genotoxicity of particulate and soluble hexavalent chromium in human lung cells. *Mutat Res Genet Toxicol Environ Mutagen*. 517(1-2): 221-229.

World Health Organisation. 2010. Risk of a range of cancers in professional painter.

World Health Organisation, International agency for research in cancer. 2002. IARC monographs on the evaluation of carcinogenic risk to humans. 82: 1-557.

Wu KG, Chang CY, Yen CY, *et al*. 2018. Associations between environmental heavy metal exposure and childhood asthma: A population based study. *J Microbiol Immunol Infect*. 1-11.

Ynalvez R, Gutierrez J and Gonzalez-Cantu H. 2016. Mini-review: toxicity of mercury as a consequence of enzyme alteration. *BioMetals*. 29(5): 781-788.

Yoshizuka M, Mori N, Hamasaki K, *et al*. 1991. Cadmium toxicity in the thyroid gland of pregnant rats. *Exp Mol Path*. 55: 97-104.

Yuan G, Dai S, Yin Z, *et al*. 2014. Toxicological assessment of combined lead and cadmium: Acute and sub-chronic toxicity study in rat. *Food Chem Toxicol*. 65: 260-268.

Yurchenco PD, Birk DE and Mecham RP. 2003. Extracellular matrix assembly and structure. Academic press; San Diego. pp4-23.

Zalup RK AS. 2003. Molecular handling of cadmium in transporting epithelia. *Toxicol Appl Pharmacol*. 186(3): 163-188.

Zelikoff JT, Parsons E and Schlesinger RB. 1993. Inhalation of particulate lead oxide disrupts pulmonary macrophage mediated functions important for host defense and tumor surveillance in the lung. *Environ Res*. 62: 207-222.

Zhao CZ, Fang XC, Wang D, *et al*. 2010. Involvement of type II pneumocytes in the pathogenesis of chronic obstructive pulmonary disease. *Respir Med*. 104: 1391-1395.

Zhu H, Jia Y, Cao H, *et al*. 2014. Biochemical and histopathological effects of subchronic oral exposure of rats to a mixture of five toxic elements. *Food Chem Toxicol*. 71: 166-175.

## Annexure 1

The Research Ethics Committee, Faculty Health Sciences, University of Pretoria complies with ICH-GCP guidelines and has US Federal wide Assurance.

- FWA 00002567, Approved dd 22 May 2002 and Expires 03/20/2022.
- IRB 0000 2235 IORG0001762 Approved dd 22/04/2014 and Expires 03/14/2020.



UNIVERSITEIT VAN PRETORIA  
UNIVERSITY OF PRETORIA  
YUNIBESITHI YA PRETORIA

Faculty of Health Sciences Research Ethics Committee

28/09/2017

### Approval Certificate New Application

**Ethics Reference No: 423/2017**

**Title: Effects of cadmium, chromium and mercury alone and in combination on lung tissue of Sprague-Dawley rats**

Dear Sirasha Venkentsamy Naidoo

The **New Application** as supported by documents specified in your cover letter dated 30/08/2017 for your research received on the 30/08/2017, was approved by the Faculty of Health Sciences Research Ethics Committee on its quorate meeting of 27/09/2017.

Please note the following about your ethics approval:

- Ethics Approval is valid for 2 years
- Please remember to use your protocol number (423/2017) on any documents or correspondence with the Research Ethics Committee regarding your research.
- Please note that the Research Ethics Committee may ask further questions, seek additional information, require further modification, or monitor the conduct of your research.

**Ethics approval is subject to the following:**

- The ethics approval is conditional on the receipt of **6 monthly written Progress Reports**, and
- The ethics approval is conditional on the research being conducted as stipulated by the details of all documents submitted to the Committee. In the event that a further need arises to change who the investigators are, the methods or any other aspect, such changes must be submitted as an Amendment for approval by the Committee.

We wish you the best with your research.

**Yours sincerely**

*\*\* Kindly collect your original signed approval certificate from our offices, Faculty of Health Sciences, Research Ethics Committee, Tswelopele Building, Level 4-60*

**Dr R Sommers; MBChB; MMed (Int); MPharMed, PhD**  
**Deputy Chairperson of the Faculty of Health Sciences Research Ethics Committee, University of Pretoria**

*The Faculty of Health Sciences Research Ethics Committee complies with the SA National Act 61 of 2003 as it pertains to health research and the United States Code of Federal Regulations Title 45 and 46. This committee abides by the ethical norms and principles for research, established by the Declaration of Helsinki, the South African Medical Research Council Guidelines as well as the Guidelines for Ethical Research: Principles Structures and Processes, Second Edition 2015 (Department of Health).*

☎ 012 356 3084      ✉ [deepeka.behari@up.ac.za](mailto:deepeka.behari@up.ac.za) / [fhsethics@up.ac.za](mailto:fhsethics@up.ac.za)      🌐 <http://www.up.ac.za/healthethics>  
✉ Private Bag X323, Arcadia, 0007 - Tswelopele Building, Level 4, Room 60, Gezina, Pretoria

## Annexure 2



UNIVERSITEIT VAN PRETORIA  
UNIVERSITY OF PRETORIA  
YUNIBESITHI YA PRETORIA

### Animal Ethics Committee

PROJECT TITLE	Investigating the effects of metals cadmium, chromium, alone and in combination, on the lung tissue of Sprague-Dawley rats
PROJECT NUMBER	H004-17
RESEARCHER/PRINCIPAL INVESTIGATOR	S Naidoo

STUDENT NUMBER (where applicable)	U_ 11131978.
DISSERTATION/THESIS SUBMITTED FOR	MSc Anatomy

ANIMAL SAMPLES	Previously collected H006-15 and H007-15	
NUMBER OF ANIMALS	To be reported	
Approval period to use animals for research/testing purposes		March 2017-March 2018
SUPERVISOR	Dr. HM Oberholzer	

**KINDLY NOTE:**

Should there be a change in the species or number of animal/s required, or the experimental procedure/s - please submit an amendment form to the UP Animal Ethics Committee for approval before commencing with the experiment

<b>APPROVED</b>	Date	27 March 2017
CHAIRMAN: UP Animal Ethics Committee	Signature	

S4285-15



Contents lists available at ScienceDirect

Environmental Toxicology and Pharmacology

journal homepage: [www.elsevier.com/locate/etap](http://www.elsevier.com/locate/etap)

## Oral exposure to cadmium and mercury alone and in combination causes damage to the lung tissue of Sprague-Dawley rats



Sirasha Venketsamy Kooopsamy Naidoo<sup>a</sup>, Megan Jean Bester<sup>a</sup>, Sandra Arbi<sup>a</sup>, Chantelle Venter<sup>b</sup>, Priyanka Dhanraj<sup>a</sup>, Hester Magdalena Oberholzer<sup>a,\*</sup>

<sup>a</sup>Department of Anatomy, Faculty of Health Sciences, University of Pretoria, Private Bag x323, Arcadia, 0007, South Africa

<sup>b</sup>Laboratory for Microscopy and Microanalysis, University of Pretoria, South Africa

### ARTICLE INFO

#### Keywords

Heavy metals  
Cadmium  
Mercury  
Reactive oxygen species  
Lungs  
Toxicity

### ABSTRACT

Environmental presence and human exposure to heavy metals in air and cigarette smoke has led to a worldwide increase in respiratory disease. The effects of oral exposure to heavy metals in liver and kidney structure and function have been widely investigated and the respiratory system as a target is often overlooked. The aim of the study was to investigate the possible structural changes in the lung tissue of Sprague-Dawley rats after oral exposure for 28 days to cadmium (Cd) and mercury (Hg), alone and in combination at 1000 times the World Health Organization's limit for each metal in drinking water. Following exposure, the general morphology of the bronchiole and lungs as well as collagen and elastin distribution was evaluated using histological techniques and transmission electron microscopy. In the lungs, structural changes to the alveoli included collapsed alveolar spaces, presence of inflammatory cells and thickening of the alveolar walls. In addition, exposure to Cd and Hg caused degeneration of the alveolar structures resulting in confluent alveoli. Changes in bronchiole morphology included an increase in smooth muscle mass with luminal epithelium degeneration, detachment and aggregation. Prominent bronchiole-associated lymphoid tissue was present in the group exposed to Cd and Hg. Ultrastructural examination confirmed the presence of fibrosis where in the Cd exposed group, collagen fibrils arrangement was dense, while in the Hg exposed group, additional prominent elastin was present. This study identified the lungs as target of heavy metals toxicity following oral exposure resulting in cellular damage, inflammation and fibrosis and increased risk of respiratory disease where Hg showed the greatest fibrotic effect, which was further, aggravated in combination with Cd.

### 1. Introduction

The main source of heavy metal exposure is through the anthropogenic sources such as transport, agriculture, mining and other related operations (Venter et al., 2017). Established routes of exposure are absorption through the skin, oral cavity and via inhalation (Awofolu et al., 2005). Air pollution is the most common cause of respiratory disease that affects the structure and the functioning of the airways and the respiratory components of the lungs. The most common respiratory diseases associated with exposure are asthma, bronchitis, chronic cough, chronic obstructive pulmonary disease (COPD), idiopathic pulmonary fibrosis, lung cancer, pneumonia and tuberculosis. The World Health Organization (WHO) (2000) reported an increase in the prevalence of respiratory diseases from 100 to 400 million from 2006 to 2010 (Mamuya et al., 2007).

Exposure is often not limited to a single metal and depends on the

type of mining; the method of extraction, the degree to which safety measures are implemented as well as other activities such as cigarette smoking that can result in exposure to several components at different concentrations. Incorrect disposal of heavy metals may also result in the leaching of waste into various water sources and thus polluting the water (McCarthy, 2011). The United States Environmental Protective Agency (EPA) in 2013 analysed municipal water supplies for the following heavy metal concentrations; aluminium (Al), copper (Cu), arsenic (As), mercury (Hg) and lead (Pb). Luo et al. (2011) showed a high concentration of cadmium (Cd), Pb, and nickel (Ni) exceeding the limit of 1000ppm and suggested that industrial contaminants have leached into the municipality water supply. Studies in South Africa examined and reported elevated levels of heavy metals in the drinking water near a mining industry in the Witwatersrand region (Naicker et al., 2003). This water is used for drinking, washing and recreational purposes. Exposure to heavy metals are found to have numerous detrimental

\* Corresponding author.

E-mail address: [nanette.oberholzer@up.ac.za](mailto:nanette.oberholzer@up.ac.za) (H.M. Oberholzer).

<https://doi.org/10.1016/j.etap.2019.03.021>

Received 13 February 2019; Received in revised form 20 March 2019; Accepted 27 March 2019

Available online 28 March 2019

1382-6689/ © 2019 Elsevier B.V. All rights reserved.

effects on human health. According to Rehman et al. (2018), constant exposure to heavy metals often leads to the accumulation of heavy metals in various parts of the body. Accumulated heavy metals may interfere or alter the functioning of essential molecules such as carbohydrates, proteins and lipids through the induction of oxidative stress. As a result, numerous metabolic processes and mechanisms are affected. This is often followed by a cascade of detrimental effects including neuronal damage, cardiovascular disorders, kidney and liver damage and several types of cancers (Rehman et al., 2018).

The effects of metals such as Hg and Cd on the liver and kidneys, common organs of toxicity, has been widely investigated in several animal models (Jarup, 2003; Leem et al., 2015). However, little is known regarding oral absorption on lung function. Workers in primary metal industries are also at a risk of exposure, as Cd is a pulmonary irritant and fatal when inhaled (Nawrot et al., 2010). Increased blood levels of Cd is associated with a decrease in pulmonary function (Bertin and Averbeck, 2006; Huff et al., 2007; Nawrot et al., 2010). Hg is toxic to humans and causes severe alterations such as DNA mutation that activates oncogenesis, resulting in the transformation of normal cells into tumour cells (Onyido et al., 2004). Previous studies indicated that both the inorganic and organic form of Hg accumulates over a period of time in the endocrine organs (e.g. pituitary gland and hypothalamus) (Zhu et al., 2014; Martin and Griswold, 2009). Little is known regarding the effect of metals such as Cd and Hg that are often part of mixtures, where the observed effect would be a function of concentration, exposure time as well as the unique tissue, cellular and biochemical targeting of each metal.

As Cd and Hg are common contaminants of water, the aim of this study was to investigate the morphological changes in the lung tissue and the presence of fibrosis in male Sprague-Dawley rats after oral exposure to relevant dosages of Cd and Hg, alone and in combination. The rationale for using 1000x the acceptable exposure limits as established by the WHO, for a short period of time, is to identify specific cellular targets that can later be further evaluated in chronic models of exposure. Also, the lungs are often overlooked when the toxicity of heavy metals after oral exposure is being investigated and therefore this study aimed to determine whether oral exposure to heavy metals can also contribute to lung damage.

## 2. Materials and methods

### 2.1. Implementation of the Sprague-Dawley rat model

Forty-eight male Sprague-Dawley rats (250–300 g) were used in this study and maintained at the University of Pretoria's Biomedical Research Centre (UPBRC). These rats were provided with irradiated commercial Epol rat pellets and water *ad libitum*. All experimental protocols complied with the requirements of the University of Pretoria's Animal Ethics Committee (ethical clearance number: H004-17). The animals were housed in conventional cages complying with the sizes laid out in the SANS 10,386:2008 recommendations. A room temperature of 22 °C (± 2 °C); relative humidity of 50% (± 20%) and a 12-hour light/dark cycle were maintained during the entire study. The rats were allowed to acclimatise for seven days prior to the start of the experiment, which was conducted over the following 28 days. The rats were randomly divided into 4 groups of 6 rats per group and the groups were control, Cd, Hg and Cd+Hg.

### 2.2. Administration of heavy metals

Cadmium chloride (CdCl<sub>2</sub>) [Merck (Pty) Ltd, South Africa] and mercury chloride (HgCl<sub>2</sub>) [Merck (Pty) Ltd, South Africa] were dissolved in sterile water and administered daily to the rats via oral gavage. The control group received saline via oral gavage. Weekly dosages were adjusted based on the changes in the mass of the rats. The dosage given to the rats was calculated from the WHO water limits for

consumption by 60 kg human consuming 1.41 water per day. The conversion of human dosages to rat dosages was calculated according to the method of Reagan-Shaw et al. (2008) and represented a rat equivalent dosage of ± 1000 times the WHO limits in drinking water for human consumption. Dosages were 0.696 mg/kg/day and 1.148 mg/kg/day for rats exposed to Cd and Hg respectively while rats in the Cd + Hg received 0.696 mg/kg and 1.148 mg/kg Cd and Hg respectively.

### 2.3. Termination

The rats were terminated after 28 days exposure via isoflurane overdose, according to standard methods employed by the UPBRC. Lung tissue was harvested for morphological and ultrastructural analyses.

### 2.4. Light microscopy

The lung tissue was fixed in 2.5% glutaraldehyde (GA) / formaldehyde (FA), washed with phosphate buffer (pH 7.4) and dehydrated in ascending ethanol concentrations. The tissue was then infiltrated and embedded with paraffin wax. Sections of 3–5 µm were made with a Leica RM 2255 wax microtome (Leica Microsystems, Wetzlar, Germany). The slides were then stained with Haematoxylin and Eosin (H&E), Picro-Sirius red and Verhoeff van Gelson to evaluate general morphology, collagen and elastin distribution, respectively.

### 2.5. H&E staining

The slides were placed in xylene for 10 min. The sections were rehydrated in a series of decreasing concentrations of EtOH; two changes of 100% EtOH, 90% and 70% each for 1 min. The slides were then placed in ddH<sub>2</sub>O for 1 min, haematoxylin for 15 min and Scott's buffer for 8 min. The slides were then rinsed with ddH<sub>2</sub>O and then dipped in eosin, 70% EtOH, 90% EtOH, 100% EtOH and xylene. The coverslips were mounted with Entellan<sup>®</sup> mounting medium. The sections were viewed using a Zeiss AXIO Imager.M2 light microscope (Carl Zeiss Microscopy, Munich, Germany).

### 2.6. Picro-Sirius red staining

Picro-Sirius red (PR) staining was performed in order to evaluate and differentiate between collagen fibre types. PR stains collagen and with polarised light microscopy, the collagen fibres are birefringent due to their molecular arrangement (Borges et al., 2007). Thin fibres are viewed as yellow – green birefringence are usually associated with collagen type III while thick fibres appear yellow-orange to orange-red colours and usually consist of type I collagen that have stronger birefringence with polarised light (Velindala et al., 2014). To prepare the PR stain, 0.5 g Sirius red dye was dissolved in 500 ml of aqueous solution of picric acid. Acidified water was used for washing. The tissue was dewaxed and rehydrated, followed by staining in haematoxylin for 8 min and rinsed in running tap water for 10 min. The tissue was placed in the PR solution for one hour and then washed twice with acidified water. The tissue was then dehydrated three times in 100% ethanol and cleared in xylene. The samples were visualised with a Zeiss AXIO Imager.M2 light microscope (Carl Zeiss Microscopy, Munich, Germany) with a polarising filter.

### 2.7. Verhoeff Van Gelson stain

For the Verhoeff van Gelson (VvG) stain, 5% alcoholic haematoxylin was prepared with 5 g of haematoxylin dissolved in 100 ml of 100% ethanol. A 10% aqueous ferric chloride solution was prepared with 10 g of ferric chloride dissolved in 100 ml of distilled water. The Weigert's iodine solution consisted of, 2 g of potassium iodide and 1 g of iodine

dissolved in 100 ml of distilled water. The VvG working solution was prepared by mixing together 20 ml of 5% alcoholic haematoxylin, 8 ml of ferric chloride and 8 ml of Weigert' iodine solutions. The tissue was deparaffinised and hydrated in distilled water followed by staining with VvG solution for an hour. The tissue was then rinsed with tap water for 6 s and was then differentiated using a 2% of ferric chloride solution for 6 s. The tissue sections were again rinsed with distilled water and were then treated with 5% of aqueous sodium thiosulfate for 1 min, followed with another distilled water rinse and Van Gieson counterstain solution for 6 s. Dehydration of the tissue sections was performed with 95% ethanol, two rinses of 100% ethanol and finally cleared in two rinses of xylene. The samples were visualised with a Zeiss AXIO Imager.M2 light microscope (Carl Zeiss Microscopy, Munich, Germany).

### 2.8. Transmission electron microscopy

The tissue samples were fixed in 2.5% GA/FA, washed three times in 0.075 M sodium phosphate buffer (pH 7.4) and then placed in the secondary fixative (1% osmium tetroxide) solution for one hour. Following secondary fixation, the samples were rinsed again as described above. The samples were then dehydrated in 30%, 50%, 70%, 90% and three changes of 100% ethanol and were embedded in epoxy resin. Ultra-thin sections (70–100nm) were cut with a diamond knife using an ultramicrotome. Samples were then contrasted with uranyl acetate and lead citrate, and examined with a JEOL transmission electron microscope (TEM) (JEM 2100 F, Tokyo, Japan).

### 3. Results

Fig. 1 is a comparison of the general structure and arrangement of the alveoli between the control (Fig. 1A) and experimental groups (Fig. 1B–D). In Fig. 1A, well defined alveolar spaces (A) can be seen with thin epithelial walls, fine interstitium (asterix) and along the alveolar wall are capillaries containing red blood cells (RBC), all forming the air-blood barrier and respiratory membrane. Pneumocyte type I (P1) and II (P2) can also be identified in the interstitium of alveolar walls. Fig. 1B–D is representative of the lung tissue of Sprague-Dawley rats exposed to the heavy metals alone and in combination (Cd, Hg and

Cd + Hg). Fig. 1B and C are representative of the Cd and Hg single metal exposure groups respectively and Fig. 1D is representative of the combination group. In all metal exposed groups, a thickened inter-alveolar space (dashed arrow) is present with increased prominence of the interstitial connective tissue (arrows) and cell nuclei. The presence of RBC is more pronounced along the alveolar wall and surrounding the alveolar spaces in the exposed groups compared to the control and is most obvious in the single metal exposed groups (Fig. 1B and C).

Fig. 2 shows the collagen distribution within the alveoli in the control (Fig. 2A) and experimental groups (Fig. 2B–D). In Fig. 2A, predominantly yellow – green birefringence is present in the connective tissue of the interstitium indicative of collagen type III fibres. Slight orange – red birefringence is shown with arrows and is indicative of collagen type I fibres. The Cd exposed group (Fig. 2B) showed some increased orange-red birefringence (collagen type I) when compared to control, indicated with arrows. The Hg exposed group (Fig. 2C) showed primarily orange-red birefringent collagen in the alveoli, which is a strong representation of collagen type I presence and fibrotic tissue. The Cd + Hg exposed group (Fig. 2D) also had an increase of collagen type I in comparison to control, as evident with the orange – red birefringent collagen (arrows) and is similar to that observed in the Cd exposed group.

Fig. 3A–D are light micrographs representing the bronchiole structure of the control (Fig. 3A) and exposed groups (Fig. 3B–D). Fig. 3A shows the typical structure of a bronchiole with an intact epithelial lining (E) and a regular arrangement of smooth muscle (SM) surrounding the bronchiole. Fig. 3B and D (asterix) show desquamation of the epithelium resulting in cellular debris within the bronchioles, and stratification of the bronchiole epithelium, (indicated by SE). Also, the smooth muscle surrounding the bronchioles in both Cd and the combination groups appears to have an irregular displacement. In the Hg exposed group (Fig. 3C), the infiltration of inflammatory cells was observed by the presence of bronchus associated lymphoid tissue (BALT) which was not observed in the control samples.

Fig. 4A–D are light micrographs of the bronchiole structures stained with PR and viewed with polarised light. The bronchioles showed a prominent change of the collagen fibres between the control (Fig. 4A) and exposed (Fig. 4B–D) groups. As seen in Fig. 4A, the control has type

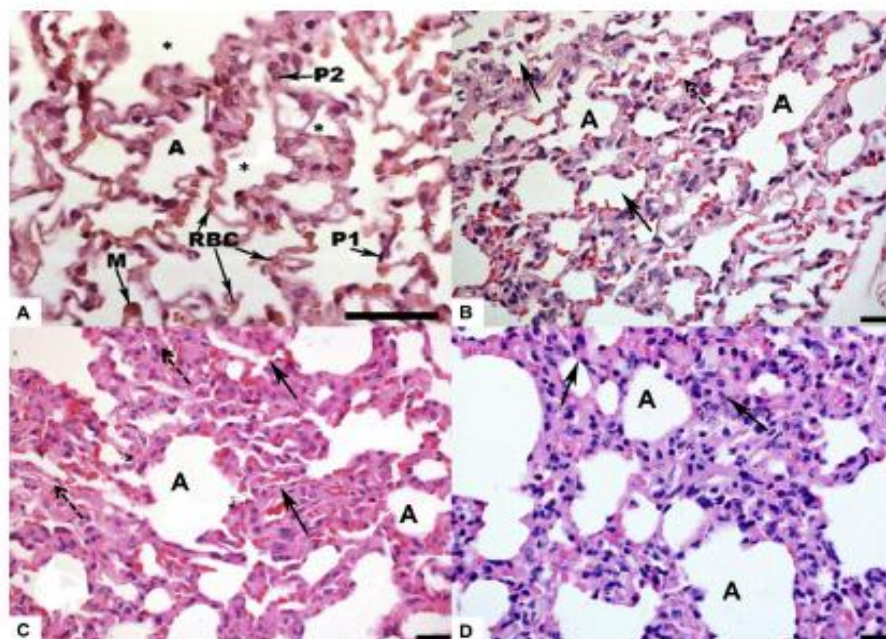


Fig. 1. General structure of the lung alveoli and interalveolar wall. H & E staining. A: Control; B: Cd; C: Hg; D: Cd + Hg. Labels: A: alveolar spaces; P1: Type I pneumocyte; P2: type II pneumocyte; RBC: red blood cell; M: alveolar macrophage. Asterix: fine interstitium; Arrow: thick interstitium; Dashed arrow: collapsed alveolar space (Scale bar in A = 50  $\mu$ m and B–D = 20  $\mu$ m).

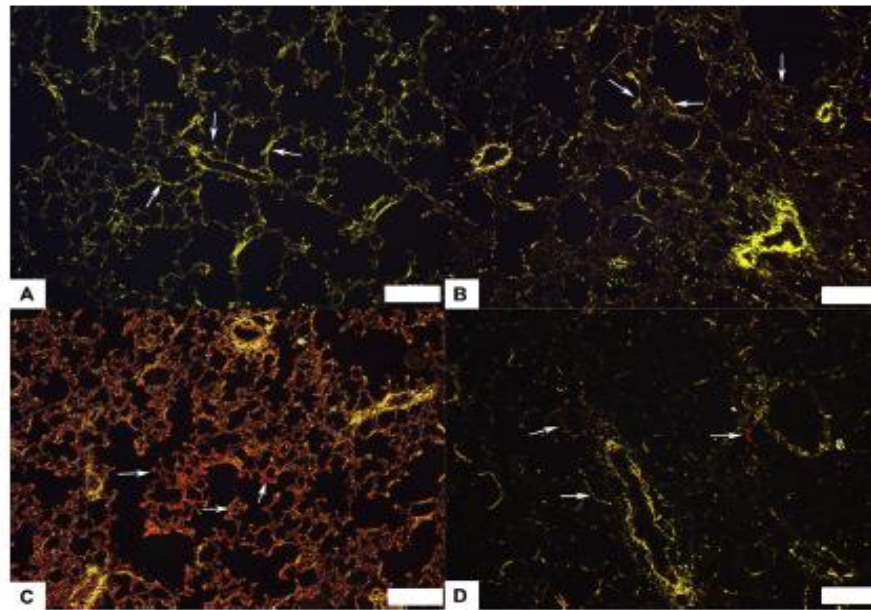


Fig. 2. Collagen distribution in the alveoli. PR staining viewed with polarised light. Images show collagen distribution in A: control, B: Cd, C: Hg and D: Cd + Hg groups. Arrows indicating the distribution of collagen type III (yellow – green birefringence) and type I fibres (orange – red birefringence) (Scale bars = 20  $\mu$ m).

III collagen fibres (green birefringence) that are arranged more loosely and thinner whereas Type I collagen fibres are more dense and thicker as observed in the exposed groups shown in Fig. 4B–D with red and orange interwoven birefringence. The control (Fig. 4A) has an interwoven distribution of green and yellow collagen fibres. In the Hg and combination exposed groups, there was a decrease in type III collagen

(green - yellow birefringence) and increase in type I collagen (orange – red birefringence) along the epithelial lumen (thin white arrow) and the epithelium (thick white arrow).

Fig. 5A–D focuses on the arrangement of elastic fibres in the bronchioles of control compared to the exposed groups. The elastic fibres in the exposed groups (Fig. 5B–D) appear irregular and not

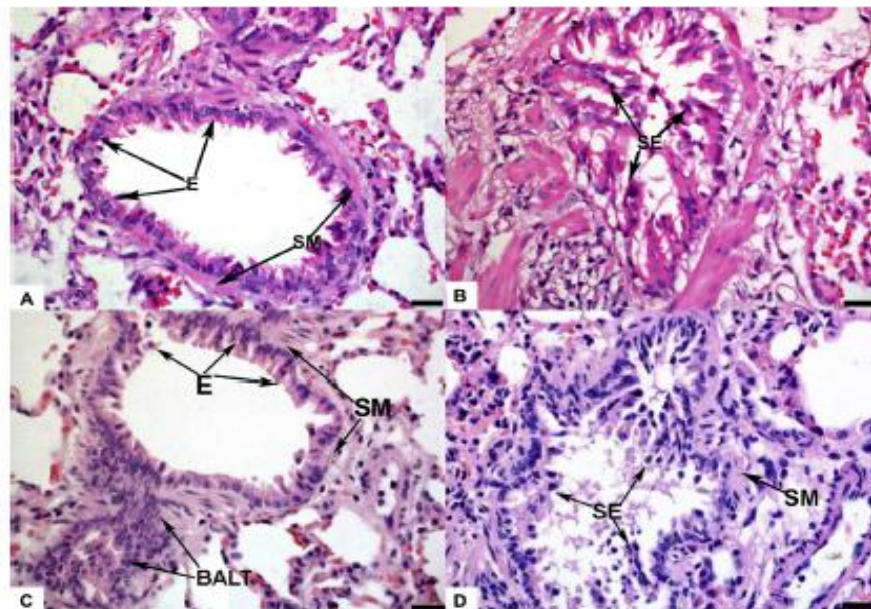


Fig. 3. General structure of the bronchioles. H&E staining. A: Control; B: Cd; C: Hg; D: Cd + Hg. Labels: E: bronchial epithelium; SM: smooth muscle in the lamina propria; SE: stratification of epithelium; BAL: bronchus associated lymphoid tissue; \*: desquamated epithelial cells (Scale bars = 20  $\mu$ m).

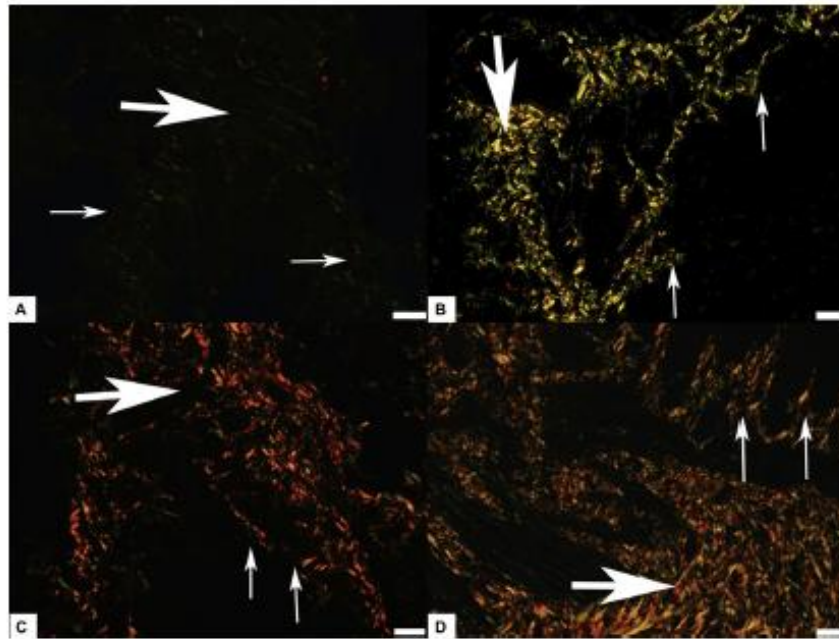


Fig. 4. Collagen distribution in the bronchioles. PR staining and viewed with polarized light. A: Control; B: Cd; C: Hg; D: Cd + Hg. Thin white arrows indicate an increase in fibre thickness associated with the bronchioles mucosa and thick arrows indicates an increase in the submucosa. Collagen type III (yellow – green birefringence) and type I fibres (orange – red birefringence) (Scale bars = 20  $\mu$ m).

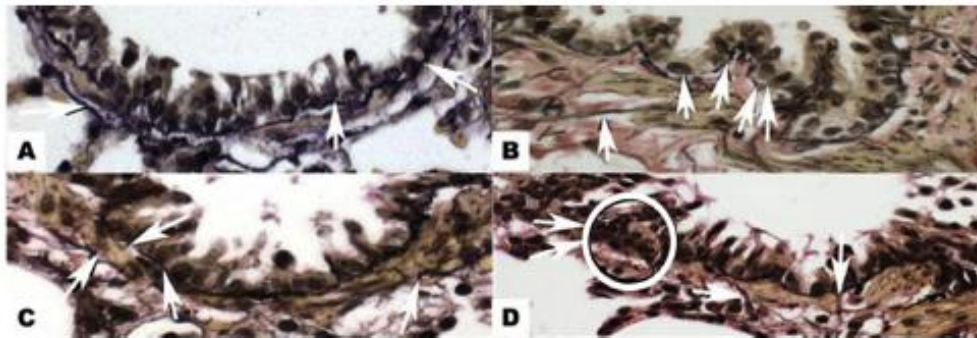


Fig. 5. Mucosa of the bronchioles. VvG staining A: Control; B: Cd; C: Hg; D: Cd + Hg. Elastic fibres are indicated by the white arrows and smooth muscle stains pink. Circled: BALT (Scale bars = 20  $\mu$ m).

continuous with the basement membrane of the epithelial lining of the bronchioles, when compared to the control (Fig. 5A). Smooth muscle stains pink and increased amounts and altered distribution of smooth muscle is observed in Fig. 5B–D.

Fig. 6A–D represents the ultrastructural features of the bronchioles in control (Fig. 6A) and metal exposed groups (Fig. 6B–D). Collagen fibres were observed in the control group, indicated by the black arrow in Fig. 6A. More prominent and densely arranged collagen fibril bundles were observed in the heavy metal exposed groups (Fig. 6B–D, black arrow) located in between the elastin fibres (arrowhead). Prominent elastin bundles (white arrowheads) were evident in the exposed groups. The collagen distribution is prominent in both single exposure groups Cd (Fig. 6B) and Hg (Fig. 6C) compared to the control (Fig. 6A). Collagen bundles appear most densely arranged and coiled in the Cd group, while the Hg group presented with additional fragmented elastin. In the Cd + Hg group (Fig. 6D); both collagen and elastin are more noticeable.

#### 4. Discussion

To determine the effects of oral exposure to heavy metals, changes in the functioning and morphology of the liver and kidneys are usually investigated (Kenston et al., 2018). In the present study, the effect of oral exposure to Cd and Hg alone and combination at 1000 times the WHO acceptable water limits on lung tissue was evaluated. Changes to the structure of the lungs and bronchiole were determined and this included the alveoli, air-blood barrier morphology and the distribution of connective tissue; collagen and elastin.

In the lungs of exposed rats, the interalveolar spaces appeared thickened associated with an increase in the presence of RBC, which indicates endothelial damage that can adversely affect the functioning of the air-blood barrier. Heavy metal induced oxidative stress causes membrane damage, which can lead to membrane destabilisation and disintegration (Stajn et al., 1997). Damage to the air-blood barrier and increase in permeability of the pulmonary epithelium leads to plasma protein extravasation (Valcheva-Kuzmanova et al., 2014) resulting in pulmonary oedema. Pneumocyte type II cells are vulnerable to oxidative stress and Hg induces type II epithelial cell damage via the

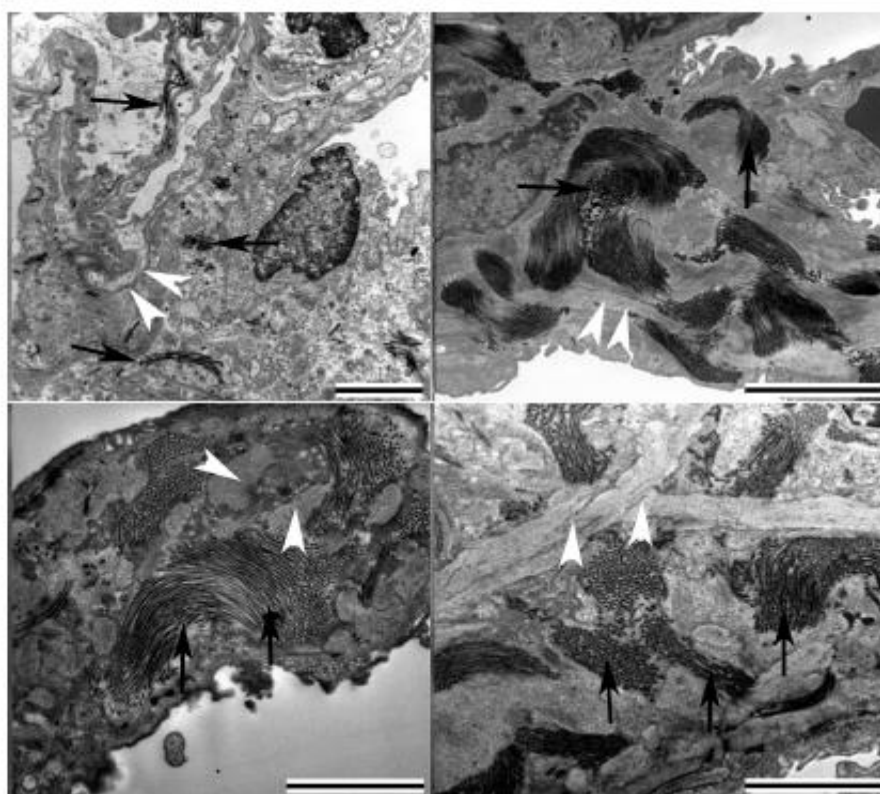


Fig. 6. Transmission electron micrographs of bronchioles A: Control; B: Cd; C: Hg; D: Cd + Hg. Black arrows: collagen fibres; white arrowheads: elastin bundles (Scale bars = 2  $\mu$ m).

oxidative stress associated mitochondrial cell death pathway (Lu et al., 2010). Shedding of the epithelial cells and cellular debris resulting in the obliteration of the bronchiolar lumen was observed in the lungs of rats exposed to Cd and Cd + Hg groups (Fig. 3B and D).

In the exposed rats, the smooth muscle in the bronchioles is irregularly displaced and BALT appears to be more prominent in exposed groups (Fig. 3C). Irregular displacement and smooth muscle accumulation are events also observed in the histopathology of asthma (Bai and Knight, 2005). Inflammatory cells are recruited into the tissue from the circulation when local defences systems fail. The influx of inflammatory cells into the interstitium and bronchoalveolar space, is considered an important factor in the progression of lung injury (Gronnes and Soehnlein, 2011). Inflammatory cell infiltration, specifically mast cell infiltration has been linked to airway hyper responsiveness (Brightling et al., 2005). An increase in bronchial smooth muscle is associated with lung dysfunction in severe asthma (Bousquet and Jeffery, 2000; Kaminska et al., 2009). Smooth muscle itself is able to recruit inflammatory cells that participate in the inflammatory activation loop (Berger et al., 2003). Improper tissue repair and epithelial regeneration after injury can result in excessive fibroproliferation and inflammation in the sub-epithelial structures. This is often observed in obliterative bronchiolitis and injury to the bronchiolar epithelium (Barker et al., 2014). Exposure to Cd and Cd + Hg (Fig. 3B and D) also caused basement membrane detachment, resulting in bronchiole epithelium stratification and the presence of cellular debris in the lumen. These changes are consistent with histological changes observed in asthma and chronic bronchitis (Bai and Knight, 2005; Salvato, 1968).

Evaluation of the effects on collagen and elastic fibre distribution in the lungs of exposed rats showed an increased collagen deposition and

differences in the type of collagen deposited in the interalveolar septa. For all rats exposed to metals there was an increase in collagen deposition, with collagen type I being the prominent type.

Elastic fibres in bronchioles are associated with the basement membrane and facilitates bronchial patency during respiration. Exposure to Cd, Hg and Cd + Hg (Fig. 5B–D) resulted in irregular elastic fibre distribution not continuous with the basement membrane. Changes in the distribution of elastic fibres are due to the elastic lamina being disrupted and delineated from the bronchioles basement membrane (Harris et al., 2016) while increased presence of elastin which may be a consequence of changes to epithelial structure and/or increased fibrosis. Increased deposition and abnormal of collagen and elastin fibres was confirmed with TEM.

Airway remodelling is associated with an increase in collagen deposition, altered distribution of collagen, mucous gland hypertrophy, smooth muscle hyperplasia or hypertrophy; all contributing to long term irreversible changes, a fixed airway obstruction and severity of asthmatic disease (Begueret et al., 2007). The increased deposition and synthesis of a collagen type often results in structural abnormalities of the connective tissue. Increased synthesis of type I collagen, as is shown in Fig. 4B–D, is often associated with fibrosis (Arbi et al., 2015). Interwoven red-orange birefringence indicative of collagen type I, which is associated with fibrosis, was observed for the Hg and Cd + Hg exposure groups.

While the bronchioles showed a prominent increase in type I collagen fibres in the exposed groups, irregular displacement of elastin fibres around the bronchioles, not being continuous with the basement membrane of the bronchiole compared to control, was observed. Transmission electron microscopy analysis showed an increase in

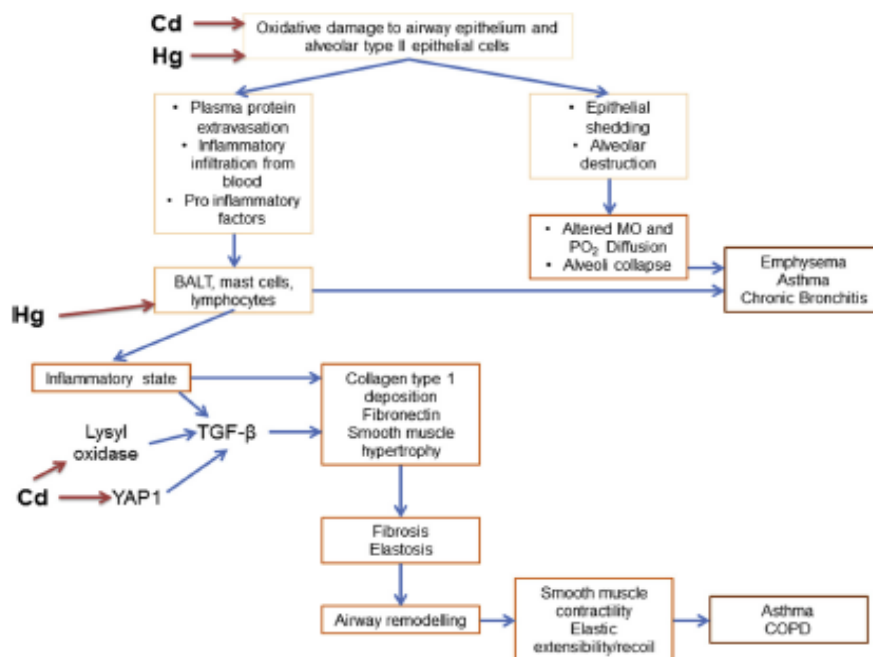


Fig. 7. Flow diagram of the hypothesised mode of action of Cd and Hg on lung tissue, contributing to lung pathologies associated with asthma, chronic bronchitis, COPD and pulmonary fibrosis.

collagen and elastin bundles of the exposed groups compared to control.

Damage to the elastic fibres can occur as a result of damage or inflammation. In asthma, elastic fibres show a thickened and patchy morphology as well as fibre tangling which may be the result of repair elicited by chronic inflammation. Elastosis in the airways and a gradual remodelling of the airways through reorientation of fibres has also been observed in chronic lung disease (Bergeron et al., 2009; Kumar, 2001; Yang et al., 2016). Alveolar wall destruction and reduced elastic recoil due to the destruction of elastin and increase deposition of collagen are characteristic features of emphysema (Zhou et al., 2018).

Effects of Hg on the lungs have largely been described as a result of exposure to Hg vapour via inhalation. Occupational or accidental exposure to Hg vapour has been shown to lead to acute respiratory failure (Smiechowicz et al., 2017; Rowens et al., 1991; Asano et al., 2000; Moromisato et al., 1994; Lim et al., 1998) pulmonary oedema and acute interstitial pulmonary fibrosis (Jaeger et al., 1979). Similar to the present study, Celikoglu et al. (2015) observed in rats that were daily orally exposed to 1 mg/kg for 28 days, Hg caused alveolar oedema, haemorrhage, interalveolar thickening, inflammatory cell infiltration and fibrosis.

Collagen found within smooth muscle affects muscle contractility, as was observed in collagen deposition in detrusor muscle and urinary retention (Bellucci et al., 2017). Severe and non-severe asthma patients present with thickened airway smooth muscle and thicker extracellular matrix (ECM) deposition (Begueret et al., 2007). Smooth muscle activation in the airways would cause excessive bronchoconstriction, and increased muscle mass would further promote this effect. The response of excessive bronchoconstriction is linked directly to underlying inflammation. An increase in transforming growth factor beta (TGF-β) has been observed in asthmatic airways (Redington et al., 1997; Vignola et al., 1997) and TGF-β is known to induce fibronectin and collagen type I deposition in bronchial smooth muscle cells through connective tissue growth dependant and independent pathways (Johnson et al., 2006). Bronchial smooth muscle cells are therefore able

to control their own environment (Bara et al., 2010). Changes of elastin were shown to cause limitations to the airflow through the airways and into the alveoli (Black et al., 2008). In the present study electron microscopy revealed the increased abundance of elastin and collagen bundles in the bronchioles (Figs. 4 and 6) indicating the possible contribution of Cd and/or Hg to the development of asthma.

Heavy metals induce oxidative stress which has been implicated in the fibrogenesis through the induction of fibrogenic cytokines such as TGF-β, connective tissue growth factor (CTGF), and platelet-derived growth factor (PDGF) (Shroff et al., 2014). The cytokines contribute to an increase in collagen synthesis and deposition by stimulating the differentiation of fibroblasts from mesenchymal, epithelial and endothelial cells (Barker et al., 2014). High collagen III to collagen I ratio is observed in early fibrosis while a low collagen III to collagen I ratio is observed in late fibrosis, associated with idiopathic pulmonary fibrosis. Furthermore idiopathic pulmonary fibrosis is a self-perpetuating fibrosis through a positive feedback mechanism (Murtha et al., 2017).

The involvement of inflammation and inflammatory mechanisms in promoting pulmonary fibrosis has been well described (Kolshian et al., 2016). Recently a new pathway for Cd-induced collagen stimulation and further matrix stiffening has been described involving Yes-associated protein 1 (YAP1) activation (Li et al., 2017), whose function is to mediate TGF-β induced signalling in the lung (Pefani et al., 2016). Activation of YAP1 causes matrix stiffening, which further promotes nuclear localisation of YAP1, so that it moves from the cytoplasm to the nucleus where it binds to Smad2/3 and activates fibrosis mediated transcription factors (Li et al., 2017). Lysyl oxidase has been found to be a target of cigarette smoke of which Cd is a major component (Li et al., 2011). Cd down regulates the expression of lysyl oxidase at mRNA, protein and catalytic levels in lung cells, both *in vitro* and *in vivo*. An inhibition of lysyl oxidase which is Cu dependant and catalyses the cross linking of collagen and elastin, stabilising the ECM. The limitation of Cu cofactor by Cd accelerates collagen and elastin damage. These changes are important in the development of emphysema (Zhao et al., 2006). Low dose Cd induces peribronchiolar fibrosis characterised by

luminal loss and remodelling in small airways and (Li et al., 2017). Peribronchiolar fibrosis can occur before the onset of emphysema (Hogg et al., 2004) and may be present together with alveolar wall loss (Lang et al., 1994; Vlahovic et al., 1999). Cd has been suggested to be attributed to pulmonary emphysema through altered redox balance and macrophage dysfunction (Ganguly et al., 2018) and Hg has been shown to cause oxidative stress in lungs (Ansar and Iqbal, 2015). These hypothesised mechanisms are summarised in Fig. 7.

Changes to lung function is often reported to be due to heavy metals such as Cd and Hg being air pollutants. However, increasing exposure to water contaminated with Cd and Hg, may via a similar pathway of oxidative stress, alter the structure of lung tissue leading to the development of associated disease especially if exposure is to metals as part of mixtures as is reported for Cd and Hg in the present study. The reported ability of Hg to stimulate the immune system (Weigand et al., 2015) could explain the elevated fibrosis and elastin damage and ECM remodelling in the Cd and Hg exposure group. Along with the fibrotic induction with oxidative stress caused by both metals individually, Hg has an additional pro-inflammatory effect, which may contribute to the elevated damage observed in the combination group.

## 5. Conclusion

This study showed that environmental exposure to heavy metals Cd and Hg in water results in fibrosis associated with an increase in type I collagen synthesis in the airways and alveoli. Additional irregular smooth muscle arrangement and destruction of elastic fibres in the bronchiole further also contributes to pathology. In the lungs, alveolar type II epithelial cell damage as a result of an increased oxidative environment, initiates an inflammatory reaction and subsequent fibrosis, which is further amplified by the metals ability to directly contribute to the inflammatory and fibrotic process. The clinical implications of exposure to water contaminated with Cd and Hg is an increased risk for the development of asthma, chronic bronchitis and potentially COPD.

## Acknowledgements

The authors wish to thank the National Research Foundation for the funding of this study (Grant number: 92768).

## References

Ansar, S., Iqbal, M., 2015. Effect of dietary antioxidant on mercuric chloride induced lung toxicity and oxidative stress. *Toxicol. Rev.* 34 (4), 168–172.

Arbi, S., Eksteen, E.C., Obeholzer, H.M., et al., 2015. Premature collagen fibril formation, fibroblast-mast cell interaction and mast cell mediated phagocytosis of collagen in keloids. *Ultrastruct. Pathol.* 1–9.

Asano, S., Ito, K., Kurisaki, E., et al., 2000. Acute inorganic mercury vapor inhalation poisoning. *Pathol. Int.* 50 (3), 169–174.

Awofolu, O.R., Mbolekiwa, Z., Mthembu, V., et al., 2005. Levels of trace metals in water and sediment from Tyume River and its effects on an irrigated farmland. *AJOL* 331 (1), 87–94.

Bai, T.R., Knight, D.A., 2005. Structural changes in the airways in asthma: observations and consequences. *Clin. Sci.* 108 (6), 463–477.

Bara, I., Ozler, A., de Lara, T., et al., 2010. Pathophysiology of bronchial smooth muscle remodelling in asthma. *Eur. Respir. J.* 36, 1174–1184.

Barker, A.F., Bergeron, A., Rom, W.N., Hertz, M.I., 2014. Obliterative bronchiolitis. *N. Engl. J. Med.* 370, 1820–1828.

Begueret, H., Berger, P., Vernejoux, J.M., et al., 2007. Inflammation of bronchial smooth muscle in allergic asthma. *Thorax* 62 (1), 8–15.

Bellucci, C.H., Ribeiro, W.D.O., Hemery, T.S., et al., 2017. Increased detrusor collagen is associated with detrusor overactivity and decreased bladder compliance in men with benign prostatic obstruction. *Prostate Int.* 5 (2), 70–74.

Berger, P., Girodet, P.O., Begueret, H., et al., 2003. Trypsin-stimulated human airway smooth muscle cells induce cytokine synthesis and mast cell chemotaxis. *FASEB J.* <https://doi.org/10.1096/fj.03-0041>.

Bergeron, C., Al-Ramli, W., Hamid, Q., 2009. Remodelling in asthma. *Proc. Am. Thorac. Soc.* 6, 301–305.

Bertin, G., Averbeck, D., 2006. Cadmium: cellular effects, modifications of biomolecules, modulation of DNA repair and genotoxic consequences (a review). *Biochim.* 88, 1549–1559.

Black, P.N., Ching, P.S., Beaumont, B., et al., 2008. Changes in elastic fibres in the small airways and alveoli in COPD. *Eur. Respir. J.* 31, 998–1004.

Borges, L.F., Gutierrez, P.S., Maran Sebastião, H.R.C., et al., 2007. Picro picosidus-polarization staining method as an efficient histopathological tool for collagenolysis detection in vesical prolapse lesions. *Micron*. 38, 580–583.

Bousquet, J., Jeffery, P., 2000. Asthma from bronchoconstriction to airways inflammation and remodeling. *Am. J. Respir. Crit. Care Med.* 161, 1720–1745.

Brightling, C.E., Ammit, A.J., Kaur, D., et al., 2005. The CXCL10/CXCR3 Axis mediates human lung mast cell migration to asthmatic airway smooth muscle. *Am. J. Respir. Crit. Care Med.* 171, 1103–1108.

Celiloglu, E., Aslanurk, A., Kalender, Y., 2015. Vitamin E and sodium selenite against mercuric chloride induced lung toxicity in the rats. *Braz. Arch. Biol. Technol.* 58 (4), 587–594.

Ganguly, K., Leivinen, B., Palmberg, L., Åkesson, A., Lindén, A., 2018. Cadmium in tobacco smoked: a neglected link to lung disease? *Eur. Respir. Rev.* 27 (147), 170–179.

Grommes, J., Soehnlein, O., 2011. Contribution of neutrophils to acute lung injury. *Mol. Med.* 17, 293–307.

Harris, W.T., Boyd, J.T., McPhail, G.L., et al., 2016. Constrictive bronchiolitis in adolescents with cystic fibrosis with refractory pulmonary decline. *All Annals ATS* 13 (12), 1–34.

Hogg, J.C., Chu, F., Utokaparch, S., et al., 2004. The nature of small-airway obstruction in chronic obstructive pulmonary disease. *N. Engl. J. Med.* 350, 2645–2653.

Huff, J., Lunn, R.M., Waalkes, M.P., et al., 2007. Cadmium-induced growth factor induces extracellular matrix in asthmatic airway smooth muscle. *Am. J. Respir. Crit. Care Med.* 173, 32–41.

Kaminska, M., Foley, S., Maghni, K., et al., 2009. Airway remodeling in subjects with severe asthma with or without chronic persistent airflow obstruction. *J. Allergy Clin. Immunol.* 124 (1), 45–51.

Keiston, S.S.F., Su, H., Li, Z., et al., 2018. The systemic toxicity of heavy metal mixtures in rats. *Toxicol. Res.* 7, 396–407.

Kolshian, S., Fernandez, I.E., Eickelberg, O., Hard, D., 2016. Immune mechanisms in pulmonary fibrosis. *Am. J. Respir. Cell Mol. Biol.* 55, 309–322.

Kumar, R.K., 2001. Understanding airway wall remodeling in asthma: a basis for improvements in therapy. *Pharmacol. Ther.* 91, 93–104.

Lang, M.R., Flaux, G.W., Gillod, M., et al., 1994. Collagen content of alveolar wall tissue in emphysematous and non-emphysematous lung. *Thorax* 49, 319–326.

Laem, A.Y., Kim, S.K., Chang, J., et al., 2015. Relationship between blood levels of heavy metals and lung function based on the Korean National Health and Nutrition Examination Survey IV-V. *Int. J. Chron. Obstruct. Pulmon. Dis.* 10, 1559–1570.

Li, W., Zhou, J., Chen, L., Luo, Z., Zhao, Y., 2011. Lysyl oxidase, a critical intra- and extracellular target in the lung for cigarette smoke pathogenesis. *Int. J. Environ. Res. Public Health* 8 (1), 161–184.

Li, F.J., Szulc, R., Li, H., Wang, Z., et al., 2017. Low-dose cadmium exposure induces peribronchiolar fibrosis through site-specific phosphorylation of vimentin. *Am. J. Physiol. Lung Cell Mol. Physiol.* 313 (1), 80–91.

Lim, H.E., Shim, J.J., Lee, S.Y., et al., 1998. Mercury inhalation poisoning and acute lung injury. *Korean J. Intern. Med.* 13 (2), 127–130 5930.

Lu, T.H., Chen, C.H., Lee, M.J., et al., 2010. Methylmercury chloride induces alveolar type II epithelial cell damage through an oxidative stress-related mitochondrial cell death pathway. *Toxicol. Lett.* 194 (3), 70–78.

Luo, H., Xu, P., Roane, T.M., et al., 2011. Microbial desalination cells for improved performance in wastewater treatment, electricity production, and desalination. *Bioresour. Technol.* 105, 60–66.

Mamuya, S.H.D., Bratveit, M., Mazhala, Y., Moen, B.E., 2007. High prevalence of respiratory symptoms among workers in the development section of a manually operated coal mine in a developing country: a cross sectional study. *BMC Public Health* 2458, 7–17.

Martin, S., Griswold, W., 2009. Human health effects of heavy metals. *Environ. Sci. Technol. Briefs Citizens* 15, 1–6.

McCarthy, T.S., 2011. The impact of acid mine drainage in South Africa. *SA J. Sci.* 107 (5), 5–6.

Moromoto, D.Y., Anas, N.G., Goodman, G., 1994. Mercury inhalation poisoning and acute lung injury in a child. Use of high frequency oscillatory ventilation. *Chest* 105 (2), 613–615.

Murtha, L.A., Schullig, M.J., Mabotwana, N.S., Hasty, S.A., Waters, D.W., Burgess, J.K., Knight, D.A., Boyle, A.J., 2017. The processes and mechanisms of cardiac and pulmonary fibrosis. *Front. Physiol.* 8, 777–789.

Nackler, K., Gukrowska, E., McCarth, T.S., 2003. Acid mine drainage arising from gold mining activity in Johannesburg, South Africa and environs. *Environ. Pollut.* 122 (1), 29–40.

Nawrot, T.S., Staessen, J.A., Roels, H.A., et al., 2010. Cadmium exposure in the population: from health risks to strategies of prevention. *Biomol. Res.* 23 (5), 769–782.

Ouyido, I., Noor, A.R., Bunce, E., 2004. Biomolecule–Mercury interactions: modalities of DNA base–Mercury binding mechanisms. *Remediation Strategies. Chem Rev* 104 (12), 5911–5930.

Pefani, D.E., Pankova, D., Abraham, A.G., et al., 2016. TGF- $\beta$  targets the Hippo pathway scaffold RASSF1A to facilitate YAP/SMAD2 nuclear translocation. *Mol. Cell* 63, 156–166.

Reagan-Shaw, S., Nihal, M., Ahmad, N., 2008. Dose translation from animal to human studies revisited. *FASEB J.* 22 (3), 659–661.

Redington, A.E., Madden, J., Frew, A.J., et al., 1997. Transforming growth factor-beta 1 in asthma. Measurement in bronchoalveolar lavage fluid. *Am. J. Respir. Crit. Care Med.* 156, 642–647.

- Rehman, K., Fatima, F., Wahed, I., et al., 2018. Prevalence of exposure of heavy metals and their impact on health consequences. *J. Cell. Biochem.* 119, 157–184.
- Rewens, B., Guerrero-Betancourt, D., Gordale, C.A., et al., 1991. Respiratory failure and death following acute inhalation of mercury vapor. A clinical and histologic perspective. *Chest*. 99 (1), 185–190.
- Salvato, G., 1968. Some histological changes in chronic bronchitis and asthma. *Thorax* 23 (2), 168–172.
- Shroff, A., Manalis, A., Jagdeo, J., 2014. Oxidative stress and skin fibrosis. *Curr. Pathobiol. Rep.* 2, 257–267.
- Smiechowicz, J., Skoczynska, A., Nieckała-Szwarc, A., et al., 2017. Occupational mercury vapour poisoning with a respiratory failure, pneumomediastinum and severe quadriplegia. *SAGE Open Med. Case Rep.* 5, 1–4.
- Staji, A., Ziki, R.V., Ognjanovic, B., et al., 1997. Effect of cadmium and selenium on the antioxidant defence system in rat kidneys. *Comp. Biochem. Physiol.* 2, 167–172.
- Valcheva-Kuzmanova, S., Stavreska, G., Dancheva, V., et al., 2014. Effect of *Azadirachta indica* fruit juice on amiodarone-induced pneumotoxicity in rats. *Pharmacogn. Mag.* 10, 132–140.
- Velindala, S., Gaikwad, P., Ella, K.K.R., Bhargonde, K.D., Hunsingi, P., Anop, K., 2014. Histochemical analysis of polarizing colours of collagen using Picro Sirius red staining in oral submucous fibrosis. *J. Oral Health* 6 (1), 33–38.
- Vester, C., Oberholzer, H.M., Cummings, F.R., et al., 2017. Effects of metals cadmium and chromium alone and in combination on the liver and kidney tissue of male Sprague-Dawley rats: An ultrastructural and electron-energy-loss spectroscopy investigation. *Microsc. Res. Tech.* 80 (8), 878–888.
- Vignola, A.M., Chaner, P., Chiappam, G., et al., 1997. Transforming growth factor- $\beta$  expression in mucosal biopsies in asthma and chronic bronchitis. *Am. J. Respir. Crit. Care Med.* 156, 591–599.
- Vlahovic, G., Russell, M.L., Mercer, R.R., Crapo, J.D., 1999. Cellular and connective tissue changes in alveolar septal walls in emphysema. *Am. J. Respir. Crit. Care Med.* 160, 2086–2092.
- Weigand, K.L., Reno, J.L., Rowley, B.M., 2015. Low-level mercury causes inappropriate activation in T and B lymphocytes in the absence of antigen stimulation. *J. Arkansas Acad. Sci.* 69 (1), 116–123.
- WHO (World Health Organisation), 2000. Cadmium: Air Quality Guidelines, 2nd. World Health Organisation, Regional Office for Europe, Copenhagen, Denmark Chapter 6.3.
- Yang, L., Li, J., Mo, H., Pidaparti, R.M., Witten, T.M., 2016. Possible role of collagen reorientation during airway remodeling on mucosal folding. *J. Eng. Math.* 96, 37–56.
- Zhao, Y., Gao, S., Chou, L.N., et al., 2006. Inhibition of the expression of lysyl oxidase and its substrates in cadmium-resistant rat fetal lung fibroblasts. *Toxicol. Sci.* 90 (2), 478–489.
- Zhou, Y., Horowitz, J.C., Naba, A., et al., 2018. Extracellular matrix in lung development, homeostasis and disease. *Matrix Biol.* 73 (77), 104.
- Zhu, H., Jia, Y., Cao, H., et al., 2014. Biochemical and histopathological effects of sub-chronic oral exposure of rats to a mixture of five toxic elements. *Food Chem. Toxicol.* 71, 166–175.